Universität Hamburg

The role of the exocyst complex in neural cell adhesion molecule mediated morphogenesis in *Mus musculus* (Linnaeus, 1758)

Dissertation

zur Erlangung des Doktorgrades des Departments Biologie der Fakultät für Mathematik, Informatik und Naturwissenschaften an der Universität Hamburg

vorgelegt von Yana Chernyshova

Hamburg, 2008

Gutachter

Prof. Dr. M. Schachner

Prof. Dr. K. Wiese

Genehmigt vom Department Biologie
der Fakultät für Mathematik, Informatik und Naturwissenschaften
an der Universität Hamburg
auf Antrag von Frau Professor Dr. M. SCHACHNER
Weiterer Gutachter der Dissertation:
Herr Professor Dr. K. Wiese
Tag der Disputation 20. Juni 2008

Hamburg, den 05. Juni 2008

Professor Dr. Jörg Ganzhorn
Leiter des Departments Biologie

HPI
Heinrich-Pette-Institut für Experimentelle Virologie
und Immunologie an der Universität Hamburg

Carol Stocking, Ph.D.
FG Molekulare Pathologie
Fon (040) 480 51-273
Fax (040) 480 51-187
stocking@hpi.uni-hamburg.de

HPI · Martinistraße 52 · 20251 Hamburg

Fachbereich Biologie
Universität Hamburg
Martin Luther King-Platz 2
D-20146 Hamburg

Hamburg, 31. März 2008

Sehr geehrte Damen und Herrn,

hiermit bestätige ich, dass die von Frau Yana Chernyshova mit dem Titel "The role of the exocyst complex in neuronal cell adhesion molecule mediated morphogenesis in *Mus musculus* (Linnaeus, 1758)" vorgelegte Doktorarbeit in korrektem Englisch geschrieben ist.

Mit freundlichen Grüssen,

Dr. Carol Stocking

Leiterin der FG Molekulare Pathologie
Heinrich-Pette-Institut
(Amerikanerin)

Abstract

The exocyst complex plays a pivotal role in polarized exocytosis in a variety of cells being involved in the polarized protein delivery and morphogenesis of neurons. The molecular cues that target the exocyst complex to the sites of exocytosis remain, however, poorly understood. Present study shows that the exocyst complex binds to the intracellular domain of the neural cell adhesion molecule NCAM and this binding is enhanced in response to ligand-induced clustering of NCAM at the cell surface. NCAM promotes tyrosine phosphorylation of the exocyst complex and is required for the efficient recruitment of the exocyst complex to growth cone plasma membranes. Clustering of NCAM at the surface of growth cones induces Ca2+ dependent vesicle exocytosis which is blocked by an inhibitor of L-type voltage dependent Ca2+ channels. NCAM deficiency results in reduced tethering of the trans-Golgi network (TGN) derived organelles near the leading edge of growth cones and is accompanied by abnormal accumulation of the TGN derived organelles in growth cones and neurites of NCAM-deficient neurons. This work reveal a novel role for a cell adhesion molecule in that it regulates addition of the new membrane to the cell surface of growth cones in developing neurons.

Contents

Abbreviations

µ	Micro (10^{-6})
°C	Degree Celsius
-/-	NCAM deficient
+/+	NCAM wild type
aa	Amino acid
Ab	Antibody
Amp	Ampicillin
APS	Ammonium per sulphate
BCA	Bicinchoninic acid
bp	Base pairs
BSA	Bovine serum albumin
CAM	Cell adhesion molecule
cDNA	Complementary deoxyribonucleic acid
CHO	Chinese Hamster Ovary
DNA	Deoxyribonucleic acid
E. coli	Escherichia coli
EDTA	Ethylene diamine tetraacetic acid
ELISA	Enzyme-linked immunosorbent assay
ER	Endoplasmatic reticulum
f.c.	Final concentration
Fab	Fragment antigen binding
Fc	Fragment crystallizable
FGF	Fibroblast Growth Factor
FGFR	Fibroblast Growth Factor Receptor
FGFRI	Fibroblast Growth Factor Receptor inhibitor
FN	Fibronectin
FNIII	Fibronectin III
g	Standard gravity is used as a unit of acceleration
GFP	Green fluorescent protein
GPI	Glycosylphosphatidylinositol
GST	Glutathione S transferase

HEPES	4-(2-Hydroxyethyl)piperazine-1-ethanesulfonic acid
His	Histidine
Homobuffer	Buffer for homogenization
ID	Iintracellular domain
Ig	Immunoglobulin
IgG	Immunoglobulin subclass G
IPTG	Isopropyl-β-D-1-thiogalactopyranoside
kb	Kilo base pairs
ko	Knockout
l	Liter
LB	Luria Bertani medium
LB/amp	LB with ampicillin concentration 100 μg/ml
LSM	laser scanning microscope
LTP	Long term potentiation
m	Milli (10^{-3})
M	Concentration of solution in mol/l
mRNA	Messenger ribonucleic acid
MW	Molecular weight
n	Nano (10^{9})
NCAM	Neural Cell Adhesion Molecule
NCAM ID	Intracellular domain of NCAM
nm	Nanometer
NTA	Nitrilotriacetic acid
OD	Optical density
PAGE	Polyacrylamide gel electrophoresis
PBS	Phosphate buffered saline
PCR	Polymerase chain reaction
PSA	Polysialic acid
Pi	Inorganic phosphate
PMSF	Phenyl methyl sulfonyl fluoride
RCF	Relative centrifugal force
RIPA	RadioImmunoPrecipitation Assay
RNA	Ribonucleic acid

RNAse	Ribonuclease
rpm	Rotations per minute
RT	Room temperature
SDS	Sodium dodecylsulfate
SDS-PAGE	Sodium dodecyl sulphate poly acrylamide gel electrophoresis
s	Second
SNARE	Soluble N-ethylmaleimide-sensitive factor attachment protein receptor
TBS	Tris buffered saline
TEMED	N,N,N',N'-Tetramethylethylenediamine
TGN	Trans-Golgi network
Tris	Tris(-hydroxymethyl)-aminomethane
Triton X-100	Tolyethylene glycol p-(1,1,3,3-tetramethylbutyl)-phenyl ether
Tween 20	Polyoxyethylene (20) sorbitan monolaurate
V	Volt
wt	Wild type
Y	Tyrosine

1. Introduction

1.1. Exocytosis and participants of vesicle fusion

Transport vesicles destined for the surface plasma membrane normally leave the *trans*-Golgi network in a steady stream. The membrane proteins and the lipids in these vesicles provide new components for the surface plasma membrane. The fusion of the vesicles with the plasma membrane is called exocytosis.

The supply of newly synthesized membrane components necessary to sustain neurite growth is enormous. New membrane is delivered at the sites of insertion into the plasma membrane via vesicle carriers, whose nature and composition is still debated. In developing neurons, organelles bearing synaptic vesicle antigens undergo active exo-endocytosis. This recycling is present in all developing processes, rather than being restricted to a specific compartment, as it occurs in mature neurons (Matteoli et al., 1992). It has also been proposed that membrane addition is accomplished by fusion of large plasmalemma precursor vesicles different from synaptic vesicles and belonging to the constitutive secretory pathway (Pfenninger and Friedman, 1993). Studies with antisense oligonucleotides as well as with clostridial toxins suggest that insertion of the new membrane into the growing axon is accomplished by means of a fusion machine similar to that employed for the fusion of synaptic vesicles (Higgins et al., 1997).

The advances concerning the molecular mechanisms of synaptic vesicle fusion have led to the development of a model believed to hold true for several intracellular fusion events (Südhof, 1995). According to the so-called SNARE hypothesis, a central role in the process is played by the compartment-specific coupling between proteins localized on the donor vesicular compartment (v-SNAREs) and the acceptor target compartment (t-SNAREs) (Söllner et al., 1993).

This basic membrane recognition and fusion machinery is regulated to fit the needs of individual trafficking steps, specific differentiated cells, and particular physiological states. For example, exocytosis in the nerve terminal is tightly coupled to calcium concentration. Additionally, polarized cells such as neurons and epithelial cells must strictly regulate the sites of fusion of vesicles with subregions of the target membrane defined by particular SNARE proteins.

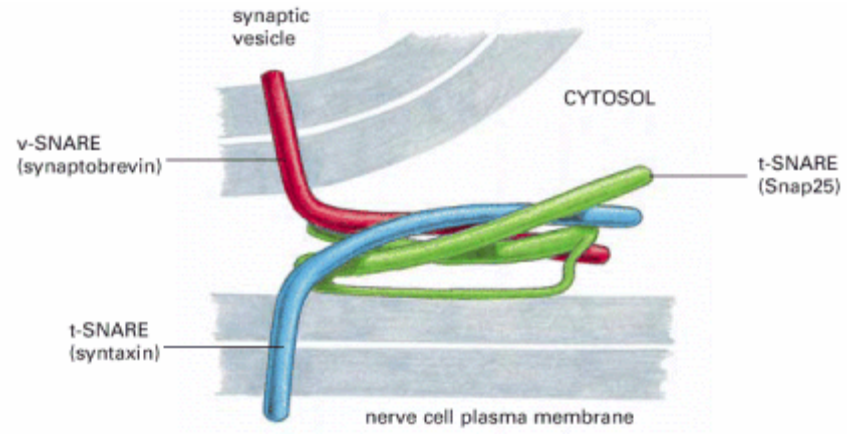

Figure 1. The structure of SNAREs.

The SNAREs responsible for docking synaptic vesicles at the plasma membrane of nerve terminals consist of three proteins. The v-SNARE synaptobrevin, and the t-SNARE syntaxin are both transmembrane proteins and each contributes one α-helix to the complex. The t-SNARE Snap25 is a peripheral membrane protein that contributes two α-helices to the four-helix bundle. *Trans*-SNARE complexes always consist of four tightly intertwined α-helices, three contributed by a t-SNARE and one by a v-SNARE. The α helices are shown as rods for simplicity (Sutton et al., 1998).

The final stage of fusion involves the formation of a bundle of four parallel core SNARE domains, one contributed by the vesicle and three contributed by the target membrane (Figure 1). Such a *trans*- SNARE complex bridges the two membranes, and its formation is thought to overcome the energy barrier preventing two membranes from fusing. Only particular combinations of four core SNAREs are able to promote fusion in vitro (McNew et al., 2000; Parlati et al., 2000). A simple model is therefore that the SNARE complement of a vesicle and a potential target membrane is necessary and sufficient to determine their compatibility for fusion.

Several aspects of this model have recently been questioned. In particular, it is unclear whether further factors provide specificity, help in SNARE assembly or even assist in the fusion event itself. The rate of *trans* complex formation is too slow *in vitro* to account for the rate of membrane fusion observed *in vivo*, which suggests that accelerating factors are involved (Fasshauer et al., 2002). There is also evidence that in some cases fusion events are regulated downstream of SNARE complex assembly, although the generality of this is unclear (Muller et al., 2002). Most debate, however, has focused on whether interactions between v- and t-SNAREs can account for the specificity of membrane transport events (Pelham, 2001). Biochemical and genetic studies have identified several proteins that appear to play a role in membrane transport steps after vesicle formation.

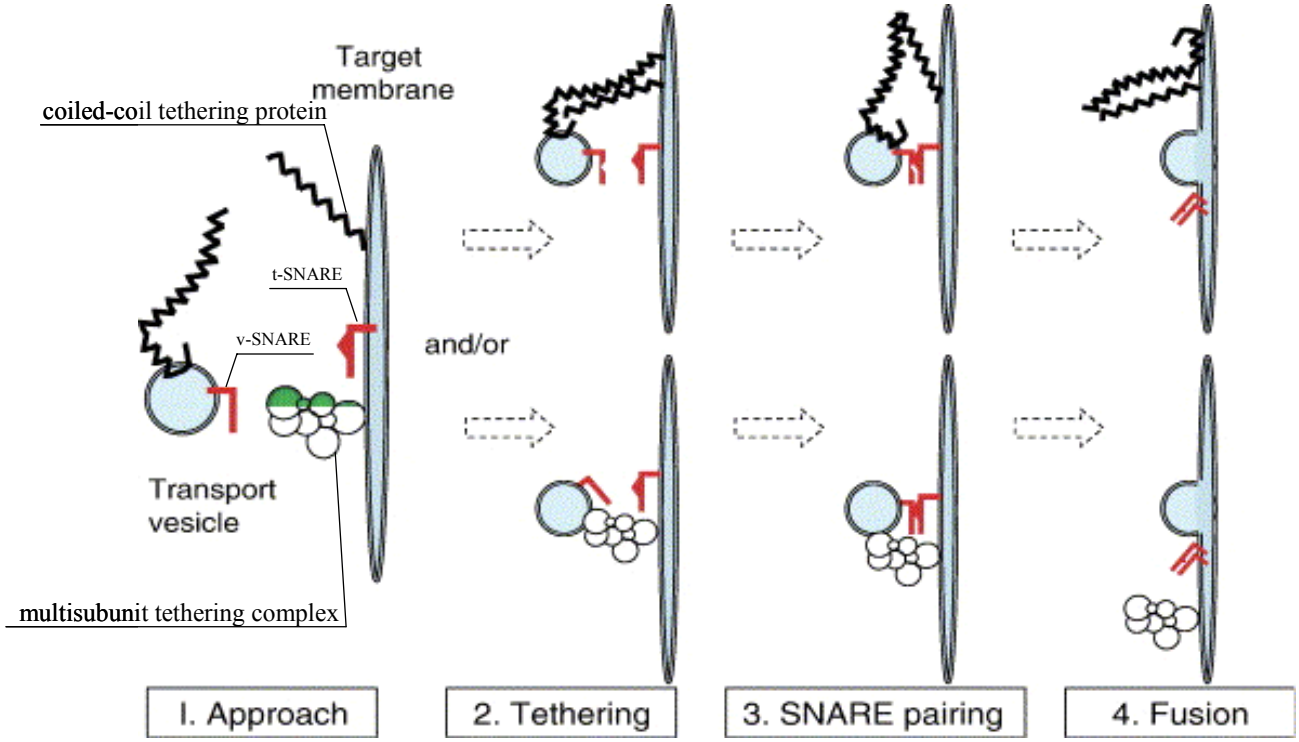

Figure 2. A model for membrane tethering.

(1) A transport vesicle approaches the target membrane. The movement can be by diffusion or by a motor-mediated process. (2) The transport vesicle is tethered to the target membrane by coiled-coil proteins or through multimeric tethering complexes. Tethering can occur at distances of >200 nm. It has been proposed that tether assembly may precede vesicle budding, and thus couple vesicle production with targeting to the appropriate target membrane. (3) The cognate v-SNARE on the transport vesicle and t-SNAREs on the target compartment pair to form *trans*-SNARE complexes. This process is sometimes referred to as "docking". (4) The assembly of SNARE complexes drives membrane fusion. Transported cargo is incorporated into the membrane of the target compartment (Lupashin and Sztul, 2005).

These factors could contribute to the fidelity of vesicle fusion and function in a process that has become known as tethering (Figure 2). This is the formation of physical links, often over considerable distances, between two membranes that are due to fuse, before *trans*- SNARE complex formation (Guo et al., 2000; Lowe, 2000; Waters and Hughson, 2000). Tethering might represent the earliest stage at which specificity is conferred on a fusion reaction.

What is the evidence that SNAREs do not provide all the specificity in vivo? The ubiquitous distribution of SNAREs on some membranes is not sufficient to account for the fusion of vesicles to localized regions of those membranes. For example, the yeast plasma membrane SNAREs Sso1p and Sso2p are distributed over the entire plasma membrane, and yet vesicles fuse with only certain parts of the membrane during periods of polarized growth (Brennwald et al., 1994). Cleavage of squid synaptic SNAREs with toxins prevents SNARE complex

formation but results in the association of more, not fewer, vesicles with the membrane (Hunt et al., 1994). Similarly, the percentage of tethered neuronal vesicles is significantly higher in flies lacking syntaxin or synaptobrevin than in wild type flies (Broadie et al., 1995). These results are consistent with SNAREs being involved in membrane fusion but dispensable for a prior tethering event that initially attaches the vesicle to its target without causing it to fuse. Vesicle tethering has been observed in an in vitro reconstituted system, which demonstrated that ER-derived vesicles attach to the Golgi apparatus, losing their ability to diffuse freely, in a reaction that is independent of functional SNARE proteins (Cao et al., 1998). A large number of factors proposed to be involved in tethering have been identified. In many cases, the mode of action of these factors remains obscure. Although it is still far from clear how tethering occurs at a molecular level, connections between the variety of tethering factors are becoming apparent and may prove useful in elucidating their roles.

Two broad classes of molecules are proposed to have a role in tethering: a group of long, coiled-coil proteins and several large, multisubunit complexes (Figure 2). The former have the potential to form homodimeric coiled coils with lengths up to several times the diameter of a vesicle. In yeast, one example is Uso1p, whose importance in tethering is clear since it is an essential protein and the only cytosolic factor required for the tethering of ER-derived vesicles to washed acceptor membranes (Barlowe, 1997). The formation of long coiled coils by Uso1p has been observed by electron microscopy (Sapperstein et al., 1995; Yamakawa et al., 1996). These structures have led to the idea that the large coiled-coil proteins are anchored at one end to a membrane, which allows them to "search" the surrounding space for a passing vesicle, which is then bound by the other end (Figure 2). Whereas this is an attractive model, there is currently a lack of direct evidence for it.

Although the coiled-coil proteins are known in many cases to bind to a target membrane and/or vesicle, their receptors on the membranes are generally not known.

The second class of tethering factor is multisubunit complexes. The overall molecular function of the complexes is still unknown, but biochemical studies have revealed their subunit compositions and interactions with other membrane-trafficking components. Seven large, conserved complexes have been proposed to play roles in vesicle tethering at distinct trafficking steps. In most cases these complexes were initially identified and characterized in yeast (Figure 3).

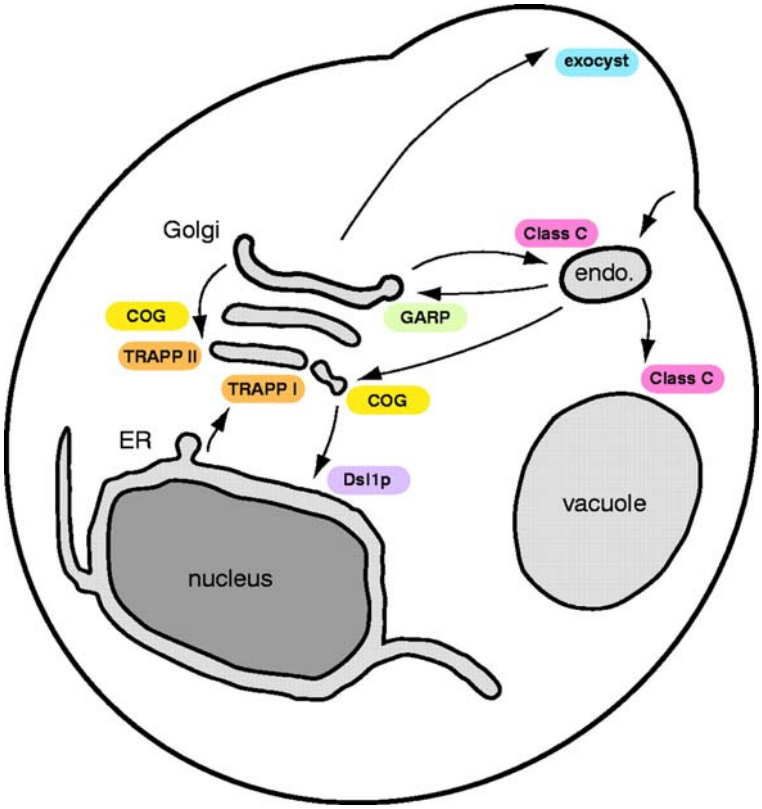

Figure 3. Tethering factors distribution in the yeast secretory pathways.

Tethering multi-subunit complexes are placed next to the transport step they facilitate or adjacent to the compartment to which they localize (Whyte and Munro, 2002).

An important but unresolved question is how tethering factors promote fusion of the vesicle to the correct target. The mechanism may be purely kinetic, with the vesicle being tethered within the vicinity of its destination and having an increased probability of undergoing SNARE-mediated fusion. Alternatively, the mechanism may be thermodynamic, the tethering factors actively promoting SNARE-mediated fusion in response to vesicle binding. This might be either by release of inhibition of SNAREs or by activation of the SNAREs on the vesicle and target. Of course, both kinetic and thermodynamic mechanisms could operate simultaneously, mediated by the same or different sets of tethering factors. One possibility is that the long, coiled-coil proteins are kinetic tethers that passively hold the vesicle and do not need to transduce signals about vesicle binding along their length, whereas the multi-protein complexes are thermodynamic tethers that actively promote interaction between vesicle and target. Whether there is any cross-talk between the two classes of tethering factors has yet to be explored.

Probably the best-characterised tethering complex is the exocyst. It is the tethering complex responsible for exocytosis at the plasma membrane (TerBush et al., 1996; Kee et al., 1997).

The exocyst complex merits detailed consideration since it plays a role in the delivery of vesicles to the plasma membrane of polarized epithelial cells (Grindstaff et al., 1998) and functions in neurite outgrowth in the nervous system (Vega and Hsu, 2001).

Overall, specialized molecular complexes (e.g. the exocyst complex) are assembled within distinct membrane domains to achieve localized delivery and fusion of intracellular vesicles but their receptors on the target membranes are generally not known.

Perfect candidates for such receptors would be transmembrane proteins which are concentrated at the target membrane. In neurons the exocyst complex plays a role in neurite outgrowth: it draws transport vesicles to the site of active membrane addition and growth to the growth cone. The proteins which are known to be concentrated in growth cones are the recognition molecules. One of the possible candidates is NCAM, an adhesion molecule that has multiple functions. NCAM will be described in the following chapters in detail.

1.2. The exocyst complex

The exocyst complex is comprised of eight subunits. Genes of six subunits were defined as secretory mutants in yeast (Sec3, -5, -6, -8, -10, and -15) (Novick et al., 1981). These six yeast proteins are found in a complex with a molecular mass of 743 kDa. The exocyst complex exhibits a restricted localization at the distal end of the budding cell, the site of active vesicle fusion (Finger and Novick, 1997). These data suggest that the exocyst complex is important in defining the site of vesicle fusion, possibly linking the machinery responsible for bud site selection and polarization to the secretory apparatus.

1.2.1. Structure of the exocyst complex

The exocyst is a multisubunit complex that is conserved among eukaryotes. It appears to function primarily as a "tether", directing secretory vesicles to specific sites on the plasma membrane, where their fusion is then brought about by SNAREs (Hsu et al., 1999). The components of the exocyst were initially identified as products of *sec* genes in yeast, but a complex of homologous proteins was subsequently isolated from rat brain. It is now thought that the exocyst (alternatively known as the Sec6/Sec8 complex) probably plays an essential role in the post-Golgi secretory pathways of all eukaryotes. Its importance is highlighted by the observation that mice lacking at least one of the exocyst subunits die at an early stage during embryogenesis. In polarised epithelial cells the complex is required for the delivery of secretory vesicles to the basolateral membrane and is localized to the tight junctions (Hsu et

al., 1999, Matern et al., 2001). Immunocytochemical studies of its distribution in cultured hippocampal neurons suggest that it is also involved in membrane addition at axonal and dendritic growth cones, and plays a key role in synaptogenesis (Matern et al., 2001).

The exocyst complex contains single copies of eight subunits Sec3, Sec5, Sec6, Sec8, Sec10, Sec15, Exo70 and Exo84 (Figure 4), that exhibit between 21% and 24% sequence identity between yeast and mammals (Hsu et all., 1999; Matern et al., 2001). In mammals, the subunits range in size from 75 kDa (Exo70) to 111 kDa (Sec8), giving a total molecular mass of the complex of 736 kDa. Electron microscopy examination of the glutaraldehyde-fixed complex purified from rat brain, following rotary shadowing with platinum, has revealed a "body" approximately 30 nm long and 13 nm wide, to which two "arms" of approximately 15 nm long and 6 nm wide are attached. The latter appear to be attached to the body via a flexible region because they extend away from the body at varying angles (Hsu et al., 1998). Information on the arrangement of the subunits within the complex has been obtained by genetic approaches in yeast, by yeast two-hybrid assay and by co-immunoprecipitation of in vitro translated, radiolabelled components (Hsu et al., 1999). Such studies have identified interactions between Sec15 and Sec10, Sec8 and Sec10, Sec5 and Sec6, and Sec6 and Exo70. There is also an interaction between Sec3 and Sec5 and between Sec3 and Sec8. In addition to these strong interactions identified by yeast two-hybrid assay, numerous weak interactions were also detected. The existence of weaker interactions brings up the possibility that the stability of the intact complex may be achieved through a series of higher order interactions not detectable by the pairwise protein interaction studies using the two-hybrid assay (Matern et al., 2001). Sec15 in yeast is the subunit responsible for association of the exocyst with secretory vesicles, via interaction with the GTP-bound form of the rab GTPase Sec4. The G-protein that plays a corresponding role in mammals is RalA. It is a small GTPase that is enriched in brain and associated with synaptic vesicles. Mammalian exocyst binds via Sec5 to the GTP-bound form of RalA. Depletion of cellular RalA disrupts the association of exocyst subunits with each other, suggesting that Ral–exocyst interactions are required to promote assembly of the full octameric complex (Sugihara et al., 2002; Moskalenko et al., 2002).

Sec3 has been identified as a spatial landmark for polarized secretion in yeast, targeting the exocyst complex to specific domains of the plasma membrane. The other exocyst components link Sec3 and Sec15 via a series of protein-protein interactions, resulting in the polarized targeting of secretory vesicles to appropriate sites of exocytosis. The figure 4 shows a hypothetical arrangement of subunits in the yeast and mammalian exocyst complex.

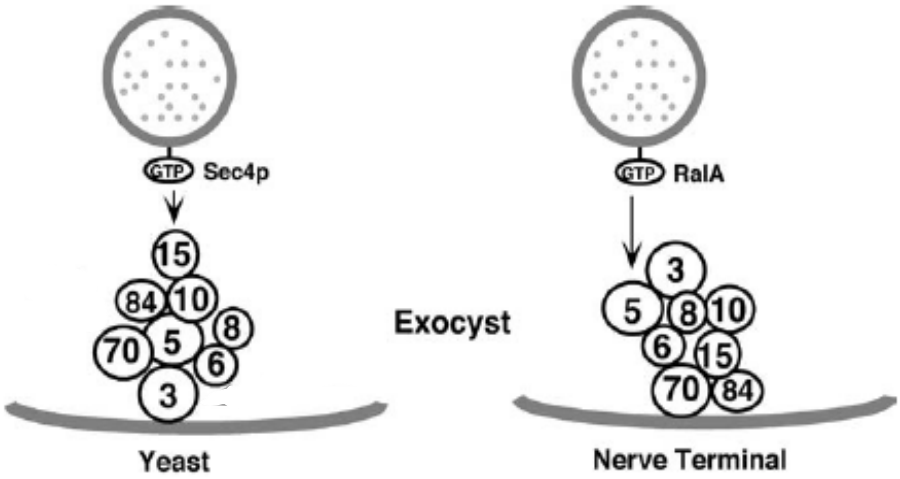

Figure 4. Hypothetical arrangement of subunits in the exocyst complex.

The exocyst complex comprises eight proteins: Sec3, Sec5, Sec6, Sec8, Sec10, Sec15, Exo70, and Exo84. The organization of these proteins in the complex is depicted based on reported protein-protein interactions for yeast and mammalian exocyst components. The interaction between the exocyst and vesicle-associated GTPases (Sec4p and RalA) are indicated by arrows (Li and Chin, 2003).

1.2.2. Subcellular localization of the exocyst complex

The exocyst complex is ubiquitously expressed, suggesting that it may be a core component of the vesicle targeting machinery in every cell. Mammalian exocyst complex are expressed in brain, spleen, lung, liver, kidney, and pancreas. Interestingly, the highest exocyst subunit expression is found in brain, an organ with highly polarized cells (Guo at al., 1997; Kee et al., 1997; Sjölinder et al., 2002).

With the cell biological approach, exocyst complex localization has been investigated by antibody detection of endogenous exocyst subunits and by green fluorescent protein (GFP) tagging of exogenously introduced exocyst subunits. Anti-exocyst subunit antibodies have detected two major exocyst subcellular distribution patterns in cells with no extensions or processes emanating from the cell body. In MDCK epithelial and pancreatic acinar cells, the Sec6 and Sec5 subunits were found to have both perinuclear and plasma membrane enrichment (Shin et al., 2000; Yeaman et al., 2001). In particular, plasma membrane-localized exocyst staining was enriched at the tight junctions (Grindstaff et al., 1998; Yeaman et al., 2001) or the lateral membrane (Kreitzer et al., 2003) in MDCK cells. Sec10 also exhibited

similar tight junction enrichment (Lipschutz at al., 2000). When MDCK cells were treated with the calcium chelator EGTA to disrupt cell-cell contacts among these cells, plasma membrane-localized Sec8 was found to redistribute into the cytoplasm (Grindstaff et al., 1998). Thus the plasma membrane localization of at least one exocyst subunit is dependent on cell polarity and/or cell-to-cell contacts.

In cells with processes or extensions emanating from the cell body, the exocyst complex subunits have been found at the perinuclear region, as well as throughout the processes with enrichment at the tip of' the processes. In neuroendocrine PC12 cells Exo70 localization was dependent on the differentiation state of the cell (Vega and Hsu, 2001). In undifferentiated PC12 cells, Exo70 displayed perinuclear enrichment. On the addition of' nerve growth factor to promote neurite outgrowth, Exo70 was found distributing from the perinuclear region into the growing neurite and became enriched in the growth cone. Antibodies against four other exocyst subunits, Sec6, Sec8, Sec15, and Exo84, showed similar localization (Wang and Hsu, 2003). In cultured hippocampal neurons, Sec6 and Sec8 were also found in the cell body, axons, and dendrites (Hazuka et al., 1999). In cultured kidney glomerular visceral epithelial cells Sec6 and Sec8 were also found in the cell body, with enrichment at the terminus of processes (Simons et al., 1999). GFP-tagged Exo70 showed plasma membrane enrichment (Matern et al., 2001).

Localized exocyst enrichment in the cell is likely due to the anchoring or active recruitment of the exocyst complex by insoluble cellular structures. In agreement, sedimentation studies have shown that the majority of the exocyst complex cosedimented with an insoluble cellular fraction in rat brain (Hsu et al., 1996). The question now is: what is the cellular structure that associates with tile exocyst complex. In MDCK cells, pharmacological, biochemical, and cell biological studies showed that the exocyst complex is localized to the *trans*-Golgi network at the perinuclear region and to the plasma membrane, where it colocalized with adhesion junction proteins including ZO-l, cortical actin, E-cadherin, α-catenin, and occuludin (Grindstaff et al., 1998; Yeaman et al., 2001). Exocyst complex subunits Sec6 and Sec8 colocalized with vesicles carrying exocytic cargoes. Blockage of exocytosis inhibited recruitment of the exocyst complex to the plasma membrane. Treatments that block exocytosis in MDCK cells, such as low temperature and expression of kinase-inactive protein kinase D, also caused the accumulation of exocyst subunits at the perinuclear region. Thus it was hypothesized that there is a steady state distribution of the exocyst complex between the *trans*-Golgi network and the plasma membrane. In addition, the introduction of various

monoclonal antibodies against Sec6 and Sec8 into permeabilized MDCK cells resulted in protein cargo accumulation either at the perinuclear region or near the plasma membrane, implying that the exocyst complex may function at multiple stages in Golgi-to-plasma membrane vesicle trafficking.

There is evidence suggesting that the exocyst complex is associated with cytoskeletal elements such as septins and microtubules in neuroendocrine PC12 cells (Vega and Hsu 2001, 2003). Thus exocyst localization is dependent on the proteins or cellular structure with which it associates.

1.2.3. The exocyst complex function

Present work is focused on exocyst functioning in growth cones of neurons in the brain. But in order to reveal more complete description of the processes exocyst complex is involved in, the evidences obtained from the studies done on different organisms and different subcellular regions will be given.

Understanding of the biological functions of the exocyst complex in higher eukaryotes has been obtained by perturbing exocyst function in tissue culture cells or in whole organisms. In the MDCK epithelial cell line, the introduction of anti-exocyst Sec8 subunit monoclonal antibodies into permeabilized cells disturbed protein targeting to the basolateral, but not to the apical, plasma membrane domain of these cells (Grindstaff et al., 1998). Similarly, the inhibition of exocyst function with anti-exocyst Sec3 subunit monoclonal antibodies in pancreatic ucinar primary cells also disrupted the delivery of calcium signaling proteins to the apical plasma membrane domains of these cells, indicating that delivery and fusion of vesicles containing calcium signaling proteins was disturbed (Shin et al., 2000). In the neuroendocrine PC12 cell line, the overexpression of an exocyst Sec10 deletion dominant negative construct prevented neurite outgrowth (Vega and Hsu, 2001). Thus, perturbations in exocyst function can affect protein targeting to specific plasma membrane domains and neurite outgrowth.

In the mammalian system, the exocyst complex has also been shown to be required for vesicle trafficking. In mice with the exocyst subunit Sec8 knocked out, animals die shortly after the induction of gastrulation (Friedrich at al., 1997), suggesting that the exocyst function is essential for development. In yeast exocyst null mutants are also nonviable.

When Sec5 subunit of exocyst complex was knocked out in the fruit fly *Drosophila melanogaster*, the flies died as growth-arrested larva precluding a more detailed analysis of the role of the complex (EauClaire and Guo, 2003; Murthy et al., 2003). Therefore flies with

eyes composed exclusively of cells homozygous for Sec5 mutation were generated in otherwise heterozygous animals. Membrane traffic in neurons of this mutant flies was studied at the cellular level. It was shown that neurite outgrowth in culture was inhibited in Sec5 mutants once maternally supplied Sec5 was exhausted. Using a T cell transmembrane protein, CD8, as a plasma membrane protein marker, it was shown that exocytosis at the plasma membrane was defective in Sec5 mutants, whereas the synthesis of CD8 protein and the generation of CD8-containing vesicles were normal (Murthy et al., 2003). This is similar to what was observed in temperature-sensitive yeast exocyst mutants. After temperature shift, the mutant cells accumulated secretory vesicles and the exocytosis of cell wall enzyme marker such as invertase was blocked. In sharp contrast to the arrest of neurite growth and plasma membrane protein addition, it was found that synaptic transmission continued to be robust despite the decline of maternal Sec5 protein (Murthy et al., 2003). These results indicate that the exocyst complex is required for constitutive secretion where secretory vesicles are delivered from Golgi to the plasma membrane. It is not, however, necessary for regulated secretion in the form of neurotransmission where synaptic vesicles are tethered near the plasma membrane and undergo repeated local exocytosis and endocytosis cycles.

The depletion of exocyst Sec10 subunit in Drosophila by RNA interference (RNAi) also resulted in early postembryonic lethality (Andrews et al., 2002). However, tissue-specific Sec10 RNAi did not cause defect in neuromuscular junction formation. Neurotransmission in this organism was not perturbed. Instead, the ring gland, an organ specialized in hormone secretion, was affected. These results suggest that fruit fly Sec10 is required for hormone secretion but not for neurotransmission.

The exocyst functions in mediating protein targeting and it is likely to be tightly regulated to promote precise protein/membrane addition to the plasma membrane. Identification of proteins that interact with the exocyst complex will help us to understand the regulation of this complex as well as the regulation of exocytosis. Research on both yeast and mammalian cells identified several members of the Ras family of small GTPases that interact and regulate the exocyst (Lipschutz and Mostov, 2002; Novick and Guo, 2002). Because the small GTPases have multiple effectors, exocyst function could be coordinated with other cellular processes also controlled by these G proteins.

A yeast exocyst component Sec15, can associate with secretory vesicles and interact specifically with the rab GTPase, Sec4, in its GTP-bound form. Sec4 may control the assembly of the exocyst. The exocyst may therefore function as a rab effector system for targeted secretion. In turn in mammalian cells in addition to Sec5-RalA, a GTP-dependent

interaction was found between Rab11 and Sec15. Rab11 is thought to regulate endosomal/plasma membrane interactions by controlling membrane traffic through recycling endosomes. Rab11 localizes to the recycling endosome, trans-Golgi network (TGN), and post-Golgi vesicles (Chen, 1998; Deretic, 1997; Ullrich, 1996). Hence, exocyst functions as a Rab11 effector in mammalian cells (Zhang et al., 2004). A study on *Drosophila melanogaster* also reported the interaction between Sec15 and Rab11. Sec15 in fly photoreceptors colocalizes with Rab11 and loss of Sec15 affects rhabdomere morphology (Wu, 2005).

The exocyst complex is proposed to play a role in regulating protein synthesis. In support of this model, the overexpression of exocyst subunits Sec6 and Sec10 has been found to promote the synthesis of a subset of proteins. Specifically, in MDCK cells, the overexpression of Sec10 was found to increase the synthesis of basolateral, but not apical, plasma membrane proteins (Lipschutz et al., 2000). In oligodendrocytes, the overexpression of Sec8 was found to increase the protein level of a subset of proteins such as myelin basic protein and myelin-associated glycoprotein (Anitei et al., 2006). Consistently, the knockdown of Sec8 decreased the protein level of myelin basic protein. These findings suggest that Sec8 and Sec10 may play a role in regulating the initiation of exocytosis starting at the protein synthesis process. This hypothesis is further supported by the *in vitro* interaction and co-immunoprecipitation of the Sec10 subunit with the ER (endoplasmic reticulum) translocon protein (Lipschutz et al., 2003). In addition, it is interesting to note that sec8 has been found to associate with different adaptor proteins such as PSD-95 (postsynaptic density-95), SAP102 (synapse-associated protein of 102 kDa) and CASK (Ca^{2+}/calmodulin-dependent serine protein kinase), which enables exocyst to associate with a variety of proteins on secretory vesicles (Anitei et al., 2006; Riefler et al., 2003; Sans et al., 2003). These associations bring up the possibility that the exocyst complex may also play a role in the sorting and targeting of various proteins to different plasma membrane domains. In this regard, the overexpression of Sec10 subunit promoted protein insertion into the basolateral, but not the apical, plasma membrane domain (Lipschutz et al., 2000).

It is suggested that the exocyst complex serves as a link between microtubule organization and vesicle targeting. One speculates that the exocyst complex may function as a remodeling factor for microtubules. It was shown that the intact exocyst complex, as well as the Exo70 subunit alone, can inhibit tubulin polymerization *in vitro* (Wang et al., 2004). These findings, along with a previous report showing that localized destabilization of microtubules can

promote plasma membrane addition (Zakharenko and Popov, 1998), led to a hypothesis that Exo70 overexpression may disrupt microtubule network and increase plasma membrane addition. Indeed, the overexpression of Exo70 resulted in localized disruption of microtubule network in the cell and increased plasma membrane addition in the form of long and thin plasma membrane protrusions. The formation of these Exo70-induced membrane protrusions was greatly inhibited by stabilizing microtubules with taxol (Wang et al., 2004). These *in vitro* and *in vivo* observations are consistent with a role for Exo70, and thus exocyst, in modulating microtubule dynamics underlying plasma membrane addition.

Characterization of the exocyst complex assembly and function in yeasts suggests that the exocyst is a dynamic complex assembled from subunits that form a targeting patch on the plasma membrane and a vesicle-associated subcomplex, which function together to both target and tether secretory vesicles to sites of membrane expansion (Boyd et al., 2004). The mammalian exocyst is responsible for appropriate targeting and tethering of relevant secretory vesicles to specific dynamic plasma membrane domains, including the basolateral surface of polarized epithelial cells, growth cones of differentiating neuronal cells, sites of synapse formation and the leading edge of migrating epithelial cells (Guo et al., 2000; Hsu et al., 2004). The exocyst has also been implicated in insulin-dependent delivery of GLUT-4 vesicles to the plasma membrane in adipocytes (Inoue et al., 2003).
In conclusion, the exocyst is an essential component in the exocytosis pathway in all cell types and organisms studied so far. Elucidation of the biological functions of the exocyst will not only contribute to our understanding of vesicle traffic, but will also provide insights into the mechanisms of many complex biological processes including polarized growth.

1.3. NCAM

1.3.1. Structure of NCAM

The neural cell adhesion molecule (NCAM) was the first cell adhesion molecule identified in the nervous system (Brackenbury et al., 1977). NCAM belongs to a group of transmembrane or membrane-associated Ig-CAMs since the extracellular part of NCAM contains five Ig-like domains. Next to Ig-like domains NCAM has two fibronectin type III-like motifs which were originally identified as a 90-residue repeated module in the extracellular matrix (ECM) molecule fibronectin (Kornblihtt et al., 1985). Three major isoforms of NCAM are generated by alternative splicing of a single gene. According to their apparent molecular masses, they

are termed NCAM120, NCAM140 and NCAM180. NCAM120 is anchored to the membrane by glycosylphosphatidylinositol, whereas NCAM140 and NCAM180 are transmembrane glycoproteins with large cytoplasmic domains of different lengths (Figure 5).

In contrast to NCAM140 the cytoplasmic domain of NCAM180 contains an additional insert of 267 amino acids, encoded by the alternatively spliced exon 18, whereas the rest of cytoplasmic region (119 amino acids) is identical to NCAM140.

There are several soluble forms of NCAM which can be generated by truncation, proteolysis or shedding (Gower et al., 1988; Rønn et al., 2000).

Several other splice variants are possible. For example the product of the 30 bp VASE exon (variable alternative spliced exon) can be present within the fourth immunoglobulin-like domain of NCAM (Barbas et al., 1988). Expression of the VASE exon reduces the neurite outgrowth-promoting activity of NCAM (Chen et al., 1994; Lahrtz et al., 1997)

.

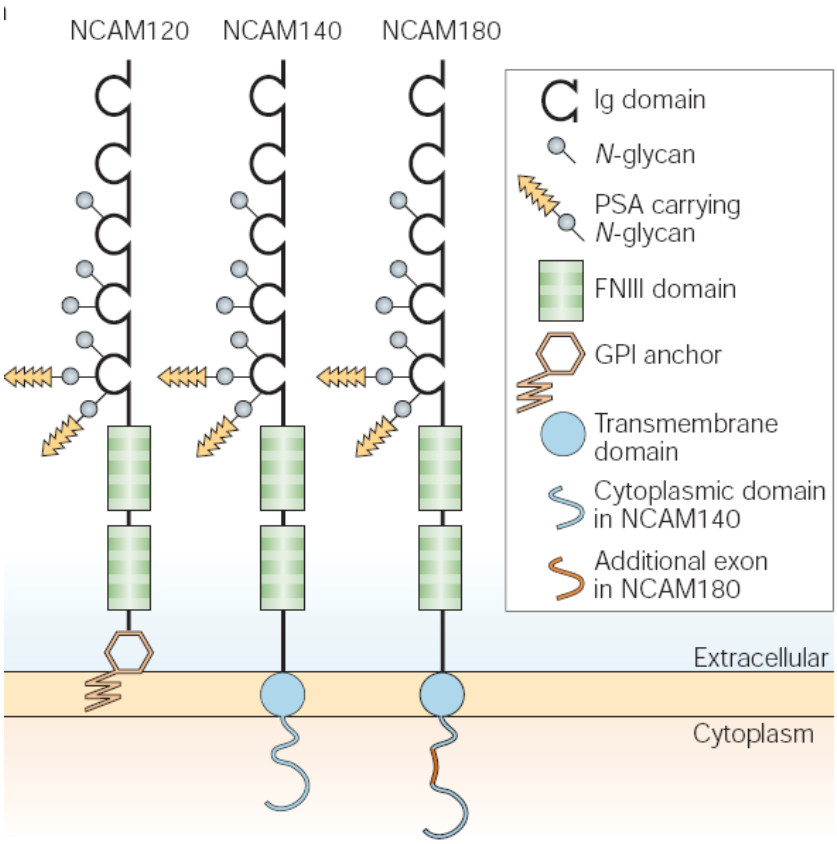

Figure 5. Schematic structure of the three main isoforms of NCAM.

Structure of three main isoforms of NCAM named according to their molecular weights. NCAM isoforms can be either GPI-anchored or exist as transmembrane isoforms with a small or large cytoplasmic domain. The

glycosylphosphatidylinositol (GPI)-anchored NCAM120 and the transmembrane NCAM140 and NCAM180 consist of five immunoglobulin (Ig)-like domains and two fibronectin-type III repeats (FNIII). All three isoforms can carry PSA. The cytoplasmic domains of NCAM140 and NCAM180 differ in length (Kleene and Schachner, 2004).

1.3.2. Expression and subcellular localization

The NCAM isoforms have different expression profiles, and thus are likely to play different roles in the organism. Generally NCAM is ubiquitously expressed. It can be found on neurons, Schwann cells, oligodendrocytes, astrocytes and muscle cells (Moore and Walsh, 1986; Neugebauer et al., 1988; Seilheimer and Schachner, 1988). Some cell types or subcellular structures specifically express one of the three main isoforms. The 180 kDa isoform, for instance, is strongly associated with synapses. Its long cytoplasmic tail interacts with the spectrin-actin cytoskeleton and thereby stabilizes synapse formation (Pollerberg et al., 1987; Persohn et al., 1989). NCAM120 is predominantly found in glia rather than in neurons. It is strongly expressed by oligodendrocytes, by muscle cells and within the spinal cord (Kiss et al., 2001). NCAM120 is also the major isoform in sensory neurons of dorsal root ganglia (Rosen et al., 1992). NCAM140 is detectable on pre- and post-synaptic membranes, whereas NCAM180 accumulates in the postsynaptic densities of synapses of mature neurons (Persohn et al., 1989; Pollerberg et al., 1985). Both transmembrane isoforms are downregulated in aging mice.

It has been reported that the expression of NCAM is regulated by nerve growth factors such us NGF in rat PC12 cells (Prentice et al., 1987). NGF treatment was associated with a 4- to 5-fold increase in NCAM180 surface protein levels, resulting from activation of NCAM expression.

All three isoforms of NCAM are found to be present in specialized membrane subcompartments, the lipid rafts. Four cysteine residues in the cytoplasmic domains of NCAM140 and NCAM180 adjacent to the transmembrane domain can be palmitoylated. The role of palmitoylation is to provide a second anchor in the plasma membrane to direct the protein to lipid rafts, but the molecular signals for palmitoylation are not known (Little et al., 1998). NCAM120 can be anchored to lipid rafts via GPI.

All isoforms of NCAM can carry polysialic acid (PSA) as long linear polymer chains composed of up to 200 sialic acid residues (Figure 5) (Schachner and Martini, 1995), but in the hippocampus PSA is restricted to NCAM180 (Doyle et al., 1992). PSA expression is high

during embryogenesis on growing axons and migrating cells and decreases rapidly in the adulthood. However, PSA-NCAM remains expressed in adult brain regions exhibiting a permanent capacity for structural and synaptic plasticity, including the olfactory bulb, the hippocampus and the pituitary gland (Bonfanti et al., 1992; Gubkina et al., 2001; Doherty et al., 1995).

The PSA polymer is negatively charged and strongly hydrated. Both, its size and its negative charge are believed to reduce NCAM mediated cell-cell adhesion (Rutishauser and Landmesser, 1996; Kiss et al., 2001).

1.3.4. Signal transduction events in neurite outgrowth and interaction partners of NCAM

The growth of neurite processes from the cell body involves a massive increase in cell surface area (Futerman and Banker, 1996). Membrane expansion at the growth cone requires the addition of new membranes to the growing processes. This is accomplished by the incorporation of *trans*-Golgi network (TGN) -derived exocytic vesicles into the plasma membrane. Exocytic membrane transport from the TGN to the plasma membrane occurs constitutively in all cells. In parallel, a stimuli-regulated exocytic process also exists. In neurons, the initiation of neurite outgrowth would require specifically intensified and oriented exocytosis in a particular small region of the plasma membrane that would become the growing tip of a neurite.

In some instances, adhesion molecules may act primarily to bind cell membranes to surfaces. But it now seems clear that some adhesion molecules of the immunoglobulin superfamily after the interaction with their binding partners act via the cytoplasmic domain to initiate a signal-transduction cascade as a direct consequence of an adhesive interaction.

Many studies have addressed the NCAM mediated signal transduction initiated through homophilic NCAM–NCAM interaction, or by more recently investigated heterophilic interactions. NCAM-NCAM binding involves all five Ig domains and that they interact pair-wise in an antiparallel orientation (Ranheim et al., 1996). However, other investigators have suggested that homophilic adhesion is mediated primarily by the third Ig domain in one NCAM molecule binding to the third Ig domain in a second NCAM molecule (Rao et al., 1994). There is little evidence for a role of FNIII domains in the homophilic interactions that occur between cells; however, these domains might contribute to a homophilic interaction in *cis* between NCAM molecules expressed in a single cell (Peck and Walsh, 1993).

The introduction of purified NCAM or NCAM antibody in substrate of neuronal cell culture resulted in enhanced neurite outgrowth (Doherty et al., 1989, 1990). The presence of purified NCAM or NCAM antibody in the medium of neuronal cell culture showed the similar effect. The ability of neural NCAM to support neurite outgrowth is a paradigm that has been used to elucidate signals that occur following NCAM activation.

Two major signalling pathways in NCAM mediated neurite outgrowth were discovered. First pathway involves NCAM binding to fibroblast growth factor receptor (FGFR), which results in FGFR dimerisation and autophosphorylation. Further FGFR-specific signaling pathway leads to the Ca2+ influx into the neurons as well as activation of the protein kinase C (PKC), finally resulting in neurite outgrowth (Williams et al., 1994; Doherty et al., 1994; Saffell et al., 1997). NCAM clustering at the cell surface has been shown to be accompanied by an increase in Ca2+ concentration in the cytosol with the voltage dependent Ca2+ channels (VDCC) of the T- and L-type playing a major role in NCAM dependent Ca2+ influx to the cell (Schuch et al., 1989; Kiryushko et al., 2006).

In addition to binding and activating the FGFR, NCAM140, but not NCAM180, activates the MAP kinase pathway through Fyn and focal adhesion kinase. It leads further to activation of the MAP kinases and phosphorylation of the transcription factor cAMP-response-element-binding protein resulting in neurite outgrowth (Schmid et al., 1999).

NCAM is regarded as a stabilizer of cell–cell contacts. It is known as a linker to the cytoskeleton through its interaction with spectrin (Pollerberg et al., 1987). Formation of the NCAM-spectrin-PKCbeta2 complex is necessary for NCAM-mediated neurite outgrowth. (Leshchyns'ka et al., 2003)

Recenty it was shown that NCAM140 forms a complex with RPTPα and spectrin. NCAM activation results in the redistribution of NCAM140-spectrin-RPTPα complex to lipid rafts where RPTPα activates Fyn, which, in turn, promotes neurite outgrowth (Bodrikov et al., 2005).

Apart from mediating interactions between apposing cells or between cells and the extracellular matrix (*trans*-interactions), NCAM can associate with another cell adhesion molecule of the immunoglobulin superfamily, L1, on the same cell membrane (*cis*-interaction). The interaction between NCAM and L1 gives rise to an enhanced homophilic interaction between L1 molecules on apposing cells, a mechanism termed assisted homophilic binding (Kadmon et al., 1990).

1.3.5. NCAM deficiency

Genetic manipulations in *Drosophila* and mice have also shed light on NCAM function. Knockout studies have shown that NCAM is not essential for survival and have revealed a perhaps unexpectedly subtle phenotype (Tomasiewicz et al., 1993). The size of the olfactory bulbs is reduced NCAM deficient (NCAM-/-) mice (Cremer et al., 1994). This phenotype most likely reflects a perturbation of the cells migration into the bulb region (Ono et al., 1994). Although there is no gross decrease in hippocampal size in NCAM-/- mice there is a 30% decrease in mossy fiber density as well as a change in the organization of the remaining fibers (Cremer et al., 1997), suggesting an axonal growth and guidance function for NCAM. Moreover, studies examining the performance of NCAM-/- mice in the Morris water maze task, which involves hippocampus-dependent learning, have found that these mice have impaired acquisition in this task (Cremer et al., 1994). In support of this, organotypic slice cultures of hippocampus prepared from the NCAM-/- mice exhibit a decaying LTP compared with LTPs obtained from wild type mice (Muller et al., 1996). Also NCAM-/- mice show impaired sensitization of the startle response (Montag-Sallaz et al., 2003; Plappert et al., 2006).

NCAM-/- mice show several hallmarks of schizophrenia: increased size of lateral brain ventricles, impaired sensory motor gating manifested by reduced prepulse inhibition of acoustic startle, and deficits in hippocampal / amygdala-dependent learning and LTP (Cremer at al., 1994). One can conclude that information processing is altered in NCAM-/- mice.

Schizophrenia is a devastating disease that affects 1% of the world's population (Freedman, 2003). Psychosis is the most common clinical feature of schizophrenia, but such cognitive dysfunction as disabling of memory, information processing and attention is also observed (Lewis and Moghaddam, 2006). Schizophrenia is a neuropsychiatric disorder that is currently believed to originate from disturbances in neurodevelopment (Lieberman at al., 2001; Maynard at al., 2001).

NCAM-/- mice are more aggressive and anxious than their wild type littermates (Stork et al., 1997). They are also display defects in the structure of the hippocampus (Tomasiewicz at al., 1993), one of several brain regions implicated in schizophrenia. In particular hippocampal mossy fibers of NCAM-/- mice produce ectopic synapses due to a failure in remodeling (Seki and Rutishauser, 1998). Furthermore, there is a reduction in polysialylated NCAM, which is needed for proper axon guidance, in the brains of human schizophrenics (Barbeau et al.,

1995). Neuronal process formation in cerebral cortical structures implicated in schizophrenia, such as the prefrontal cortex, has not yet been analyzed in NCAM-/- mice.

Abnormal levels of an NCAM fragment that includes most of its extracellular domain are secreted in affected brain regions and cerebrospinal fluid of schizophrenic patients, correlating with severity of the disease (Poltorak et al., 1995; Honer et al., 1997; Vawter, 2000).

NCAM has been postulated as a candidate susceptibility gene for bipolar disorder and depression (Atz et al., 2007; Arai et al., 2004). Bipolar disorder and schizophrenia share some common susceptibility genes (Farmer et al., 2007; Leahy, 2007) and neuroanatomical characteristics, such as ventricular enlargement, decreased temporal lobe volume, and disrupted synaptic plasticity.

Levels of secreted NCAM are increased in the hippocampus of individuals with bipolar disorder (Vawter et al., 1999). Soluble NCAM is elevated in the hippocampus, prefrontal cortex and cerebral spinal fluid (CSF) of affected patients compared to normal controls (Vawter et al., 1998; Vawter et al., 1999; Poltorak et al., 1996). The elevated levels of soluble NCAM suggest that subcellular or synaptic functions of NCAM are compromised, perhaps contributing to the pathology of the disorder.

Soluble forms of NCAM are also increased in the cerebrospinal fluid of Alzheimer disease (AD) patients (Strekalova et al., 2006; Todaro et al., 2004). AD features include: neuronal death, synapse loss, reduced brain volume, disruption of the cholinergic system, and cognitive dysfunction. The hallmark features of AD are neurofibrillary plaques in the brain which are composed of amyloid β (Aβ) protein (Goedert and Spillantini, 2006; Yaari and Corey-Bloom, 2007). Significant decrease in the numbers of NCAM positive neurons was found in the frontal cortex of AD patients (Yew et al., 1999). There are conflicting reports on NCAM expression in plaques, suggesting that it may be altered in only a subset of individuals with AD (Gillian et al., 1994; Cotman et al., 1998).

All above-mentioned disorders are characterized with abnormal information processing in the brain. Since NCAM plays an important role in neurite outgrowth and synapse formation, alteration of its function during development could lead to improper cell migration and neuronal network formation, leading to pathological behavior related to disorder. The behavior in turn correlates with abnormalities found in NCAM-/- mice. Thus deep investigation of molecular mechanisms underlying NCAM mediated neurite outgrowth including vesicle exocytosis in nerve growth cones can improve our understanding of nature and causes of above-mentioned disorders.

1.3.7. The evidence for NCAM involvement in vesicle cycling and exocytosis

The function of NCAM was extensively studied in the neuromuscular junction (NMJ). Some evidence for NCAM involvement in vesicle cycling and exocytosis was also obtained from these experiments.

The NMJ is a specialized contact point of a skeletal muscle with the peripheral motorneuron terminal. NCAM-/- mice exhibit neuromuscular synaptic transmission deficits under physiological stimulation that lead to locomotor impairment (Polo-Parada et al., 2001). Transmission failure in these mice may be the result of defects in vesicle mobilization. The molecular basis of vesicle mobilization is poorly understood by now.

In addition, vesicle fusion in the normal adult NMJ is restricted to active zones at the nerve-muscle contact site (Polo-Parada et al., 2001). It is not yet understood how loss of NCAM affects synaptic maturation, vesicle cycling and targeting at the molecular level. However, some insight is offered by mice lacking only the NCAM180 isoform, where proper vesicle targeting to the active zones was disturbed at the nerve-muscular contact site. Like NCAM-/- mice deficient in all NCAM isoforms, the NCAM180-/- mice also exhibit locomotor deficits (Polo-Parada et al., 2004). These data point to improper targeting of vesicles to the active zone, as one of the causes of the synaptic deficit in NCAM-/- mice.

Neuroendocrine cells don't have the specialized synaptic structures found at the NMJ. Neuroendocrine chromaffin cells release catecholamine through exocytosis from large dense-core granules that employ molecular fusion machinery very similar to that utilized in the neuromuscular junction with the exception that the large dense core secretory granules dock and fuse with the cell surface in the absence of a specialized active zone structure. Thus it is another good tool to study NCAM involvement in exocytosis.

Several parameters of catecholamine release from chromaffin cells where tested in tissue slices prepared from NCAM+/+ as well as NCAM-/- mice. Electrochemical and electrophysiological techniques were employed to determine granule recruitment to the releasable state, fusion competence, and sustained levels of release under repetitive physiological stimulation (Chan et al., 2005).

It was found that chromaffin cells from NCAM-/- mice exhibited deficiencies in transmitter release that are analogous to those found in the neuromuscular junction. The deficit was due to an impaired recruitment of granule/vesicle from the readily releasable pool to the final highly fusogenic immediately releasable pool (Chan et al., 2005).

The results of the experiments on NMJ lead to the suggestion that NCAM may play a structural role in active zone stabilization, somewhat similar to the intercellular adhesion function served during development (Rutishauser and Landmesser, 1991, 1996). However, the data collected from the neuroendocrine chromaffin cells point to a more basic function for NCAM, this cell type does not release granules at a structurally identifiable active zone. This opens the possibility that NCAM may be an important molecule in the regulation and proper function of secretory machinery in general and is not restricted to specialized active zones found in neurons. This evidence is very valuable for the present work, since it is focused on the mechanisms of NCAM dependent exocytotic events in the neuronal growth cone, the structure which appears developmentally before synapse formation.

In addition, it was found that the NCAM-/- mice overexpress proteins vital to the secretory process (SNAP-25, Syntaxin, and Munc-13). Such an overexpression is consistent with a compensation mechanism designed to facilitate more complete fusion. This would be achieved by increasing the copy number of fusion machines per granule. However, this overexpression is insufficient to rescue the NCAM dependent trafficking deficit responsible for impaired catecholamine release.

Besides, a study on cultured hippocampal neurons showed that NCAM mediates accumulation of TGN organelles at sites of cell-to-cell contact (Sytnyk et al., 2002). In cultures of neurons from NCAM-/- mice, the number of newly formed contacts with accumulated organelles was reduced when compared with cultures from wild type mice. Moreover, organelles moved away from the contacts approximately four times more often in NCAM-/- neurons when compared with wild type neurons. Thus it was shown that NCAM is important not only for stabilization of initial contacts but also for stabilization of organelles at the specific sites of contact on the plasma membrane (Sytnyk et al., 2002).

1.4. Regulation of exocytosis by Ca2+

Calcium ions act as a second messenger inside the cell to mediate a wide spectrum of cellular functions. At their resting state, cells maintain a baseline of intracellular Ca2+ concentration at approximately 100 nM. This basal concentration is crucial for cells to respond effectively to various Ca2+ signals elicited by extracellular stimuli or membrane depolarizations that often reach a concentration of several hundreds of nanomols to a few micromols (Berridge et al., 2003; Clapham, 2007).

The stimulus-induced Ca2+ signals originate from either Ca2+ influx via plasma membrane Ca2+ channels or Ca2+ release from internal stores. The best-known Ca2+ channels in the plasma membrane of neurons are voltage-dependent Ca2+ channels (VDCCs) and neurotransmitter-gated channels.

Although Ca2+ influx through the plasma membrane conveys the first Ca2+ signal triggered by many extracellular stimuli, Ca2+ signals are often amplified by further Ca2+ release from internal stores. The most ubiquitous of the intracellular Ca2+ release mechanisms involves activation of phospholipase C (PLC). PLC catalyzes the hydrolysis of phosphatidylinositol 4,5-bisphosphate (PIP2) to yield diacylglycerol (DAG) and inositol trisphosphate (IP3). DAG activates members of the protein kinase C family, many of which play important roles in the control of cell growth. IP3 binds to IP3 receptor (IP3R) which is ligand–gated Ca2+ channel in the ER membrane, allowing the influx of Ca2+ to the cytosol (Berridge et al., 2000). Finally increased Ca2+ concentration triggers vesicle fusion.

Interestingly, exocyst complex component Sec8 and Sec6 can co-immunoprecipitate with the IP3R type 3 from pancreatic acinar cell extracts. They also co-immunoprecipitate with the plasma membrane Ca2+ pump, one of the isoform of phospholipase C, and the ER resident IP3R type1 from brain extracts. Also it was suggested that via interaction with above-mentioned proteins the exocyst complex can regulate their activity (Shin et al., 2000).

As was described above, NCAM activation on the cell surface also resultes in the Ca2+ influx in the cytoplasm. Thus both NCAM and exocyst complex can regulate Ca2+ concentration in the cell influencing exocytosis.

2. The aim of the study

The exocyst complex in neurons is important for polarized secretion and membrane addition at the tip of the growing neurite, growth cone. Since exocyst is believed to serve as a landmark for docking and fusion of transport vesicles with the plasma membrane, its accumulation in growth cones is important for efficient neurite outgrowth (Kee et al., 1997; Hazuka et al., 1999). Till now it is not clear by which processes and with help of which molecules the exocyst complex is targeted to the growth cones.

A cell adhesion molecule NCAM plays an important role in neurite outgrowth and neuronal development (Cremer et al., 1997; Doherty et al., 1990; Polo-Parada et al., 2004; Leshchyns'ka et al., 2003; Bodrikov et al., 2005). Activation of NCAM molecules at the cell surface by homophilic binding results in activation of intracellular signaling pathways finally leading to enhanced neurite outgrowth. Neurite outgrowth as a biological process requires new material insertion and membrane addition at the neurite growth cones through fusion of the transport vesicles with plasma membrane. Vesicle fusion is controlled by the exocyst complex, which is found to be accumulated in growth cones in neurons. NCAM is also present in the growth cones in big amounts. Furthermore, the exocyst complex plays a role in directing vesicles from *trans*-Golgi network to the plasma membrane, whereas NCAM in the plasma membrane can interact with TGN organelles and thus can promote their stabilization near the plasma membrane and guide their fusion (Sytnyk at al., 2002). Finally, redistribution of the exocyst complex during development from perinuclear region to neurites and growth cones depends on MAP kinase pathway activation (Vega and Hsu, 2001). In return NCAM stimulation activates MAP kinase pathway (Kolkova et al., 2000). Taking into account all facts mentioned above we determined the aims of the present study.

The aims of this study were:

- to analyze whether NCAM regulates targeting of the exocyst complex to the growth cones;
- to examine the possibility of interaction between NCAM and the exocyst complex and investigate potential functional consequences of this interaction;
- to investigate whether NCAM regulates the exocyst complex functions;
- to identify the role of NCAM in vesicle exocytosis in the growth cones of neuronal cells.

3. Materials

3.1. Chemicals

All chemicals were purchased from the following companies: Amersham Pharmacia Biotech (Freiburg, Germany), Bio-Rad (Hercules, CA, USA), Invitrogen (Karlsruhe, Germany), Carl Roth (Karlsruhe, Germany), Macherey-Nagel (Duren, Germany), Merck (Darmstadt, Germany), Serva (Heidelberg, Germany) and Sigma-Aldrich (St. Louis, MO, USA). Glutathione-agarose was obtained from Sigma-Aldrich. Ni-NTA agarose was purchased from Qiagen (Hilden, Germany).

3.2. List of buffers and solutions (in alphabetical order)

1.	0.4 M sucrose in TBS (For membrane expansion assay)	0.4 M sucrose 150 mM NaCl 50 mM Tris-HCl, pH 7.4
2.	0.75 M sucrose in Tris-HCl buffer (For growth cone isolation)	0.75 M sucrose 1 mM $MgCl_2$ 1 mM $CaCl_2$ 5 mM Tris-HCl, pH 7.4
3.	1 M sucrose in Tris-HCl buffer (For growth cone isolation)	1 M sucrose 1 mM $MgCl_2$ 1 mM $CaCl_2$ 5 mM Tris-HCl, pH 7.4
4.	5mM Tris-HCl	5mM Tris adjusted to pH 7.4 with 37% HCl
5.	Ampicillin stock solution (1000x)	100 mg/ml in H_2O, store in aliquots in - 20°C
6.	Blocking buffer (Western blot)	5 % skimmed milk powder 0.1 % Tween 20 in TBS pH 7.4
7.	Buffer for lysis of bacterial cell culture (Purification of GST-tagged recombinant proteins)	1% Triton X-100 in PBS pH 7.4

8.	Buffer for the lysis of bacterial cell culture (Purification of His-tagged recombinant proteins)	50 mM NaH_2PO_4 300 mM NaCl 10 mM imidazole pH 8.0
9.	Buffer for membrane expansion assay	100 mM sucrose 20 mM glucose 200 mM NaCl 10 mM KCl 2.4 mM NaH_2PO_4 44 mM HEPES 2.4 mM $MgCl_2$ pH 7.4
10.	De-staining solution (For coomassie staining of SDS-PAGE gels)	40 % ethanol 10% acetic acid
11.	Elution buffer for His-tagged recombinant proteins (Purification of recombinant proteins)	50 mM NaH_2PO_4 300 mM NaCl 200 mM imidazole pH 8.0
12.	Homobuffer (For whole brain homogenization)	320 M sucrose 1 mM $MgCl_2$ 1 mM $CaCl_2$ 5 mM Tris-HCl, pH 7.4
13.	Incubation buffer (For protein redistribution to the growth cone membrane)	0.25 mM Tris-HCl, pH 7.4 150 mM NaCl
14.	IPTG (1M) stock solution (1000x)	238 mg/ml in H_2O, store in aliquots in - 20°C
15.	Modified RIPA buffer with 0.5% SDS (For immunoprecipitation)	50 mM Tris-HCl, pH 7.4 150 mM NaCl 2 mM EDTA 1 mM Na_3VO_4 1 mM NaF

		1% Nonidet P-40 0.5% SDS 100 µM PMSF (Add just before use) Protease inhibitor cocktail-EDTA free, used according to the manufacturer's instructions (Add just before use)
16.	PBS (Phosphate buffered saline)	10 mM Na_2HPO_4 2.5 mM NaH_2PO_4 150 mM NaCl 3 mM KCl pH 7.4
17.	Resolving gel composition for SDS-PAGE	375 mM Tris-HCl, pH 8.8 0.1% SDS 0.025% ammonium persulfate 0.001% TEMED Acrylamide/Bis solution 29:1 (according to % of gel required)
18.	RIPA buffer (For immunoprecipitation)	50 mM Tris-HCl, pH 7.4 150 mM NaCl 2 mM EDTA 1 mM Na_3VO_4 1 mM NaF 1% Nonidet P-40 100 µM PMSF (Add just before use) Protease inhibitor cocktail-EDTA free, used according to the manufacturer's instructions (Add just before use)
19.	SDS PAGE running buffer	25 mM Tris-HCl, pH 8.3 192 mM glycine 0.1% SDS
20.	SDS sample buffer for SDS-PAGE (5x)	62.5 mM Tris-HCl, pH 6.8 40 % glycerol 5 % 2-mercaptoethanol

		0.04 % bromphenol blue
21.	Stacking gel composition for SDS-PAGE	125 mM Tris-HCl, pH 8.8 0.1% SDS 0.06% APS 0.025% TEMED 4% Acrylamide/Bis solution 29:1 according to % of gel required)
22.	Staining solution (coomassie staining of SDS-PAGE gels)	40% ethanol 10% acetic acid 0.1% Brilliant blue R250
23.	TBS- Tween (TBST) (For immunoblotting)	50 mM Tris-HCl, pH 7.4 150 mM NaCl 0.05% Tween
24.	Transfer buffer (For electrophoretic transfer of SDS-PAGE gels)	20 % methanol 25 mM Tris-HCl, pH 8.3 192 mM glycine 0.01 % SDS
25.	TBS (Tris Buffered Saline)	50 mM Tris-HCl, pH 7.4 150 mM NaCl

3.3. Antibodies

1.	anti-Actin	Rabbit polyclonal antibody (Sigma).
2.	anti-EEA1	Mouse monoclonal antibody (BD Transduction Laboratories).
3.	anti-Exo70	Mouse monoclonal antibody against Exo70 was a kind gift from Dr. Hsu C.S. (Rutgers University, USA).
4.	anti-GAPDH	Rat monoclonal antibody (Chemicon).
5.	anti-GM130	Mouse monoclonal antibody (BD Biosciences)

6.	anti-GST	Mouse monoclonal antibody (Novagen).
7.	anti-His6	Rabbit polyclonal antibody (Cell Signaling).
8.	anti-L1	Rabbit polyclonal antibody produced against the extracellular domain of L1, generated in the lab of Dr. M. Schachner (ZMNH, Hamburg, Germany).
9.	anti-NCAM (2b2)	Rabbit polyclonal antibody produced against the extracellular domain of mouse NCAM, generated in the lab of Dr. M. Schachner (ZMNH, Hamburg, Germany).
10.	anti-NCAM (clone H28)	Rat monoclonal antibodies produced against the extracellular domain of mouse NCAM, generated in the laboratory of C. Goridis (Centre National de la Recherche Scientifique UMR 8542, Paris, France).
11.	anti-NCAM 5b8	Mouse monoclonal antibody (Developmental Studies Hybridoma Bank).
12.	anti-pY20	Mouse monoclonal antibody (Santa Cruz Biotechnology)
13.	anti-Sec8	Mouse monoclonal antibody against Sec8 was a kind gift from Dr. Hsu C.S (Rutgers University, USA).
14.	anti-Tubulin	Rabbit polyclonal antibody (Covance).
15.	anti-β1-integrin	Rabbit polyclonal antibody (Chemicon).
16.	anti-γ-adaptin	Mouse monoclonal antibody (BD Biosciences).
17.	Peroxidase-conjugated goat anti-mouse IgG + IgM (H + L)	Peroxidase-conjugated AffiniPure goat anti-mouse IgG + IgM (H + L) (Dianova).

18.	Peroxidase-conjugated mouse anti-rabbit IgG (H + L)	Peroxidase-conjugated AffiniPure mouse anti-rabbit IgG (Dianova).
19.	Peroxidase-conjugated rabbit anti-goat IgG	Peroxidase-conjugated AffiniPure rabbit anti-goat IgG (Dianova).

3.4. Bacterial cell culture medium

Bacterial media were autoclaved and antibiotics added later to warm media.

1.	LB ampicillin medium	100 mg/l ampicillin in LB-Medium
2.	LB ampicillin plates	20 g/l agar in LB-Medium 100 mg/l ampicillin
3.	LB-medium	10 g/l Bacto-tryptone 10 g/l NaCl 5 g/l yeast extract pH 7.4

3.5. Bacterial strains and cell lines

1.	*Escherichia coli* DH5α	Invitrogen
2.	*Escherichia coli* M15 [pREP4]	Qiagen
3.	CHO-K1	*Chinese Hamster Ovary* dehydrofolatreductase deficient hamster cell line. ATCC (American Type Culture Collection) CCL 61.

3.6. Plasmids

1.	pGEX Exo70	For expression of GST tagged Exo70	From Dr. Hsu C.S, (Rutgers University, USA).
2.	NCAM140-ID pQE30	For expression of histidine tagged NCAM140 intracellular domain	Leshchyns'ka et al., 2003
3.	NCAM180-ID pQE30	For expression of histidine tagged NCAM180 intracellular domain	Leshchyns'ka et al., 2003

3.7. Toxins, inhibitors and other reagents

BAPTA-AM (1,2-Bis(2-aminophenoxy) ethane-N,N,N′,N′-tetraacetic acid tetrakis)	For Ca2+ depletion. BAPTA-AM is a membrane-permeable Ca2+ chelator.	Sigma-Aldrich
Cholera toxin β subunit tagged with HRP	For labeling of GM1 ganglioside.	Sigma-Aldrich
PD173074, FGFRI	For FGFR tyrosine kinase inhibition.	Calbiochem
Pimozide	For the blocking of voltage-dependent Ca2+ channels of T-type.	Sigma-Aldrich
Dynasore	For blocking of endocytosis. Dynasore is a cell-permeable, reversible noncompetitive dynamin 1 and dynamin 2 GTPase activity inhibitor.	Sigma-Aldrich
Nifedipine	For the blocking of voltage-dependent Ca2+ channels of L-type	Sigma-Aldrich
PhosSTOP	For the inhibition of phosphatases.	Roche

Phenylmethylsulfonyl flouride (PMSF)	For inhibition of serine proteases.	Sigma-Aldrich
Sodium orthovanadate (Na_3VO_4)	For inhibition of protein tyrosine phosphatases.	Fisher

3.8. Mouse strains

C57BL/6J mice were used as control wild type mice in all experiments. NCAM-/- mice were provided by H. Cremer (Cremer et al., 1994) and were inbred for at least nine generations onto the C57BL/6J background. For all of the biochemical experiments animals of 1-3 days of age were used. To prepare cultures of hippocampal neurons, 1- to 3-day-old C57BL/6J and NCAM-/- mice from homozygous breeding pairs were used.

3.9. Centrifuges and rotors

1. Eppendorf 5804R Refrigerated Centrifuge (Eppendorf AG, Hamburg, Germany)
2. Sorvall Ultracentrifuge (Kendro, Hanau, Germany)
3. Rotors used- SA600, HB-6, SLA1500, SLA3000
4. Beckman XL-80 Ultracentrifuge (Beckman Instruments GmbH, Munich, Germany)
5. Rotors used- SW28, 80Ti, 55Ti

4. Methods

4.1. Molecular biology

4.1.1. Transformation of bacteria

100 µl of competent cells (*E. coli* strains M15, DH5α or BL21) were mixed with 100 ng of plasmid DNA and incubated on ice for 10 min. After a heat shock (50 s, 42°C) and successive incubation on ice (2 min), 400 µl of LB-medium without antibiotic were added to the bacteria and bacteria were incubated with constant shaking at 37°C for 45 min. 50 µl of transformed bacteria was plated on LB agar plates containing the appropriate antibiotics. Plates were incubated at 37°C overnight.

4.1.2. Plasmid isolation from *E. coli* cultures

Plasmid isolation from 3 ml cultures (Minipreps)

3-5 ml LB/amp were inoculated with a single colony and incubated overnight at 37°C with constant agitation. Then cells were pelleted by centrifugation (12000 g, 1 min, RT). Plasmids were isolated from the bacteria according to the manufacturer's protocol (Nucleospin kit, Macherey-Nagel).

Plasmid isolation from 500 ml cultures (Maxipreps)

For preparation of large quantities of DNA (up to 500 µg of plasmid DNA), the Qiagen Maxiprep kit was used. A single colony was inoculated in 2 ml LB/amp and grown at 37°C for 8 h with constant agitation. Afterwards, this culture was added to 500 ml LB/amp and incubated at 37°C with constant agitation overnight. Cells were pelleted using Beckmann centrifuge (6000 g, 15 min, 4°C). DNA was isolated as described in the manufacturer's protocol (see Qiagen Maxiprep kit).

4.2. Protein-biochemical methods

4.2.1. Recombinant expression of proteins in *E. coli*

The appropriate *E. coli* strain was transformed with the expression plasmid and streaked on LB/amp plates. A single colony was inoculated in a 50 ml LB/amp and incubated overnight at 37°C with constant agitation. Afterwards, bacteria were transferred into a 450 ml LB/amp and

incubated at 37°C under constant agitation until the culture had reached the OD_{600} of 0.6. Protein expression was induced by adding IPTG (0.1-0.5 mM f.c.) to the culture with further incubation for 3 h at 37°C with constant agitation. Bacteria were collected by centrifugation and stored at –20°C. Protein expression after IPTG induction was monitored every hour by SDS-PAGE.

4.2.2. Lysis of bacteria

Sonication

2 ml of bacterial culture were centrifuged (8000 g, 4°C, 10 min). The pellet was resuspended in SDS sample buffer. The suspension was lysed on ice using a sonicator (Branson Sonifier B15, level 6, 50% pulse, 5 times 20 s). The debris were pulled down by centrifugation (10000 g, 4°C, 10 min). The supernatant was subjected to SDS-PAGE.

French press

Bacteria cells were pelleted (8000g, 4°C, 10 min) and resuspended in lysis buffer (PBS, pH 7.4, 1 mg/ml lysozyme, 0.1% Triton X-100 , 5 µg/ml DNAse). The suspension was lysed by compression (Spectronic Instruments/SLM Aminco). Then the suspension was centrifuged (15000 g, 10 min, 4°C) in a Beckman centrifuge.

Mild extraction

B-PER® Bacterial Protein Extraction Reagent (Pierce) was used according to manufacturer's instructions to lyse the cells.

4.2.3. Recombinant protein purification

Further purification of recombinant proteins was done according to protocol for purification of fusion protein by affinity chromatography and protocol for elution of fusion protein with glutathione and digestion with thrombin (Karcher et al., 1996).

4.2.4. Determination of protein concentration (BCA kit)

The protein concentration was determined using the BCA kit (Pierce). Solution A and B were mixed in a ratio of 1:50 to give the BCA solution. 10 µl of the sample were mixed with 200 µl BCA solution and incubated for 30 min at 37°C. A BSA standard curve was co-incubated ranging from 0.1 to 2 mg/ml. The extinction of the samples was determined at 568 nm wave

length by μQuant^{TM} universal microplate spectrophotometer (Bio-Tek Instruments Inc., Winooski, Vermont, USA)

4.2.5. SDS-polyacrylamide gel electrophoresis

Protein samples were subjected to SDS-polyacrylamide gel electrophoresis (SDS-PAGE) under reducing conditions using the Mini-Protean II system (Bio-Rad). Gel composition is given in materials. After polymerization of the SDS-PAGE gel, the chamber was assembled as described by the manufacturer's protocol. Samples were diluted with appropriate amount of SDS sample buffer followed by boiling for 5 min at 100ºC. 5-30 μg of total protein of each sample were loaded per well. The assembly was filled with SDS running buffer and the gel was run at constant 60 V for approximately 15 min and then at 100 V. The run was stopped when the bromophenol blue running front had reached the end of the gel. Gels were either stained or subjected to Western blotting.

4.2.6. Coomassie-staining of polyacrylamide gels

After SDS-PAGE, the gels were fixed in fixing solution for 60 min and subsequently incubated with Coomassie blue solution for 2-15 h at room temperature with constant agitation. The gels were then incubated in de-staining solution until the background of the gel appeared nearly transparent.

4.2.7. Western Blot

Proteins were transferred from the gel onto nitrocellulose membrane (Protran Nitrocellulose BA 85, 0.45 μm, Schleicher & Schuell) using a MINI TRANSBLOT-apparatus (BioRad). After equilibration of the gel in transfer buffer for 5 min, the blotting sandwich was assembled as described in the manufacturer's protocol. Proteins were transferred electrophoretically at 4°C in transfer buffer at constant voltage 40 V overnight. Prestained marker from Bio-Rad Laboratories was used as a molecular weight marker and to monitor successful protein transfer after blotting.

4.2.8. Immunological detection of proteins on nitrocellulose membranes

After electrophoretic transfer membrane was washed once in TBS and incubated in 10 ml of blocking buffer for 1 h at RT. Afterwards, the primary antibody was added in the appropriate

dilution either for 2 h at RT or overnight at 4°C. The unbound primary antibodies were removed by washing the membrane 4 times 15 min with TBST. The appropriate horseradish peroxidase (HRP) -conjugated secondary antibodies were applied for 1.5 h at RT. The membrane was washed again 4 times 15 min with TBST and immunoreactive bands were visualized using the enhanced chemiluminescence detection system.
The antibody bound to the membrane was detected using the enhanced chemiluminescence detection system (Pierce). The membrane was soaked for 1 min in detection solution (1:1 mixture of solutions I and II). The solution was removed and the membrane was exposed to X-ray film (Biomax-MR, Kodak) for several time periods, starting with 30 s exposure.

4.2.9. Densitometric evaluation of band intensities

Band densities were quantified using the image processing software *Scion Image* (Scion Corporation, Frederick, MD, USA) or TINA 2.09 software (University of Manchester, UK). The developed film was scanned. The digitized picture was exported to the image processing program and band density was evaluated according to the manual.

4.2.10. Stripping and re-probing of Western blots

For detection of several proteins on the immunoblot, the nitrocellulose membranes were stripped from bound antibodies by shaking blots in stripping buffer for 10 min at room temperature. Blots were neutralized by incubation for 2 times 5 min in 1 M Tris-HCl (pH 7.5). Than the membranes again were subjected immunological detection of proteins as described above.

4.2.11. Enzyme-linked immunosorbent assay (ELISA)

Purified exo70 protein was immobilized on polyvinylchloride surface in 96-well plates (Nunc) at the concentration 100 μg/ml overnight at 4°C. Non-absorbed proteins were removed, the wells were washed three times for 5 min with TBST and blocked overnight at 4°C with 10% BSA in TBS. After blocking, the wells were subsequently incubated at 4°C overnight with the putative binding proteins (NCAM140-ID, NCAM180-ID, NCAM Fc) applied at different concentrations (150 nM to 4800 nM). Non-bound proteins were removed and the wells were washed three times for 5 min at RT to remove nonspecifically bound proteins. Specifically bound proteins were detected with the antibodies against NCAM and the appropriate HRP-

linked secondary antibodies. Non-bound antibodies were removed and the wells were washed three times for 5 min at RT. Protein binding was visualized by detecting HRP with the OPD reagent (Pierce) that resulted in coloured product, which was quantified using ELISA reader at 492 nm wave length.

4.2.12. Immunoprecipitation

Immunoprecipitation experiments were performed with antibodies against the protein of interest, using A/G protein agarose beads (Santa Cruz Biotechnology) to pull down the complex. 1 mg of total protein of brain homogenate, or growth cone fraction was incubated with 1 ml of ice-cold RIPA lysis buffer for 1 h at 4°C with constant gentle shaking. The lysate was centrifuged at 20000 g for 15 min at 4°C. The supernatant was pre-cleared with 20 µl of thoroughly resuspended A/G agarose beads by incubating for 3 h at 4°C and constant gentle shaking. After pre-clearing, the beads were pelleted down by centrifugation at 500 g for 5 min. Then the supernatant was incubated with corresponding antibodies or control Ig overnight at 4°C with constant gentle shaking followed by precipitation with protein A/G agarose beads 3 h at 4°C. The beads were washed 4 times with ice-cold RIPA buffer and 3 times with ice-cold PBS. 70 µl of SDS sample buffer were added to the beads, following by heating at 100 °C for 7 min. The beads were pelleted by centrifugation and the supernatant was collected and applied to SDS-PAGE.

4.2.13. Isolation of growth cones particles and membrane fraction from growth cone

Growth cone particles (GCPs)

GCPs were isolated according to the two-step procedure described by Pfenninger (Pfenninger et al., 1983). The brains from 1-3-day old mice were homogenized in Homobuffer. Obtained homogenate was centrifuged at 1660 g for 15 min at 4°C. The supernatant collected after this step of centrifugation was spun to equilibrium on a discontinuous sucrose density gradient 0.75/1.0/2.66 M at 242000 g for 30 min at 4°C. The fraction at the interface between load and 0.75 M sucrose contained the isolated growth cones or GCPs. This fraction was collected and resuspended in 10 ml of Homobuffer, than pelleted at 100000 g for 40 min at 4°C to obtain purified GCPs.

GCP membranes (GCMs)

GCMs were prepared from the GCPs pellet as follows: GCPs were lysed by resuspending in 1 ml of 5 mM Tris-HCl, pH 7.5 and stirring on ice for 5 min. The lysed material was spun at 100000 g for 60 min at 4°C. The obtained pellet was resuspended in 5 mM Tris-HCl, pH 7.5 and stored frozen at -20°C until used.

4.2.14. NCAM clustering with NCAM antibody in isolated growth cones

1 mg of total protein of freshly isolated GCPs was resuspended in 150 µl of Homobuffer. Samples were stimulated with 3 µl of NCAM Ab or with 1 µl of nonspecific Ig as a control for 5 min at 37 °C with constant gentle shaking. Then samples were centrifugated at 242000 g for 30 min at 4°C. Each pellet was incubated with 1 ml of ice-cold RIPA lysis buffer for 1 h at 4°C with constant gentle shaking. The consequent steps were done according to the protocol for Immunoprecipitation described above.

4.2.15. Protein redistribution to the growth cone membrane

Brains from wild type mice were homogenised in 5mM Tris-HCl buffer, pH 7.4 and spun at 100000 g for 1 h. Collected after this centrifugation supernatant contained the cytosol. GCMs were incubated with the cytosol to analyze the redistribution of the exocyst complex proteins to the growth cone plasma membrane. In some samples the isolated GCMs were treated with 0.1 M Na_2CO_3 for 8 h at 4°C to strip off peripheral proteins and any cytosolic proteins that may have co-purified with the GCMs and interfere the binding. The absence of soluble proteins Exo70 and Sec8 on stripped GCMs were analyzed by Western blot.

Treated with Na_2CO_3 GCMs as well as control untreated GCMs were incubated with 500 µg of cytosol in a total assay volume of 1ml in Incubation buffer or with empty Incubation buffer for control. After 2 h incubation at RT the GCMs were collected by centrifugation at 100000 g for 1 h. The GCMs were washed once by resuspending them in 500 µl of Incubation buffer and repeating the centrifugation. The obtained pellets were resuspended in 50 µl of Incubation buffer. After determination of the total protein concentration, samples were subjected to SDS-PAGE for analysis. Recruited exocyst complex proteins were detected by Western blot.

4.2.16. Membrane expansion assay

The labeling of the growth cone plasma membrane with HRP-coupled cholera-toxin was used as a measure of membrane area. For expansion assay, 1.3 ml of ice-cold GCPs-containing interface (Pfenninger et al., 1983) were mixed with 0.5 ml cold 2 times concentrated buffer (100 mM sucrose, 20 mM glucose, 200 mM NaCl, 10 mM KCl, 2.4 mM NaH_2PO_4, 44 mM HEPES, 2.4 mM $MgCl_2$, pH 7.3) and, after 30 min, with a further 0.8 ml of the same buffer. After an additional 20 min on ice, 250 µl aliquots of the suspension were added to assay tubes. Samples were preincubated with (and without) specified inhibitors for 30 min. Then NCAM antibodies (or preimmune serum) were added and samples were equilibrated on ice for 15 min. After this samples were warmed up in a water bath to 37°C for 5 min, and subsequently chilled in ice slurry for 5 min. Then saponin at f.c. 0.01% was added to the probes destined for total membrane estimation. After 5 min cholera-toxin-HRP was added to each tube to label membranes, incubation continued for 15 min on ice. Samples were loaded onto 0.5 ml cushions of 0.4 M sucrose in TBS and then spun at 100000 g for 1 h. The pellets were resuspended in 200 µl of water and HRP activity was measured using OPD reagent (Pierce). Each experimental set included controls stimulated with preimmune serum and samples containing 0.01% saponin. This allowed determination of the surface only (probes without saponin) and total (probes with saponin) membrane pools. The difference between the two measurements represented the size of the internal membrane pool. Changes in the internal membrane pool were taken as a measure of vesicle exo- and endocytosis.

4.3. Immuno- and cytochemistry

The experiments with primary cultures of hippocampal neurons and immunofluorescence labeling were performed in cooperation with Dr. Iryna Leshchyns'ka and Dr. Vladimir Sytnyk in the group of Melitta Schachner.

4.3.1. Cultures of hippocampal neurons

Cultures of hippocampal neurons were prepared from 1- to 3-day-old mice. Neurons were grown for 24 days in Neurobasal A medium (Invitrogen) supplemented with 2% B-27 (Invitrogen), glutamine (Invitrogen) and basic FGF (2 ng/ml, R&D Systems) on glass coverslips (for live imaging and immunocytochemsitry) coated with poly-L-lysine (100 µg/ml).

4.3.2. Immunofluorescence labeling

Immunolabeling was performed as described (Sytnyk et al., 2002). All steps were performed at room temperature. Hippocampal neurons were fixed for 15 min in 4% formaldehyde in PBS, pH 7.4, permeabilized with 0.25% Triton X-100 in PBS, pH 7.4 for 5 min and blocked with 3% BSA in PBS for 20 min. Primary antibodies were applied in 3% BSA in PBS for 2 hours and detected with corresponding secondary antibodies applied for 45 min.

4.3.3. Immunofluorescence aquisition and quantification

Immunofluorescence images were acquired at room temperature using a confocal laser scanning microscope LSM510 (Zeiss), LSM510 software (version 3, Zeiss) and oil Plan-Neofluar 40x objective (numerical aperture 1.3, Zeiss) at 3x digital zoom. Contrast and brightness of the images were further adjusted in Corel Photo-Paint 9 (Corel Corporation). For immunofluorescence quantification neurites or growth cones were outlined using ImageJ software and mean intensities within these outlines were measured.

4.3.4. Labeling of TGN-derived organelles in live neurons

Live neurons were incubated with 5 μM BODIPY FL ceramide (Invitrogen) applied in a culture medium for 30 min in a CO2 incubator, washed with the culture medium and incubated for another 30 min in a CO2 incubator.

4.3.5. Live cell imaging

Recordings of live neurons were performed using a time-lapse function of the laser scanning microscope LSM510 (Zeiss). During recordings, neurons were maintained on the microscope stage in an incubator (Zeiss) at 37^{o}C and 5% CO2. Images were acquired with a 1 s interval. Organelle mobility and fluorescence levels were analyzed using ImageJ software (National Institute of Health).

5. Results

5.1. TGN-derived organelles abnormally accumulate in neurites of NCAM-/- neurons

Previously, it was shown that the intracellular domains of NCAM molecules at the neuronal surface membrane can bind to the spectrin cytoskeleton lining the surface of the *trans*-Golgi network (TGN) derived intracellular organelles and that this interaction stabilizes TGN-derived organelles at sites of NCAM accumulation. In growing neurites, NCAM accumulates in growth cones being involved in the regulation of neurite outgrowth (Leshchyns'ka et al., 2003; Bodrikov et al., 2005; Santuccione et al., 2005). To investigate the role of NCAM in the regulation of the distribution of TGN-derived organelles in growing neurites, we compared the levels of these organelles in growth cones of wild type (NCAM+/+) and NCAM deficient (NCAM-/-) hippocampal neurons maintained in culture for 1 day. Immunolabeling of the neurons with the antibodies against a TGN-marker protein γ-adaptin showed that the number of TGN-derived organelles, identified as accumulations of γ-adaptin immunofluorescence, was increased in growth cones of NCAM-/- neurons (Figure 6). Similarly, the mean γ-adaptin immunofluorescence intensity in growth cone, a more easy-to-measure parameter, was also increased in NCAM-/- neurons (Figure 6). γ-adaptin levels were increased both in the growth cones formed on presumable axons, identified morphologically as thin long neurites, and dendrites, identified as thicker, shorter and often tapering processes (Figure 6). The molecular markers, such as MAP2 and tau, were present in all neurites of these immature neurons (not shown) in accordance with previous reports (Sytnyk et al., 2002), that precluded further distinction between axons and dendrites at the molecular level. The γ-adaptin immunofluorescence intensity was increased not only in growth cones but also along axons and dendrites of NCAM-deficient neurons (Figure 6) that may explain increased levels of γ-adaptin in NCAM-/- growth cones. However, the ratio of the γ-adaptin immunofluorescence intensity in growth cones to γ-adaptin immunofluorescence intensity in neurites was two times lower in NCAM-/- versus NCAM+/+ neurons (Figure 6) strongly suggesting that NCAM is important for preferential accumulation of TGN-derived organelles in growth cones. A similar result was obtained when TGN-derived organelles were labeled with the antibodies against another Golgi and TGN marker protein GM130 (Figure 7).

Levels of γ-adaptin and GM130 were also increased in NCAM-/- versus NCAM+/+ growth cones isolated from the brain tissue and analyzed by Western blot (Figure 8). Interestingly, however, the overall levels of these two proteins were not changed in the brain homogenates of NCAM-/- versus NCAM+/+ mice (Figure 8). This observation excludes a possibility that increased levels of γ-adaptin and GM130 in NCAM-/- neurites and growth cones are due to the overall enhanced expression of these two proteins in NCAM-/- brains. Hence, a plausible explanation for the increased levels of the TGN-derived organelles in NCAM-/- growth cones and neurites could be the inability of these organelles to fuse with the surface plasma membrane that would result in the filling of neurites and growth cones with these organelles. In support of this idea, the growth cones in NCAM-/- neurons were slightly swollen being increased in their area (Figure 9). In contrast to TGN-derived organelles, the levels in growth cones and neurites and the ratio of the levels in growth cones to the levels in neurites for the early endosomes visualized with the antibodies against the early endosome marker protein EEA1 was not changed in NCAM-/- neurons (Figure 10). Interestingly, the levels of the lysosomes visualized with the antibodies against a lysosomal marker protein Lamp1 were reduced in NCAM-/- neurites and growth cones (Figure 10) again suggesting abnormalities in the biosynthetic and protein degradation pathways. The ratio of the lysosome levels in growth cones to the lysosome levels in growth cone was not changed in NCAM-/- neurons (Figure 10). Thus our observations indicate that NCAM specifically promotes preferential accumulation of TGN-derived organelles in growth cones.

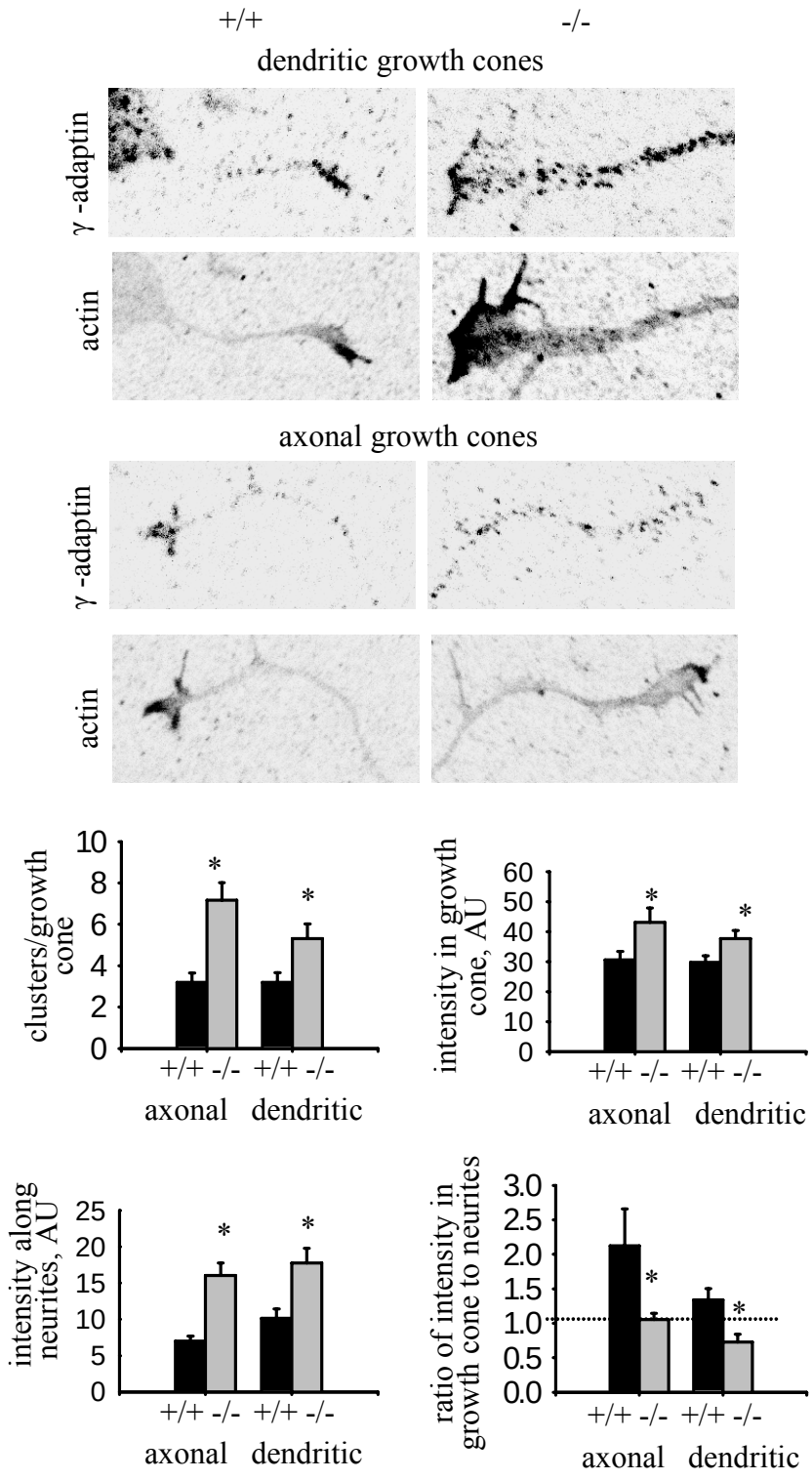

Figure 6. The numbers of TGN-derived organelles are increased but their predominant accumulation in growth cones is impaired in NCAM-/- neurons.

Hippocampal neurons maintained in culture for 24 h were labeled with the antibodies against a TGN marker protein γ-adaptin and co-labeled with the antibodies against actin to visualize growth cones. In these immature neurons, thin long neurites of a uniform diameter were identified as putative axons, while short tapering neurites were identified as dendrites. Representative examples of the axonal and dendritic growth cones are shown.

Immunofluorescence signals are shown as gray scale inverted images to better visualize the distribution of the TGN-derived organelles observed as accumulations of γ-adaptin. Note increased numbers of γ-adaptin positive organelles in NCAM-/- neurites. Note also that the predominant accumulation of γ-adaptin positive organelles in growth cones is impaired in NCAM-/- neurons. Graphs show quantitation of the immunofluorescence images (mean ± SEM, from n=100 neurons) from a representative experiment. The experiment was performed three times with the same effect. Mean numbers of γ-adaptin positive organelles per growth cone, mean intensity of γ-adaptin immunofluorescence along neurites and in growth cones and the ratio of the γ-adaptin immunofluorescence intensity in growth cones to γ-adaptin immunofluorescence intensity in neurites are shown. Note that in NCAM+/+ neurites, the ratio of the γ-adaptin immunofluorescence intensity in growth cones to γ-adaptin immunofluorescence intensity in neurites is more than 1, indicating the predominant accumulation of TGN-derived organelles in growth cones versus neurites. In contrast, this ratio is below 1 in NCAM-/- neurites. * $P<0.05$ (t-test). Experiments with primary cultures of hippocampal neurons were performed in cooperation with Dr. Iryna Leshchyns'ka and Dr. Vladimir Sytnyk in the institute of Prof. Melitta Schachner.

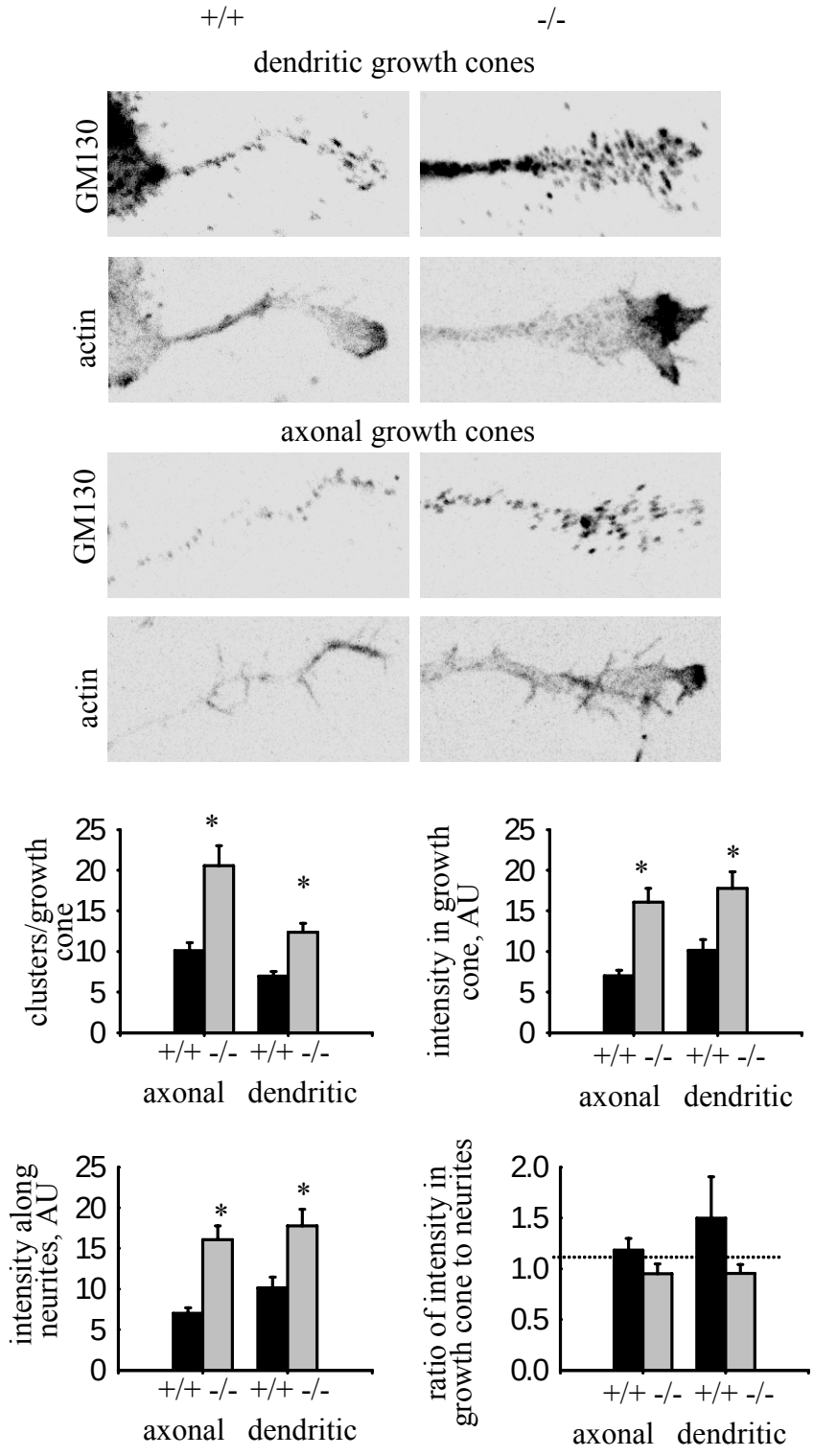

Figure 7. The numbers of Golgi-derived organelles are increased but their predominant accumulation in growth cones is impaired in NCAM-/- neurons.

Hippocampal neurons maintained in culture for 24 h were labeled with the antibodies against a Golgi marker protein GM130 and co-labeled with the antibodies against actin to visualize growth cones. In these immature neurons, thin long neurites of a uniform diameter were identified as putative axons, while short tapering neurites were identified as dendrites. Representative examples of the axonal and dendritic growth cones are shown.

Immunofluorescence signals are shown as gray scale inverted images to better visualize the distribution of the Golgi-derived organelles observed as accumulations of GM130. Note increased numbers of GM130 positive organelles in NCAM-/- neurites. Note also that the predominant accumulation of GM130 positive organelles in growth cones is impaired in NCAM-/- neurons. Graphs show quantitation of the immunofluorescence images (mean ± SEM, from n=100 neurons) from a representative experiment. The experiment was performed three times with the same effect. Mean numbers of GM130 positive organelles per growth cone, mean intensity of GM130 immunofluorescence along neurites and in growth cones and the ratio of the GM130 immunofluorescence intensity in growth cones to GM130 immunofluorescence intensity in neurites are shown. Note that in NCAM+/+ neurites, the ratio of the GM130 immunofluorescence intensity in growth cones to GM130 immunofluorescence intensity in neurites is more than 1, indicating the predominant accumulation of TGN-derived organelles in growth cones versus neurites. In contrast, this ratio is below 1 in NCAM-/- neurites.
* P<0.05 (t-test). Experiments with primary cultures of hippocampal neurons were performed in cooperation with Dr. Iryna Leshchyns'ka and Dr. Vladimir Sytnyk in the institute of Prof. Melitta Schachner.

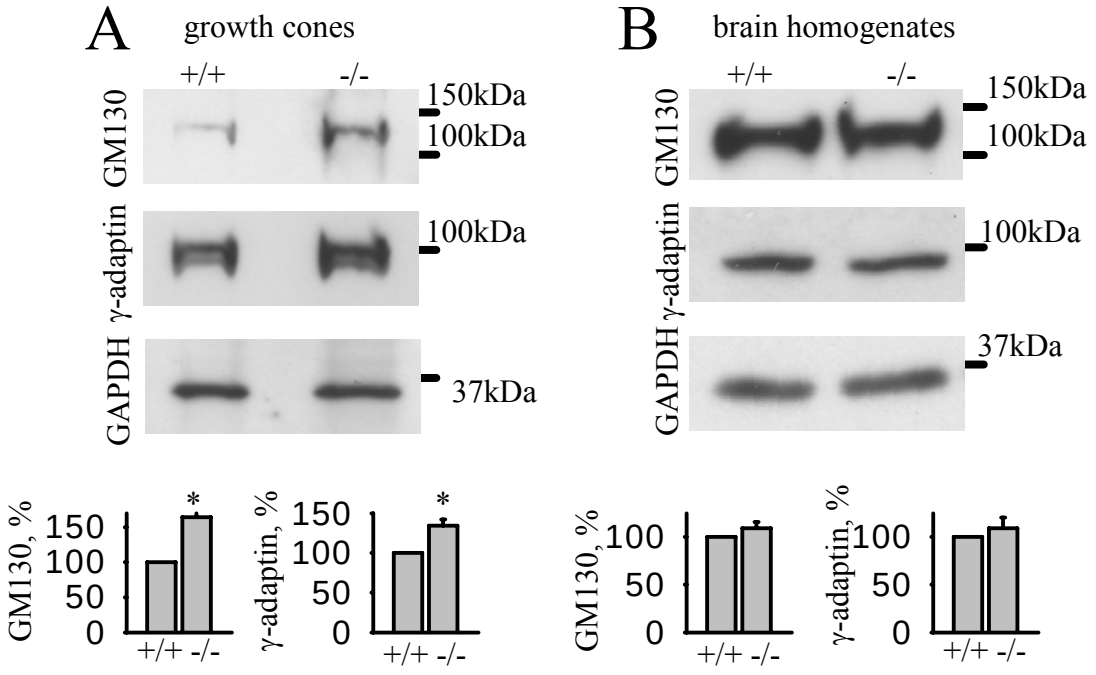

Figure 8. The levels of GM130 and γ-adaptin in growth cones and homogenates isolated from NCAM+/+ and NCAM-/- mouse brains.

Growth cones (A) isolated from NCAM+/+ and NCAM-/- brains, and NCAM+/+ and NCAM-/- brain homogenates (B) were probed by Western blot with the antibodies against GM130 and γ-adaptin. Labeling for GAPDH served as a loading control. Note that while levels of GM130 and γ-adaptin are similar in NCAM+/+ and NCAM-/- brain homogenates, the levels of these two proteins are increased in NCAM-/- versus NCAM+/+ growth cones. Graphs show optical density (mean ± SEM) of the blots from n=4 experiments with the signal intensity in NCAM+/+ probes set to 100%. * P<0.05 (t-test).

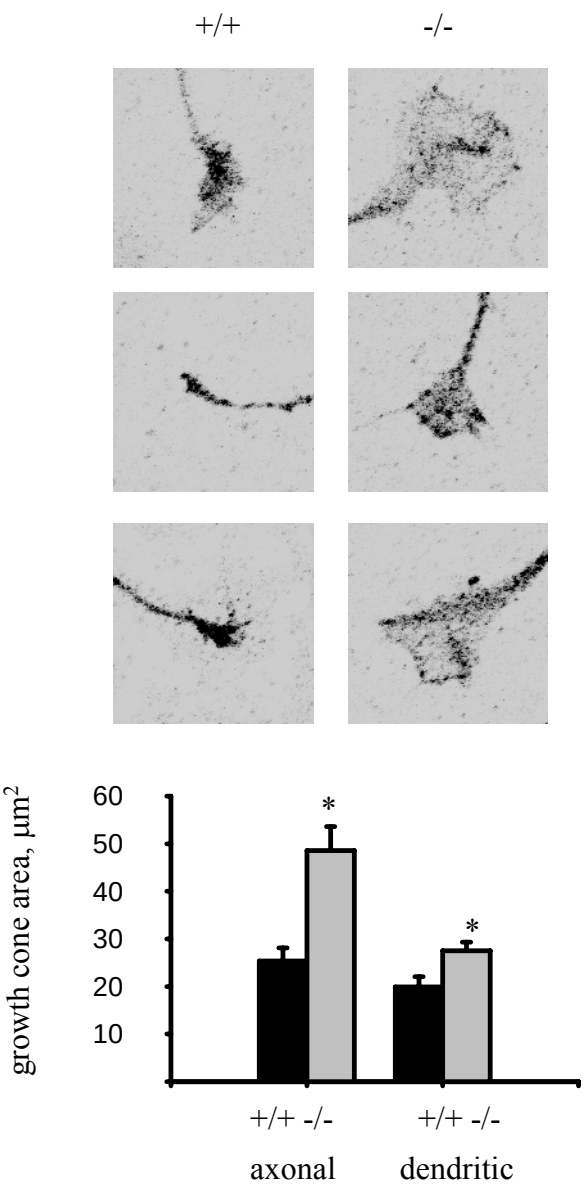

Figure 9. Growth cone area is increased in NCAM-/- neurons.

Pictures show representative examples of axonal growth cones in NCAM+/+ and NCAM-/-. Diagram shows the area (mean ± SEM, n=300) of growth cones in NCAM+/+ and NCAM-/- neurons. * $P<0.05$ (t-test). Both axonal and dendritic growth cones are enlarged in NCAM-/- neurons. Experiments with primary cultures of hippocampal neurons were performed in cooperation with Dr. Iryna Leshchyns'ka and Dr. Vladimir Sytnyk in the institute of Prof. Melitta Schachner.

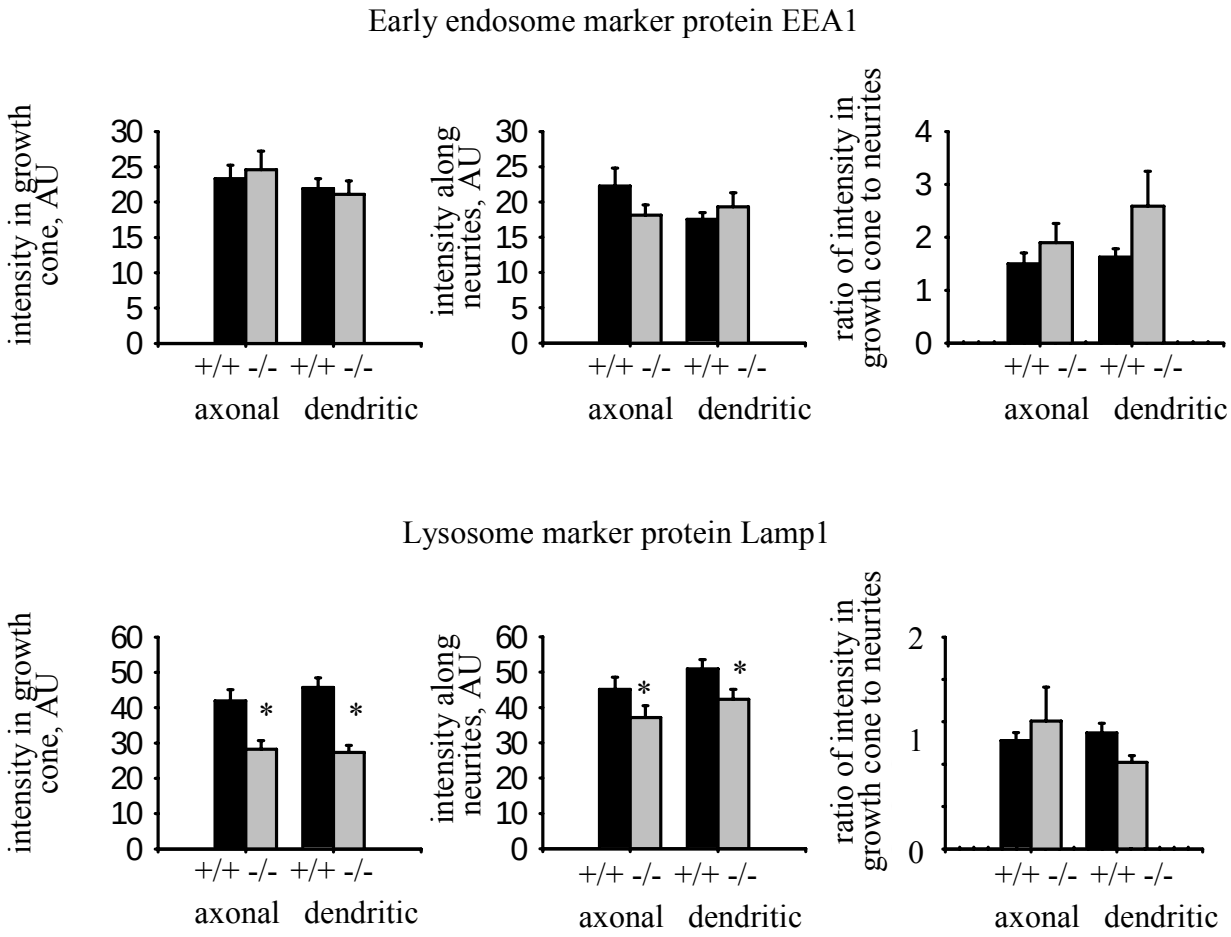

Figure 10. The distribution of the early endosomes and lysosomes between neurites and growth cones is not changed in NCAM-/- neurons.

Hippocampal neurons maintained in culture for 24 h were labeled with the antibodies against an early endosome marker protein EEA1 and lysosome marker protein Lamp1. Graphs show quantitation of the immunofluorescence images (mean ± SEM) from n=100 neurons from a representative experiment. Experiments were performed two times with the same effect. Mean intensity of EEA1 and Lamp1 along neurites and in growth cones and the ratio of the EEA1 and Lamp1 immunofluorescence intensity in growth cones to EEA1 and Lamp1 immunofluorescence intensity in neurites are shown. Note that in NCAM-/- neurons, the levels of Lamp1 immunoreactivity along neurites and in growth cones are reduced. * $P<0.05$ (t-test). Experiments with primary cultures of hippocampal neurons were performed in cooperation with Dr. Iryna Leshchyns'ka and Dr. Vladimir Sytnyk in the institute of Prof. Melitta Schachner.

5.2. Recruitment of the TGN-derived organelles to growth cone periphery is impaired in NCAM deficient neurons

The peripheral part of the growth cone is considered as a predominant site of the exocytosis of the intracellular carriers, such as TGN-derived organelles, delivering lipids and proteins to the surface of the growing neurite (Shea and Sapirstein, 1988; Dequidt et al., 2007). We analyzed the behavior of the TGN-derived organelles in growth cones by labeling these organelles in living neurons with the fluorescently labeled ceramide (Lipsky and Pagano, 1985; Pagano et al., 1991). Time lapse recordings of the growth cones of the labeled neurons showed, that organelles, observed as bright accumulations of the fluorescent ceramide, were intermittently moving within the growth cones towards the leading edge and back both in NCAM+/+ and NCAM-/- neurons occasionally entering the peripheral zone defined as the area between the midline and the leading edge of the growth cone (Figure 11). However, the relative presence of the organelles within the peripheral zone, quantified as the ratio of the ceramide fluorescence intensity within the peripheral zone to the ceramide fluorescence intensity in the central zone of the growth cone and measured over the time of time lapse recordings for each growth cone, was reduced by approximately 40% in NCAM-/- versus NCAM+/+ growth cones (Figure 12) suggesting that tethering of the TGN-derived organelles to the sites of their exocytosis at the periphery of the growth cones was reduced in NCAM-/- neurons.

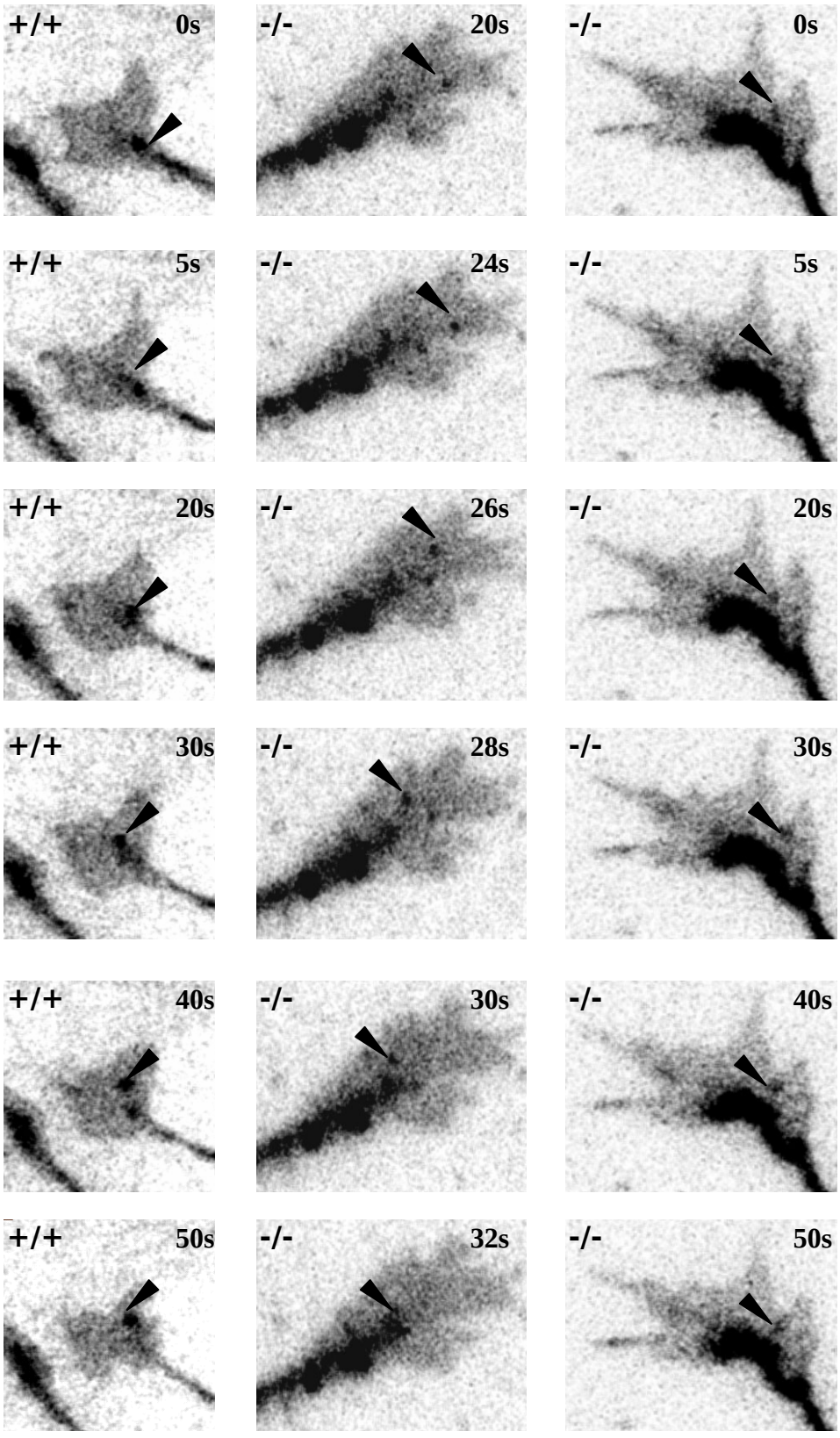

Figure 11. TGN-derived organelles are mobile in NCAM+/+ and NCAM-/- growth cones.

Time-lapse video recording of the movements of ceramide labeled TGN-derived organelles in growth cones of a hippocampal neurons maintained for 24 h in culture. Neurons were stained with BODIPY FL labeled ceramide applied to live cultures. Immunofluorescence signals are shown as gray scale inverted images to better visualize

the distribution of organelles and to accentuate the differences between genotypes. The movement of individual organelles in growth cones from NCAM+/+ and NCAM-/- neurons is depicted by arrows.

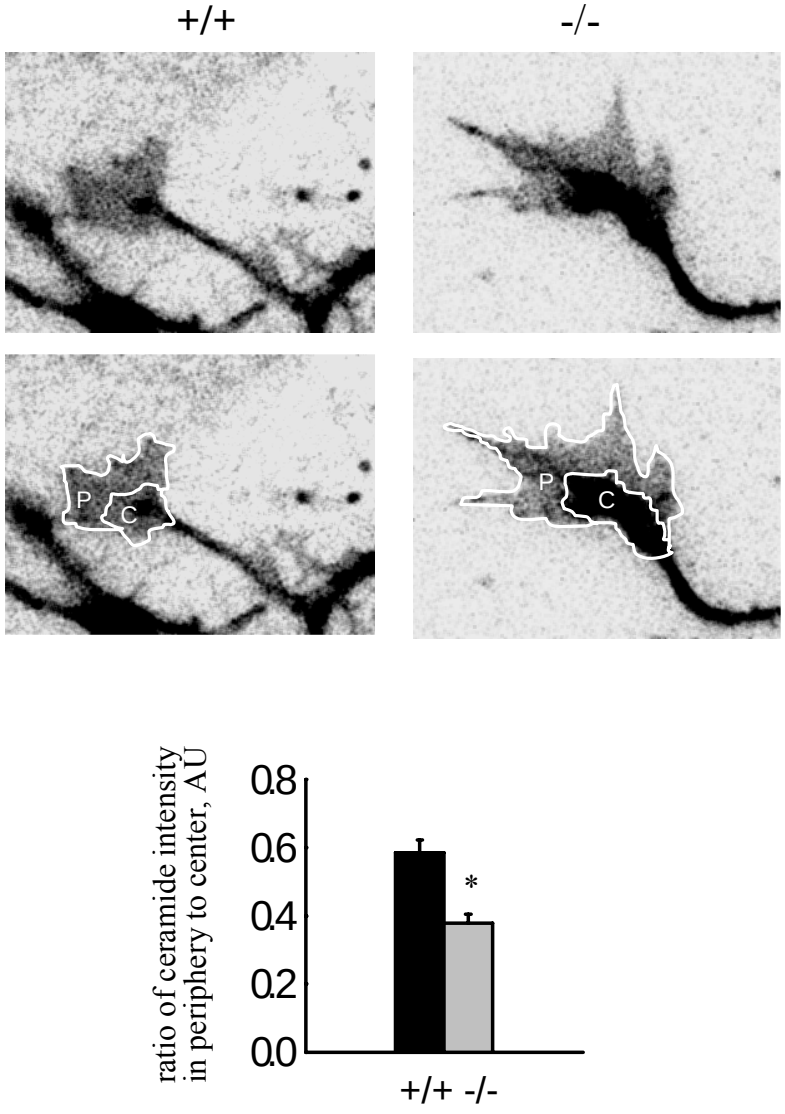

Figure 12. Localization of TGN-derived organelles in the peripheral zone of growth cones is redused in NCAM-/- neurones.

Live one day old neurons from NCAM+/+ and NCAM-/- mice were stained with BODIPY FL labeled ceramide. Examples of NCAM+/+ and NCAM-/- neurites are shown. Immunofluorescence signals are shown as gray scale inverted images to better visualize the distribution of organelles and to accentuate the differences between genotypes. Growth cones were divided in to peripheral (P) and central (C) zones. Diagram shows ratio of the ceramide fluorescence intensity at the peripheral zone to the ceramide fluorescence intensity at the central zone (mean ± SEM, n=24), which is decreased in NCAM-/- versus wild type neurites. * $P<0.05$ (t-test). Experiments with primary cultures of hippocampal neurons were performed in cooperation with Dr. Iryna Leshchyns'ka and Dr. Vladimir Sytnyk in the institute of Prof. Melitta Schachner.

5.3. NCAM interacts with the subunits of the exocyst complex

Exocyst complex plays a pivotal role in the polarized insertion of organelles in growing neurites by tethering organelles to the sites of the exocytosis (Hsu et al., 2004; Vega and Hsu, 2001). In cultured hippocampal neurons, NCAM at the cell surface of growth cones partially co-localized with the exocyst subunits Exo70 and Sec8 with the most prominent overlap in distribution of these proteins observed at the central zone of the growth cones and in filopodia (Figure 13), suggesting that NCAM may play a role in the regulation of the exocyst function. In agreement with this idea, Exo70 and Sec8 co-immunoprecipitated with NCAM from brain lysates (Figure 14) with approximately 27% of all Exo70 molecules and approximately 23% of all Sec8 molecules in brain homogenates being in complex with NCAM. Interestingly, the co-immunoprecipitation of Exo70 and Sec8 with NCAM was reduced by approximately 50% in the presence of 2 mM Ca2+ chelator EDTA (Figure 14). Hence, our observations suggest that NCAM associates with the exocyst complex in the brain in a Ca2+ dependent manner.

Co-immunoprecipitation experiments do not exclude a possibility of the interaction between proteins via intermediate binding partners. To analyze whether NCAM can directly bind to the exocyst complex subunits recombinant proteins Exo70, intracellular domains of NCAM140 and NCAM180 were produced in the bacterial expression system (Figure 15). Recombinant extracellular domain of NCAM fused to the human Fc (NCAM-Fc) was provided by Bodrikov V. (ZMNH, Hamburg, Germany). Recombinant Exo70 was immobilized on plastic surface and assayed for its ability to bind increasing concentrations of the recombinant intracellular domains of NCAM140 or NCAM180. NCAM140-ID but not NCAM180-ID bound to Exo70 in a concentration dependent manner (Figure 16). NCAM-Fc was used as a control and it did not bind to the Exo70 (Figure 16). Interestingly, addition of Ca2+ did not increase the direct interaction between NCAM140-ID and Exo70 (not shown), suggesting that the interaction between NCAM140 and Exo70 is further potentiated in the brain tissue in a Ca2+ dependent manner by yet unknown binding partners of these two proteins.

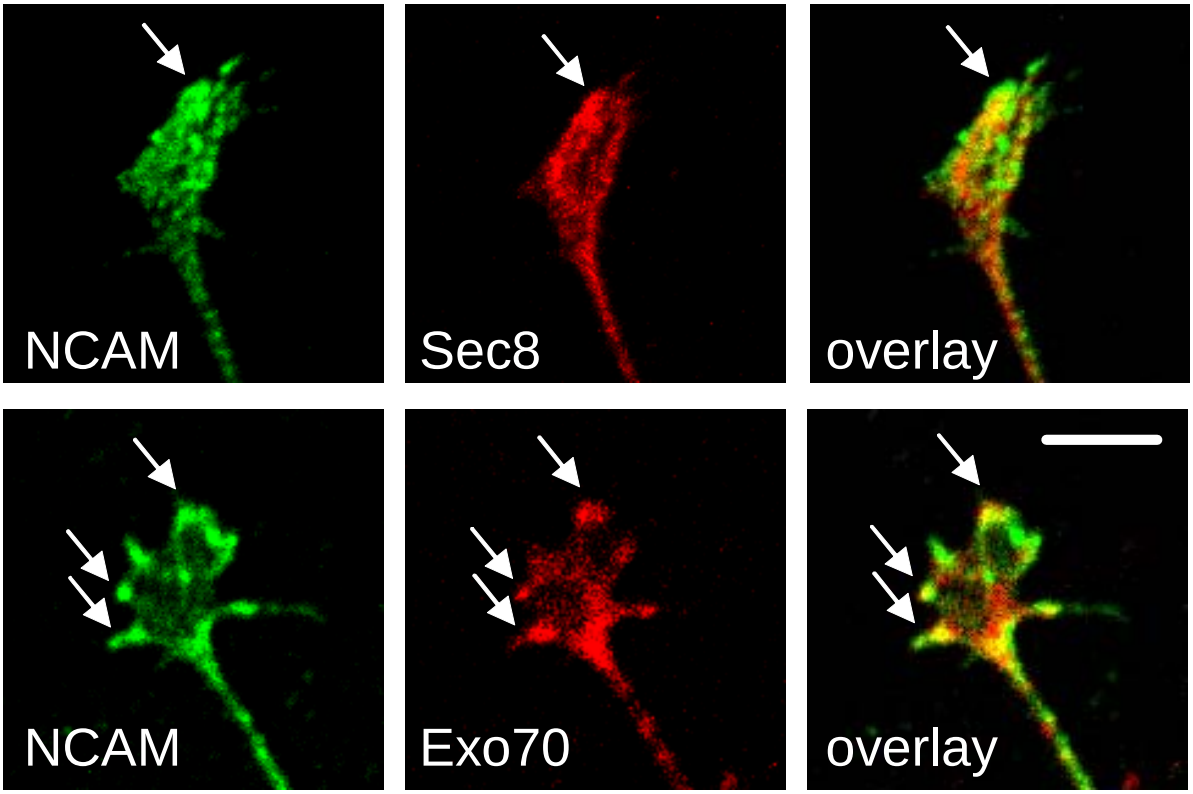

Figure 13. NCAM co-localizes with the exocyst complex components Exo70 and Sec8.

Double immunostaining of hippocampal neurons from wild type mice with antibodies against NCAM (green) and Exo70 or Sec8 (red) is shown. Yellow staining indicates co-localization of NCAM and Exo70/Sec8. The exocyst complex partially co-localized with NCAM at the base of the growth cones and at the filopodia tips (arrows). Experiments with primary cultures of hippocampal neurons were performed in cooperation with Dr. Iryna Leshchyns'ka and Dr. Vladimir Sytnyk in the institute of Prof. Melitta Schachner.

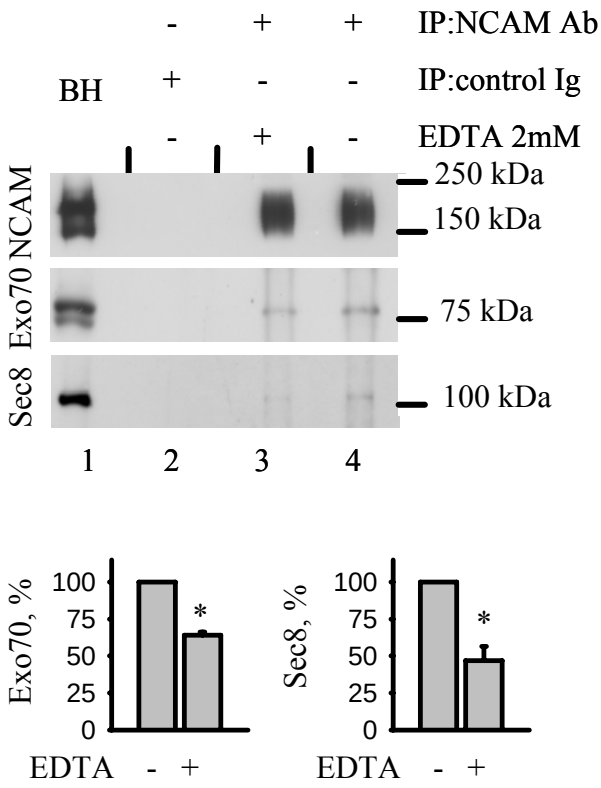

Figure 14. The exocyst complex associates with NCAM in Ca2+ dependent manner.

NCAM was immunoprecipitated from NCAM+/+ brain lysates either in the presence (lane 3) or absence (lane 4) of 2 mM EDTA. NCAM immunoprecipitates (lane 3, 4) and 10% of the brain homogenate input (BH, lane 1) were probed by Western blot with the antibodies against NCAM, Exo70 and Sec8. Mock immunoprecipitation with non-specific immunoglobulins (lane 2) served as control. Note, that Exo70 and Sec8 co-immunoprecipitated with NCAM, and that the co-immunoprecipitation efficiency was reduced in the presence of EDTA. Graphs show mean optical densities ± SEM of the blots from n=3 experiments with the signals for the EDTA non-treated group set to 100%. * P<0.05 (t-test).

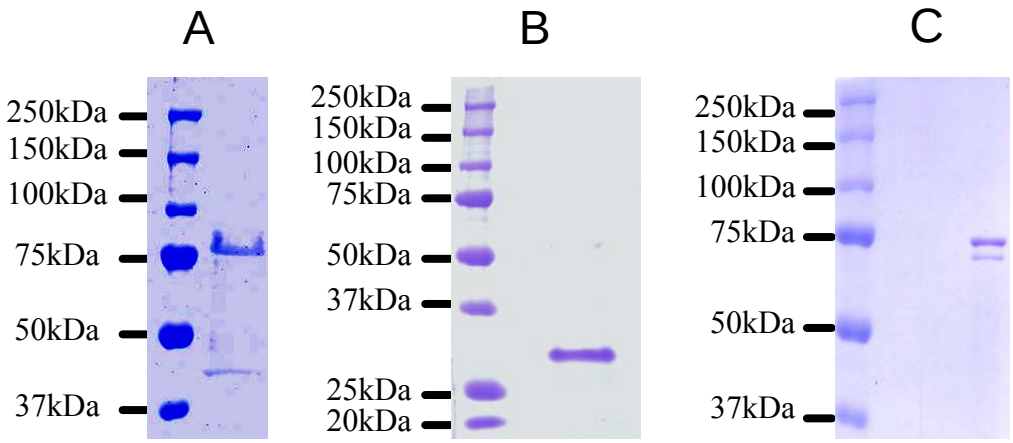

Figure 15. Purified recombinant proteins NCAM180-ID, NCAM140-ID and Exo70. Purified recombinant proteins were subjected to SDS-PAGE and visualized by Coomassie staining as a predominant bands of predicted molecular weight: (A)- NCAM180-ID, (B)- NCAM140-ID, (C)- Exo70.

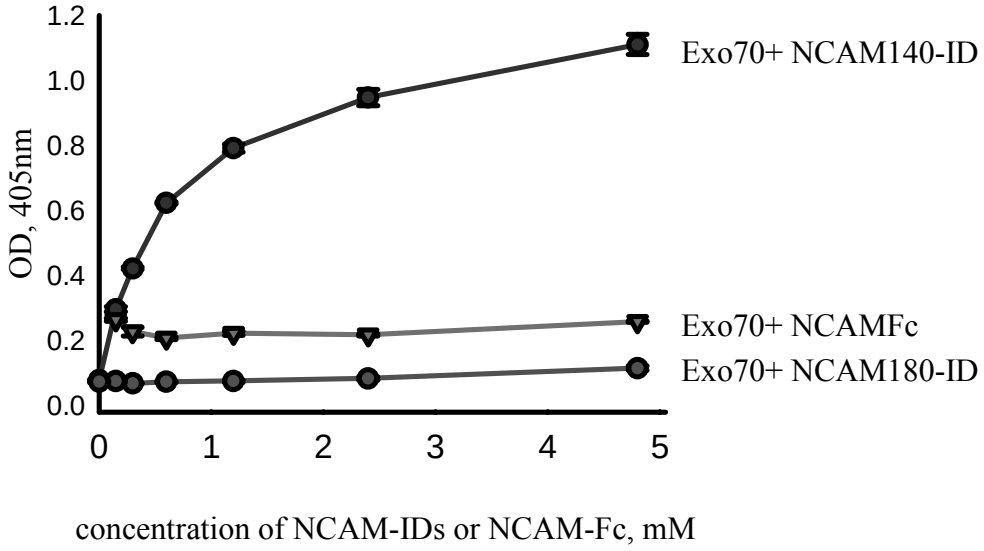

Figure 16. Intracellular domain of NCAM140 directly interacts with Exo70 subunit of the exocyst complex. Immobilized Exo70 (100 μg/ml) was incubated with NCAM140-ID, NCAM140-ID or with NCAM Fc (4800nM – 150 nM). Detection of bound proteins was carried out using the anti-NCAM antibody. Mean values of the optical density ± SEM (n=3) from a representative experiment are shown. The experiment was repeated 3 times with the same effect. Note that NCAM140-ID, but not NCAM180-ID or NCAM-Fc bound to Exo70 in a concentration dependent manner.

5.4. NCAM recruits the exocyst complex to growth cone membranes

Since NCAM binds to the exocyst complex and co-localizes with it in growth cones, we analyzed whether NCAM plays a role in the recruitment of the exocyst to the growth cones. Western blot analysis showed that the levels of Exo70 and Sec8 subunits of the exocyst complex were reduced by approximately 30% in growth cones isolated from NCAM-/- brains (Figure 17). This reduction was not due to overall decreased levels of the exocyst complex subunits in NCAM-/- brains. On the contrary, levels of Exo70 and Sec8 were increased by approximately 30% in NCAM-/- versus NCAM+/+ brain homogenates (Figure 17), also suggesting a compensatory reaction to the abnormal functioning of the exocyst complex in NCAM-/- mice. A similar result was obtained when Exo70 and Sec8 levels were analyzed by immunofluorescence labeling with respective antibodies in cultured hippocampal neurons: the levels of these two proteins measured in graphically outlined growth cones were reduced in

NCAM-/- versus NCAM+/+ neurons with the ratio of Exo70 and Sec8 immunofluorescence intensity in growth cones to the Exo70 and Sec8 immunofluorescence intensity in neurites being approximately two fold lower in NCAM-/- versus NCAM+/+ neurons (Figure 18).

As a surface plasma membrane associated protein, NCAM may influence levels of the exocyst complex in growth cones by recruiting the exocyst subunits to the surface plasma membrane. In agreement with this idea, Western blot analysis of the plasma membranes isolated from NCAM+/+ and NCAM-/- growth cones showed that the levels of Exo70 and Sec8 associated with the growth cone plasma membranes were significantly lower in NCAM-/- versus NCAM+/+ brains (Figure 19). To verify directly the role for NCAM in the recruitment of the exocyst complex subunits to the plasma membranes, plasma membranes isolated from NCAM+/+ and NCAM-/- growth cones were incubated with the soluble protein fraction (cytosol) from NCAM+/+ brains as a source of the endogenous exocyst complex subunits. The recruitment of Exo70 and Sec8 from the cytosol to the membranes was then analyzed by Western blot. This analysis showed that the levels of Exo70 and Sec8 that attached to NCAM+/+ growth cone membranes were approximately two fold higher than the levels of these proteins recruited to NCAM-/- membranes (Figure 19). A similar effect was also observed when before the recruitment assay the isolated growth cone plasma membranes were treated with 0.1M Na_2CO_3 to strip all peripheral proteins (Figure 19). Thus we conclude that NCAM promotes the recruitment of the exocyst complex subunits to the growth cone plasma membranes.

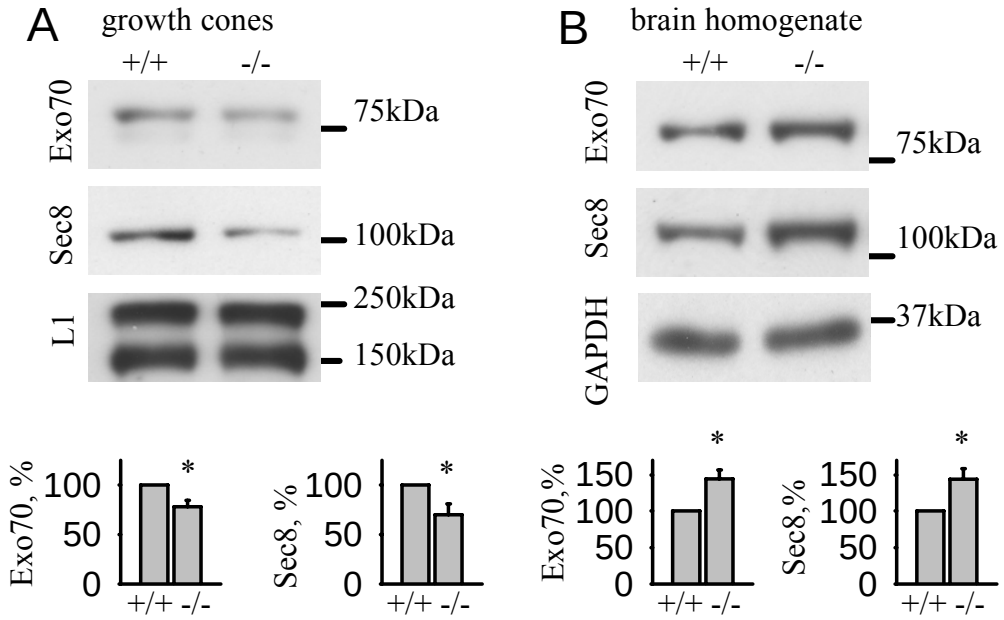

Figure 17. The expression levels of Exo70 and Sec8 are increased in NCAM-/- brain homogenates, whereas the levels of these proteins are reduced in NCAM-/- growth cones.

(A) Growth cones biochemically isolated from NCAM+/+ and NCAM-/- mice were probed by Western blot with antibodies against Exo70, Sec8 and L1. Graphs show optical density (mean ± SEM) of the blots from n=6 experiments with the signal intensity in NCAM+/+ probes set to 100%. * $P<0.05$ (t-test). Levels of Exo70 and Sec8 are reduced, whereas levels of L1 are not changed, in NCAM-/- growth cones.

(B) Brain homogenates from NCAM+/+ and NCAM-/- mice were probed by Western blot with antibodies against Exo70, Sec8 and GAPDH. Graphs show optical density (mean ± SEM) of the blots from n=6 experiments with the signal intensity in NCAM+/+ probes set to 100%. * $P<0.05$ (t-test). Levels of Exo70 and Sec8 are increased, whereas levels of GAPDH are not changed in wild-type versus NCAM-/- brain homogenates.

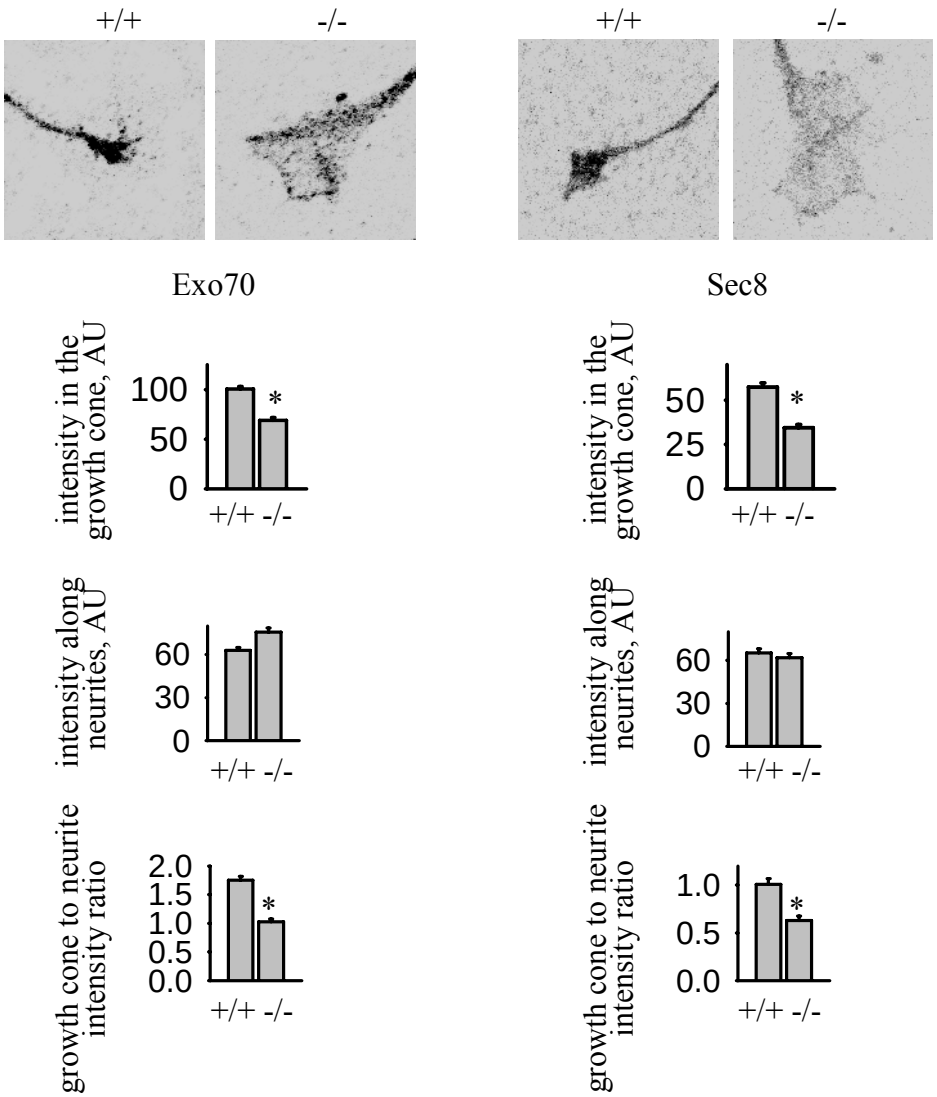

Figure 18. Exocyst complex accumulation is reduced in growth cones of NCAM-/- cultured hippocampal neurons.

Hippocampal neurons maintained in culture for 24 h were labeled with the antibodies against Exo70 and Sec8. Representative examples of axonal growth cones are shown. Immunofluorescence signals are shown as gray scale inverted images to better visualize the distribution of the exocyst complex subunits and to accentuate the differences between genotypes. Note reduced levels of Exo70 and Sec8 in NCAM-/- growth cones. Graphs show quantitation of the immunofluorescence images (mean ± SEM) from n=100 neurons of neurons from a representative experiment. The experiment was repeated three times with the same effect. Similar results were received for axonal and dendritic growth cones and all growth cones were pooled together. Mean intensity of Exo70 and Sec8 immunofluorescence along neurites and in growth cones and the ratio of the Exo70 and Sec8 immunofluorescence intensity in growth cones to Exo70 and Sec8 immunofluorescence intensity in neurites are shown. * $P<0.05$ (t-test).

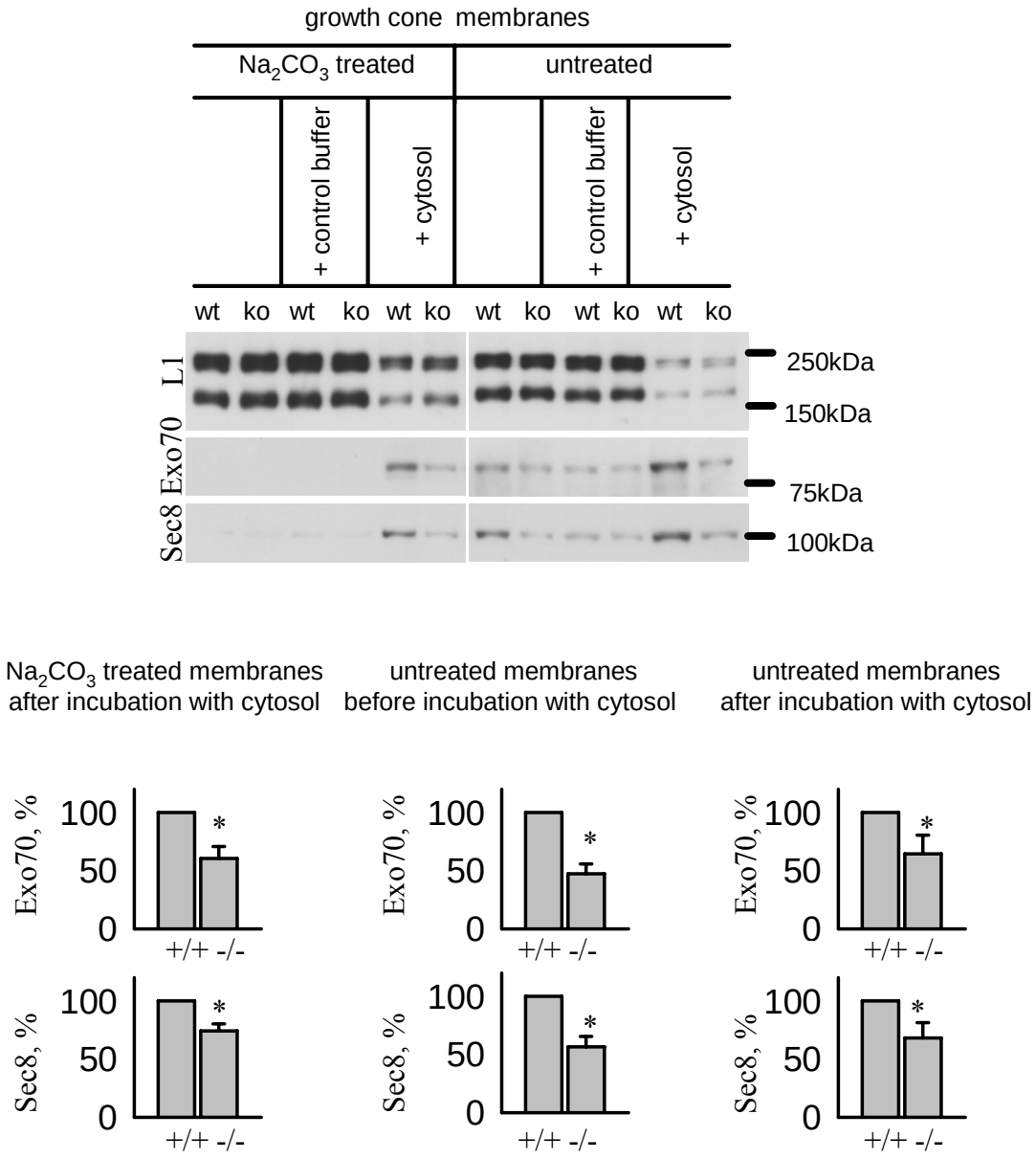

Figure 19. Exocyst complex recruitment to the growth cone membranes is reduced in NCAM-/- growth cones.

Growth cone plasma membranes from NCAM+/+ and NCAM-/- brains were incubated with the soluble fraction from NCAM+/+ brain homogenates (the cytosol that served as a source of soluble proteins). Before and after incubation the amounts of Exo70 and Sec8 bound to the membranes were estimated by Western blot. Recruitment of Exo70 and Sec8 to untreated membranes and membranes treated with 0.1M Na_2CO_3 to release peripheral proteins was analyzed. Labeling with L1 antibodies shows that similar amounts of growth cone plasma membranes were used in NCAM+/+ and NCAM-/- groups

Mean optical densities ± SEM in NCAM-/- probes normalized to NCAM+/+ levels (set to 100%) are shown. Graph shows quantitation of the blots from n=3 experiments. * $P<0.05$ (t-test). Note, that the levels of Exo70 and Sec8 co-isolated with the growth cone membranes are reduced in NCAM-/- growth cones (untreated membranes

before incubation with cytosol). Exo70 and Sec8 recruitment to NCAM-/- growth cone membranes is reduced both in untreated and Na_2CO_3 treated groups.

5.5. The exocyst complex assembly is not affected in NCAM deficient brains

Next, we analyzed whether NCAM has any role in the exocyst complex assembly by estimating the efficiency of the co-immunoprecipitation of the exocyst complex subunits with each other. Sec8 co-immunoprecipitated with Exo70 and Exo70 co-immunoprecipitated with Sec8 with a similar efficiency from NCAM+/+ and NCAM-/- brain lysates (Figure 20). Although we cannot exclude that the interactions between other subunits of the exocyst complex are affected by NCAM deficiency, these data suggest that the assembly of the exocyst complex is not affected in NCAM-/- brains.

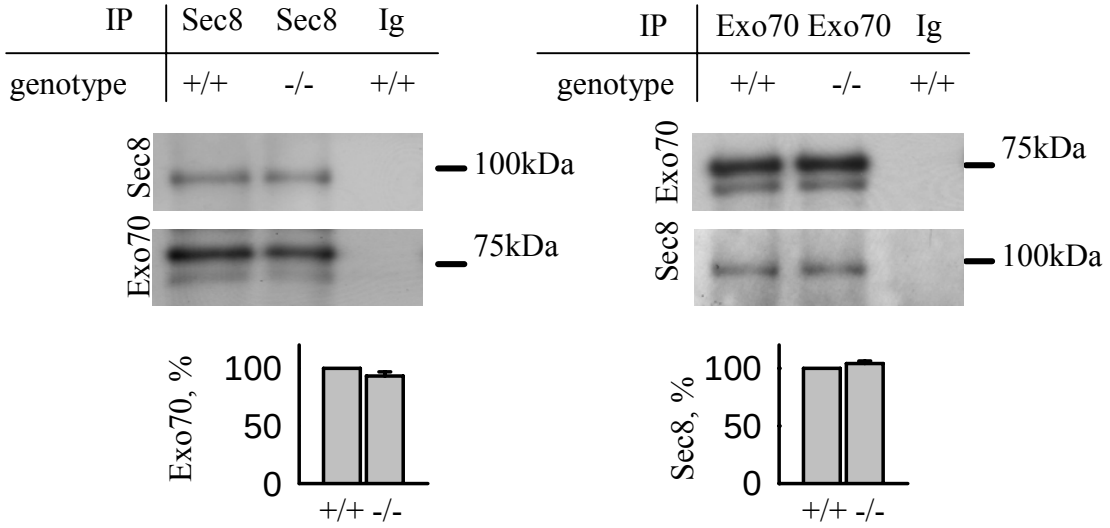

Figure 20. NCAM deficiency does not affect assembly of the exocyst complex.

Exo70 and Sec8 immunoprecipitates (IP) from NCAM+/+ and NCAM-/- brain lysates were probed by Western blot with the antibodies against Exo70 and Sec8. Note, that similar levels of Sec8 co-immunoprecipitate with Exo70, and similar levels of Exo70 co-immunoprecipitate with Sec8 from NCAM+/+ and NCAM-/- brain lysates. Mock immunoprecipitation with nonspecific immunoglobulins (IgG) served as control. Graphs show optical densities of the blots (mean values ± SEM from n= 4 experiments).

5.6. NCAM regulates phosphorylation of the exocyst complex

Clustering of NCAM at the neuronal surface induces activation of several intracellular signaling cascades (Schachner and Maness, 2007; Ditlevsen et al., 2008). NCAM deficiency results in a strong downregulation of the activity of the kinases involved in NCAM signaling,

such as Fyn tyrosine kinase (Bodrikov et al., 2005). Hence, we analyzed whether NCAM deficiency affects the phosphorylation of the exocyst complex subunits. Western blot analysis of Sec8 immunoprecipitates with the antibodies against phospho-tyrosine residues showed that Sec8 and at least one another subunit with the molecular weight of approximately 80 kDa were phosphorylated at tyrosine(s). Tyrosine phosphorylation of Sec8 was reduced by approximately 80% in NCAM-/- versus NCAM+/+ brain homogenates (Figure 21) indicating that NCAM regulates tyrosine phosphorylation of this exocyst subunit by activating an unknown kinase. No detectable labeling with the phosphotyrosine antibodies was observed for Exo70 immunoprecipitates from both NCAM+/+ and NCAM-/- brain lysates (Figure 21), suggesting that tyrosine phosphorylation does not play a role in regulation of this exocyst subunit.

Since little is known on how phosphorylation regulates the exocyst function, we analyzed the recruitment of the exocyst complex to the growth cone membranes from the cytosol preincubated with staurosporine, a general inhibitor of kinases. Inhibition of the kinase activity by staurosporine resulted in 40% reduction in Sec8 recruitment to the membranes (Figure 22). This observation indicates that the dephosphorylation of the exocyst complex subunits by phosphatases endogenously present in the cytosol, which was promoted in the presence of staurosporine, inhibited the exocyst complex recruitment to the growth cone plasma membranes. Hence, phosphorylation of the exocyst complex subunits by as yet unknown kinases is required for its efficient recruitment to the membranes. Interestingly, PP2, the inhibitor of the src family kinases and among them Fyn, did not inhibit the recruitment of Exo70 and Sec8 to the membranes (not shown) indicating that these kinases do not regulate exocyst complex recruitment to the membranes.

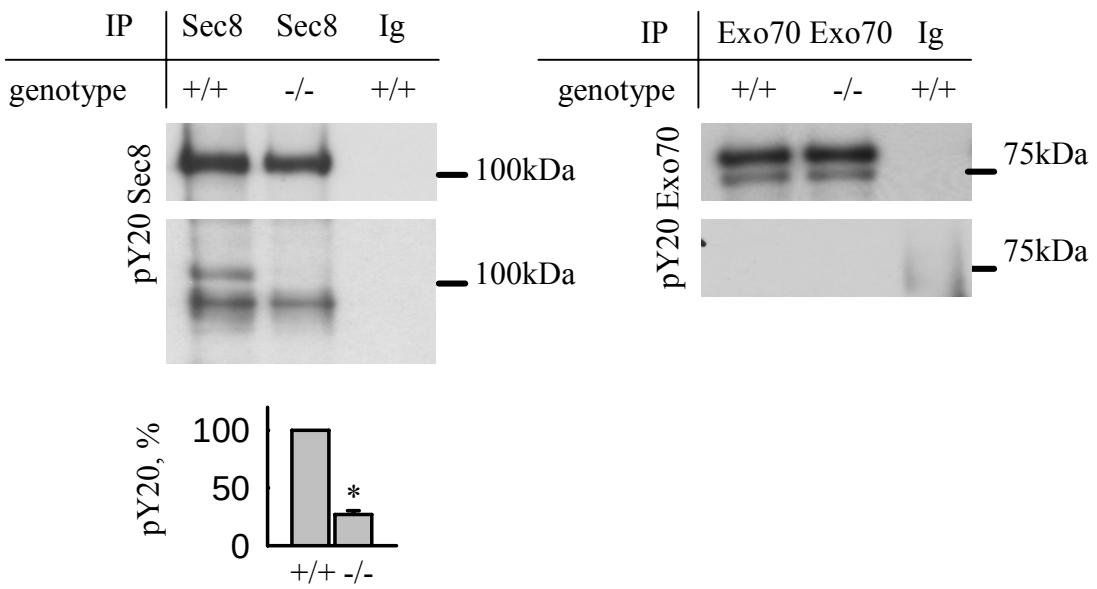

Figure 21. Phosphorylation of the exocyst complex component Sec8 is affected in NCAM-/- brain.

Sec8 and Exo70 immunoprecipitates from NCAM+/+ and NCAM-/- brain lysates were probed by Western blot with the antibodies against Sec8, Exo70 and phosphotyrosine residues (pY20). Mock immunoprecipitation with the nonspecific immunoglobulins (Ig) was performed for control. Note that the tyrosine phosphorylation of Sec8 is reduced in NCAM-/- brains. Note also subunit(s) of the exocyst complex with the molecular weight below 100 kDa that co-immunoprecipitate with Sec8 and are tyrosine phosphorylated. The phosphorylation of these proteins is less dependent on NCAM. No detectable tyrosine phosphorylation of Exo70 is observed. Graph shows mean optical densities of the blots (mean ± SEM from n=3 experiments). * $P<0.05$ (t-test).

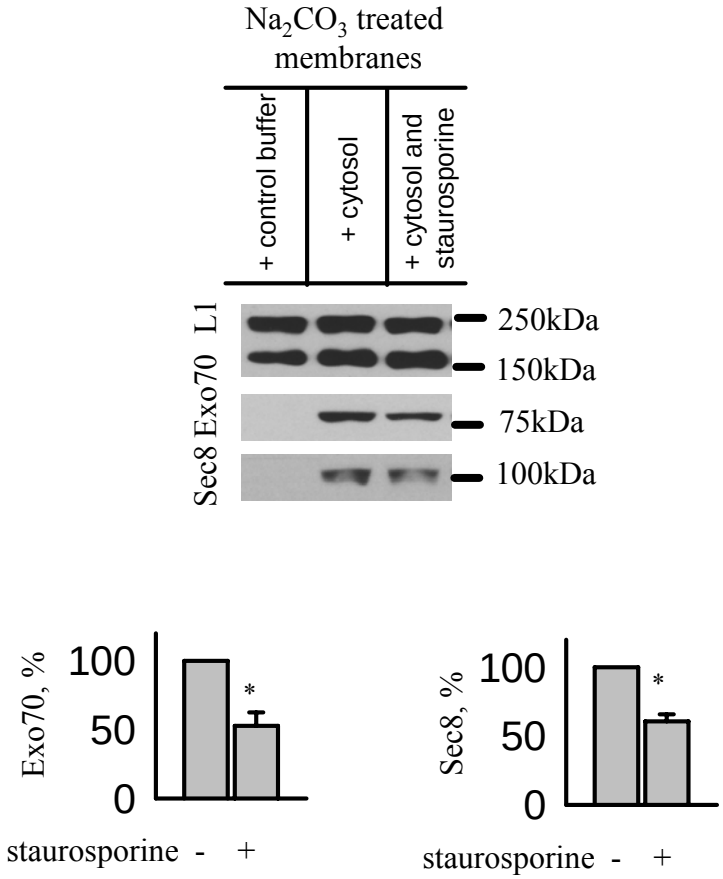

Figure 22. Exocyst complex recruitment to the growth cone membranes is reduced in the presence of kinase inhibitor staurosporine.

Membranes from NCAM+/+ growth cones were treated with alkali (Na_2CO_3) to strip peripheral proteins and incubated with cytosol from NCAM+/+ brains or control buffer used for cytosol preparation. The cytosol was either non-treated or pre-incubated with staurosporine. Recruitment of Exo70 and Sec8 from the cytosol to the membranes was analyzed by Western blot with the antibodies against Exo70 and Sec8. Labeling for L1 served as a loading control. Note, that the recruitment of Exo70 and Sec8 to growth cone membranes from the cytosol pre-incubated with staurosporine is lower then from the non-treated cytosol. Graph shows quantitation of the blots from n=3 experiments. Mean optical densities ± SEM are shown with the signals in non-treated cytosol group set to 100%. * $P<0.05$ (t-test).

5.7. NCAM clustering at the growth cone surface membrane promotes NCAM/exocyst complex formation and vesicle fusion

Clustering of NCAM at the neuronal surface membrane promotes neurite outgrowth (Hinsby et al., 2004) – a process, which is accompanied by an expansion of the surface plasma membrane in growth cones via exocytosis of the intracellular vesicles (Shea and Sapirstein, 1988; Popov et al., 1993). To analyze whether clustering of NCAM influences exocytosis of

the vesicles in the growth cones, growth cones isolated from NCAM+/+ brains were incubated with the polyclonal antibodies against the extracellular domain of NCAM to cluster NCAM at the growth cone surface. In growth cones incubated with NCAM antibodies, the levels of the Exo70 and Sec8, which co-immunoprecipitated with NCAM, were approximately two fold higher than in growth cones treated with non-specific immunoglobulins (Figure 23), showing that clustering of NCAM enhanced its association with the exocyst complex.

Exocytosis of the vesicles in isolated growth cones was analyzed by estimating the changes in the size of the internal membrane pool, representing intracellular membranous organelles. Cholera toxin, which binds exclusively and with a high affinity to the ganglioside GM1, was used to label growth cone surface membranes only, when applied to detergent non-permeabilized growth cones, and to label the total pool of membrane, when applied to detergent permeabilized growth cones. The internal membrane pool was identified as a difference between the total and surface membrane pools, and a reduction in the internal membrane pool was regarded as a measure of the exocytosis of the vesicles contained in the growth cones. Incubation of growth cones with NCAM antibodies resulted in an approximately two fold reduction in the intracellular membrane pool when compared to growth cones treated with the preimmune serum (Figure 24A) indicating that clustering of NCAM results in the exocytosis of the intracellular vesicles. No change in the intracellular membrane pool in response to NCAM antibodies was observed in NCAM-/- growth cones (Figure 24A), indicating the specificity of the effect exerted by NCAM antibodies. NCAM antibody induced exocytosis was blocked in growth cones preincubated with the membrane permeable form of the Ca2+ chelator BAPTA (Figure 24A), indicating that Ca2+ influx is required for NCAM-induced vesicle exocytsosis.

In developing neurons, NCAM induces Ca2+ influx to the cytosol via voltage-dependent Ca2+ channels (VDCC) of the T- and L-type (Schuch et al., 1989; Kiryushko et al., 2006). To analyze whether these channels play a role in Ca2+-dependent NCAM-induced exocytosis in growth cones, exocytosis was analyzed in the presence of the different inhibitors of Ca2+ channels. While NCAM-induced exocytosis was not inhibited by pimozide, a blocker of T-type VDCC, application of nifedipine, a blocker of L-type VDCC, not only blocked NCAM-induced exocytosis but also resulted in a two fold increase in the internal membrane pool when compared to preimmune serum treated growth cones (Figure 24B). A plausible explanation for this phenomenon could be that clustering of NCAM induces not only exocytosis, but also endocytosis. When NCAM-induced exocytosis was inhibited by

nifedipine, NCAM-induced endocytosis resulted in the increase of the intracellular membrane pool. Indeed, recycling of the intracellular organelles in growth cones has been described (Diefenbach et al., 1999). To get further support to this idea, growth cones were treated with dynasore, an inhibitor of dynamin dependent endocytosis (Macia et al., 2006; Nankoe and Sever, 2006). Application of NCAM antibodies to growth cones in the presence of dynasore resulted in an approximately 30% larger decrease in the intracellular membrane pool then when growth cones were treated with NCAM antibodies only (Figure 24C). The only plausible explanation for this phenomenon is that, indeed, NCAM-induced exocytosis is partially counterbalanced by NCAM-induced endocytosis, and inhibition of the latter results in a stronger reduction in the internal membrane pool. Changes in the internal membrane pool in response to application of NCAM antibodies were blocked in growth cones preincubated with nifedipine and dynasore applied together (Figure 24C), indicating that both exo- and endocytosis induced by NCAM clustering were inhibited in the presence of both drugs.

Activation of the fibroblast FGFR with consequent production of the arachidonic acid has been proposed as a mechanism for VDCC activation in response to clustering of NCAM at the neuronal surface (Kiryushko et al., 2006). Interestingly, an FGFR inhibitor, D173074, blocked NCAM-induced exocytosis in growth cones (Figure 24B). Hence, NCAM-induced exocytosis of the intracellular organelles in growth cones occurs in FGFR dependent and L-type VDCC dependent manner.

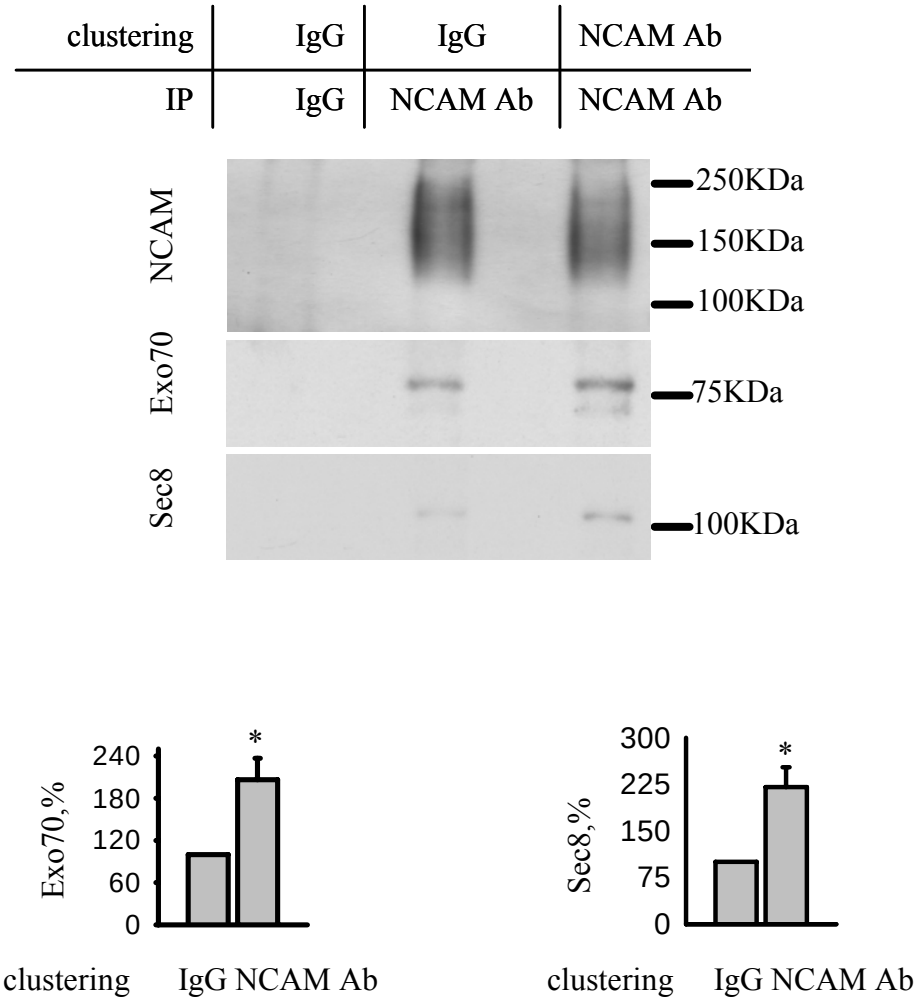

Figure 23. Clustering of NCAM enhances its association with the exocyst complex.

NCAM was clustered at the surface of NCAM+/+ growth cones with the polyclonal antibodies against the extracellular domain of NCAM (NCAM Ab). Control growth cones were treated with nonspecific rabbit immunoglobulins (IgG). NCAM was then immunoprecipitated from the growth cones and immunoprecipitates were analyzed with the antibodies against Exo70 and Sec8. Mock immunoprecipitation with nonspecific immunoglobulins served as control. Note, that co-immunoprecipitation of Exo70 and Sec8 with NCAM was increased following NCAM clustering at the surface of growth cones. Graphs show quantitation of the blots with the signals for IgG treated growth cones set to 100%. Mean values ± SEM from n=3 experiments are shown.

* $P<0.05$ (t-test).

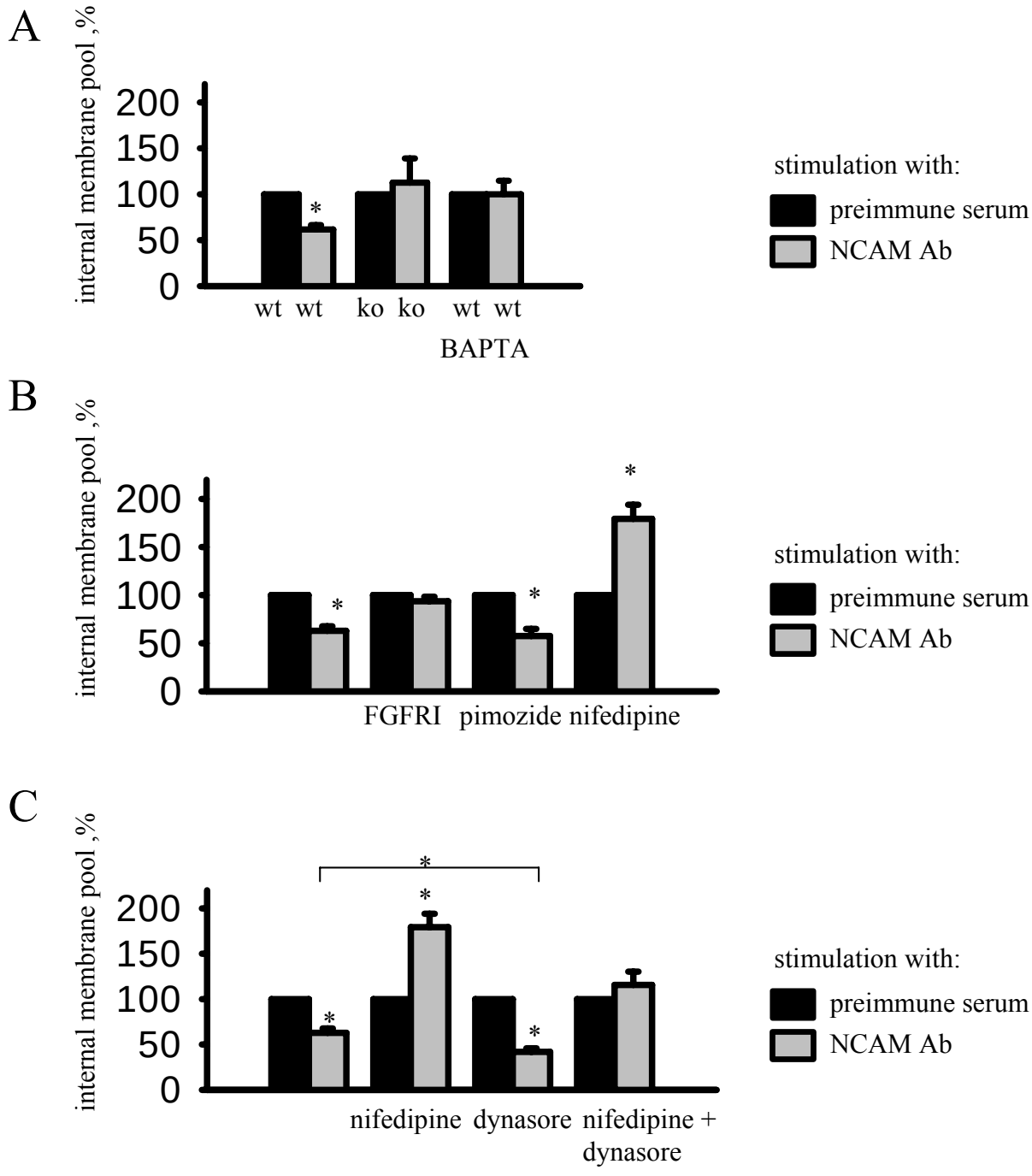

Figure 24. Clustering of NCAM promotes exocytosis of the intracellular organelles in growth cones.

A-C – Internal membrane pool was analyzed in growth cones isolated from brains of wild type mice (if different is not indicated) treated with preimmune serum or polyclonal antibodies against the extracellular domain of NCAM applied in the presence or absence of BAPTA (A), inhibitors of the FGFR and T- and L-type VDCC (pimozide and nifedipine, respectively) (B), and inhibitors of L-type VDCC (nifedipine) and dynamin dependent endocytosis (dynasore) (C). Graphs show the sizes of the internal membrane pools in growth cones treated NCAM antibody and preimmune serum (mean values ± SEM from n=3 experiments) normalized to the levels of the internal membrane pool in preimmune serum treated growth cones set to 100%. * $P<0.05$ (t-test, when compared to control preimmune serum treated growth cones or as indicated by solid line).

6. Discussion

The neural cell adhesion molecule NCAM plays an important role in neuronal development by regulating neurite outgrowth and branching. Until now, changes in cytoskeleton dynamics and gene expression were considered as the major mechanisms by which NCAM influences neuronal development. In our work we expand the repertoire of NCAM functions and show a novel role for NCAM in modulation of the plasma membrane delivery to the cell surface of growing neurites – a critical step in the process of neurite outgrowth.

Exocyst is a protein complex that has been found to be essential for exocytosis underlying neurite outgrowth (Hsu et al., 2004). Several models have been proposed on how the exocyst complex promotes exocytosis, including modulating cytoskeletons and tethering vesicles to the plasma membrane. In any case, targeting of the exocyst complex to spatially defined domains, such as growth cones, is expected to be essential for the exocyst complex function. However, the question of how the localization and function of the exocyst complex is regulated in response to extracellular cues is poorly explored. In this work, we identify the exocyst complex as a novel binding partner of NCAM. NCAM, which accumulates at the surface of growth cones and mediates the interactions between neurons and adjacent cells and the extracellular matrix, is well posed to perform this function. It is interesting in this respect that Exo70, a subunit that links NCAM to other components of the exocyst complex, binds specifically to NCAM140, the most potent outgrowth promoting NCAM isoform in neurons (Niethammer et al., 2002), that further suggests an involvement of the exocyst complex into NCAM mediated neuronal differentiation.

The association between NCAM and the exocyst complex was strongly reduced in the presence of the Ca2+ chelator EDTA. This observation suggests that the NCAM/Exocyst complex formation could be further potentiated in the brain by as yet unidentified protein(s) in a Ca2+ dependent manner. Among the possible candidates that may potentiate the NCAM/Exocyst complex formation are the components of the actin cytoskeleton, which link the exocyst to the Ca2+ signaling complexes (Shin et al., 2000) and which are connected with NCAM via spectrin (Leshchyns'ka et al., 2003). Clustering of NCAM at the cell surface is accompanied with the Ca2+ influx via L- and T-type VDCC (Schuch et al., 1989; Kiryushko et al., 2006). In agreement, clustering of NCAM at the surface of growth cones strongly potentiated the interaction between NCAM and the exocyst complex. Interestingly, the L-type but not T-type VDCCs were required for NCAM dependent exocytosis in growth cones

suggesting that the Ca2+ influx via different Ca2+ channels may have functionally distinct roles.

We found that NCAM deficiency results in the strongly reduced recruitment of the exocyst complex subunits to the growth cone membrane that points at NCAM as a cue that targets the exocyst complex to the sites of exocytosis thereby coupling exocytosis to the changes in the extracellular environment. Our data thus suggest a scenario when clustering of NCAM at the surface of a growth cone induces exocytosis of vesicles at this site thereby expanding the membrane. Interestingly, we found that the exocyst complex and, in particular, Sec8 subunit is phosphorylated at tyrosine(s). Inhibition of the kinase activity strongly reduced the recruitment of the exocyst complex to the plasma membrane indicating that phosphorylation is critical for exocyst complex function.

We concluded that NCAM promotes TGN-derived organelle exocytosis in growth cones by recruiting the exocyst complex to the growth cone plasma membrane. The suggested model for NCAM regulated fusion of TGN-derived organelles with the plasma membrane in growth cones is schematically shown on the figure 25.

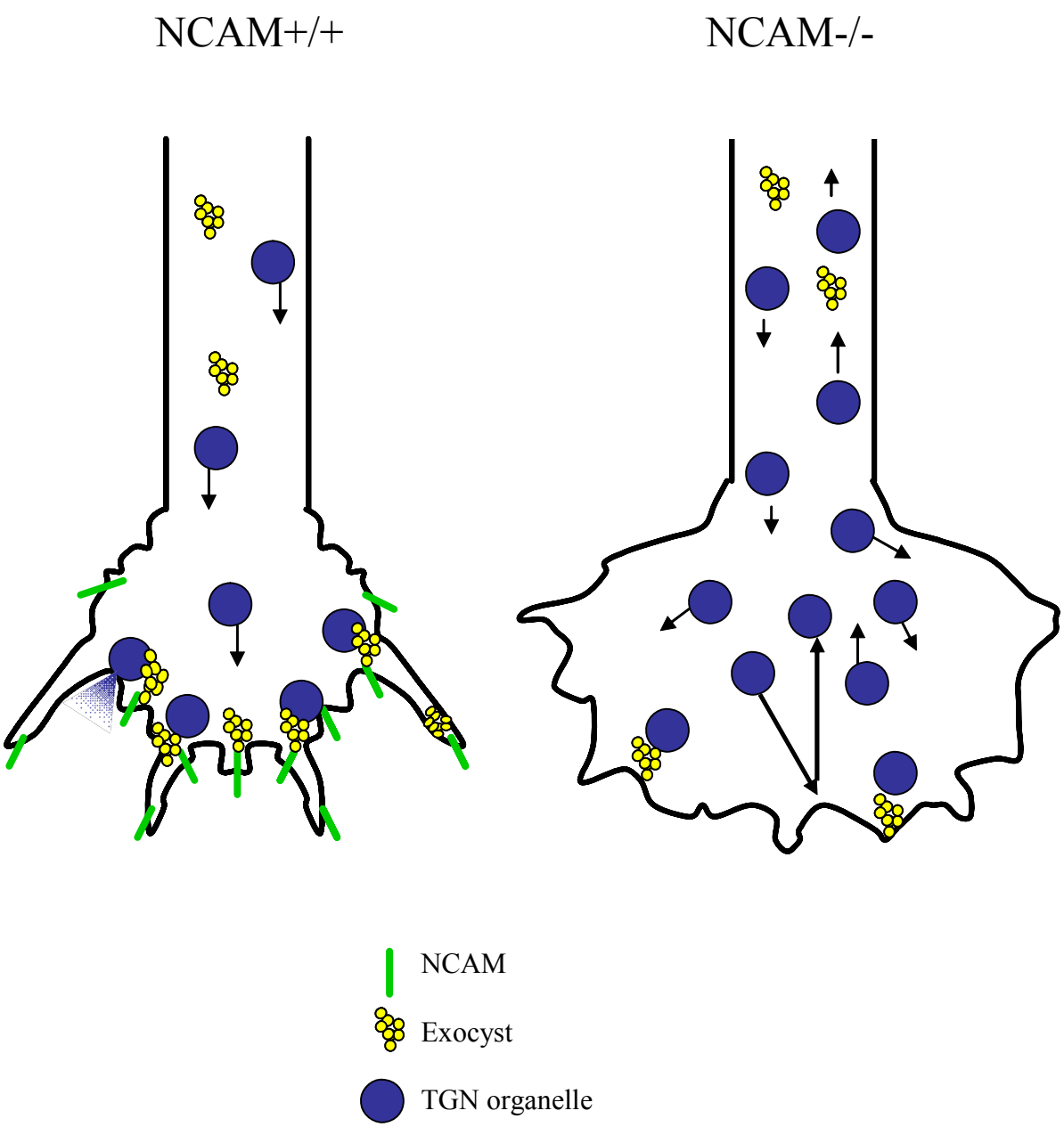

Figure 25. Schematic diagram of NCAM dependent TGN-derived organelle exocytosis in NCAM+/+ and NCAM-/- growth cones.

NCAM targets the exocyst complex to the growth cone plasma membrane. NCAM associated exocyst complex recruits TGN organelles to the growth cone and facilitates their fusion with the plasma membrane. NCAM-/- growth cones contain lower amount of the exocyst complex on the plasma membrane, thus the organelles fusion with the surface plasma membrane is decreased in NCAM-/- growth cones. The organelles which fail to fuse with the plasma membrane accumulate in the growth cone, resulting in growth cone enlargement. Some organelles that could not fuse with the plasma membrane are transported back to the neurite that results in increased organelle density in NCAM-/- neurites when compared to NCAM+/+ neurites. The direction of organelle movement is depicted by arrows.

7. Summary

Neural cell adhesion molecule (NCAM) is involved in a number of morphogenetic events, such as neuronal migration and differentiation, fasciculation and outgrowth of neurites. In NCAM mediated neurite outgrowth, activation of NCAM molecules at the cell surface by homophilic binding results in activation of intracellular signaling pathways leading to enhanced neurite outgrowth. Besides, neurite outgrowth as a biological process requires new material insertion and membrane addition at the neurite growth cones through fusion of the transport vesicles with the plasma membrane. A macromolecular complex that has been suggested to play a role in targeting and fusion of transport vesicles to the plasma membrane is the exocyst complex. Among all tested organs the highest exocyst subunit expression is found in the brain. The exocyst complex concentrates at sites of active fusion and membrane addition. In neuronal cells such sites are growth cones. While it is well established that the exocyst complex plays a role in determining the plasma membrane sites for the fusion of TGN derived vesicles, functioning as a tethering factor to guide the initial interaction of vesicles with specific regions of the plasma membrane, cues that target the exocyst complex to the plasma membrane are not well established.

In present study we characterized a novel function for a neural cell adhesion molecule, NCAM: NCAM regulates exocytosis in the growth cones of neurons by anchoring the exocyst complex to the plasma membrane of the growth cones. We showed that TGN-derived organelles abnormally accumulate in neurites and growth cones of NCAM-/- neurons when compared to NCAM+/+ neurons. A plausible explanation for the increased levels of the TGN-derived organelles in NCAM-/- growth cones and neurites could be the inability of these organelles to fuse with the surface plasma membrane that would result in the filling of neurites and growth cones with these organelles. In support of this idea, the growth cones in NCAM-/- neurons were slightly swollen being increased in their area. We observed that the recruitment of the TGN-derived organelles to the growth cone periphery was impaired in NCAM-/- neurons. The peripheral part of the growth cone is considered as a predominant site of the exocytosis. Thus the decreased amount of organelles in the peripheral part also indicates that the fusion of TGN-derived organelles is disturbed in NCAM-/- growth cones.

We found that NCAM co-localizes with the exocyst complex in growth cones and associates with the exocyst complex in a Ca2+ dependent manner. We showed for the first time that NCAM directly interacts with Exo70 subunit of the exocyst complex. Whereas expression of

the exocyst complex was enhanced in NCAM-/- brains, the levels of the exocyst complex were reduced in NCAM-/- growth cones and growth cones plasma membranes implicating NCAM in targeting of the exocyst complex to the growth cones and specific sites on the growth cone plasma membranes. We confirmed this in vitro by showing that the exocyst complex recruitment to the growth cone membranes isolated from NCAM-/- brains was reduced when compared to the growth cone membranes isolated from wild type brains.

Increased organelle accumulation and their inability to fuse with the surface plasma membrane in NCAM-/-growth cones can be thus explained by reduced levels of the exocyst complex in NCAM-/- growth cones and growth cone plasma membrane. We proved that by showing that NCAM clustering on the surface of growth cones enhanced vesicle exocytosis. We showed also that this NCAM activated vesicle exocytosis in the growth cones is Ca2+ dependent. At the same time NCAM activation enhanced the association between NCAM and the exocyst complex in isolated growth cones and the association between NCAM and the exocyst complex is Ca2+ dependent. Taking into account all our findings mentioned above we conclude that NCAM regulates fusion of TGN-derived organelles with the plasma membrane of growth cones by recruiting the exocyst complex to the growth cone plasma membrane.

8. References

Andrews HK, Zhang YQ, Trotta N, Broadie K. 2002. Drosophila sec10 is required for hormone secretion but not general exocytosis or neurotransmission. Traffic. 12:906-21.

Anitei M, Ifrim M, Ewart MA, Cowan AE, Carson JH, Bansal R, Pfeiffer SE. 2006. A role for Sec8 in oligodendrocyte morphological differentiation. J Cell Sci. 119:807-18.

Arai M, Itokawa M, Yamada K, Toyota T, Haga S, Ujike H, Sora I, Ikeda K, Yoshikawa T. 2004. Association of neural cell adhesion molecule 1 gene polymorphisms with bipolar affective disorder in Japanese individuals. Biol Psychiatry 55:804–810.

Atz ME, Rollins B, Vawter MP. 2007. NCAM1 association study of bipolar disorder and schizophrenia: polymorphisms and alternatively spliced isoforms lead to similarities and differences. Psychiatr Genet 17:55–67.

Barbas JA, Chaix JC, Steinmetz M, Goridis C. 1988. Differential splicing and alternative polyadenylation generates distinct NCAM transcripts and proteins in the mouse. EMBO J. 3:625-32.

Barbeau D, Liang JJ, Robitalille Y, Quirion R, Srivastava LK. 1995. Decreased expression of the embryonic form of the neural cell adhesion molecule in schizophrenic brains. Proc Natl Acad Sci U S A. 92:2785-9.

Barlowe C. 1997. Coupled ER to Golgi transport reconstituted with purified cytosolic proteins. J Cell Biol. 139:1097-108.

Berridge MJ, Bootman MD, Roderick HL. 2003. Calcium signalling: dynamics, homeostasis and remodelling. Nat Rev Mol Cell Biol. 4:517-29.

Berridge MJ, Lipp P, Bootman MD. 2000. The versatility and universality of calcium signalling. Nat Rev Mol Cell Biol. 1:11-21.

Bodrikov V, Leshchyns'ka I, Sytnyk V, Overvoorde J, den Hertog J, Schachner M. 2005. RPTPalpha is essential for NCAM-mediated p59fyn activation and neurite elongation. J Cell Biol. 168:127-39.

Bonfanti L, Olive S, Poulain DA, Theodosis DT. 1992. Mapping of the distribution of polysialylated neural cell adhesion molecule throughout the central nervous system of the adult rat: an immunohistochemical study. Neuroscience. 49:419-36.

Boyd C, Hughes T, Pypaert M, Novick P. 2004. Vesicles carry most exocyst subunits to exocytic sites marked by the remaining two subunits, Sec3p and Exo70p.J Cell Biol. 167:889-901.

Brackenbury R, Thiery JP, Rutishauser U, Edelman GM. 1977. Adhesion among neural cells of the chick embryo. I. An immunological assay for molecules involved in cell-cell binding. J Biol Chem. 252:6835-6840.

Brennwald P, Kearns B, Champion K, Keränen S, Bankaitis V, Novick P. 1994. Sec9 is a SNAP-25-like component of a yeast SNARE complex that may be the effector of Sec4 function in exocytosis. Cell. 79:245-58.

Broadie K, Prokop A, Bellen HJ, O'Kane CJ, Schulze KL, Sweeney ST. 1995. Syntaxin and synaptobrevin function downstream of vesicle docking in Drosophila. Neuron. 15:663-73.

Cao X, Ballew N, Barlowe C. 1998. Initial docking of ER-derived vesicles requires Uso1p and Ypt1p but is independent of SNARE proteins. EMBO J. 17:2156-65.

Chan SA, Polo-Parada L, Landmesser LT, Smith C. 2005. Adrenal chromaffin cells exhibit impaired granule trafficking in NCAM knockout mice. J Neurophysiol. 94:1037-47.

Chen A, Haines S, Maxson K, Akeson RA. 1994. VASE exon expression alters NCAM-mediated cell-cell interactions. J Neurosci Res. 38:483-92.

Chen W, Feng Y, Chen D, Wandinger-Ness A. 1998. Rab11 is required for trans-golgi network-to-plasma membrane transport and a preferential target for GDP dissociation inhibitor. Mol Biol Cell. 11:3241-57.

Chen YA, Scheller RH. 2001. SNARE-mediated membrane fusion. Nat Rev Mol Cell Biol. 2:98-106.

Clapham DE. 2007. Calcium signaling. Cell. 131:1047-58.

Cremer H, Lange R, Christoph A, Plomann M, Vopper G, Roes J, Brown R, Baldwin S, Kraemer P, Scheff S. 1994. Inactivation of the N-CAM gene in mice results in size reduction of the olfactory bulb and deficits in spatial learning. Nature. 367:455-9.

Cremer, H., G. Chazal, C. Goridis, and A. Represa. 1997. NCAM is essential for axonal growth and fasciculation in the hippocampus. Mol Cell Neurosci. 8:323-335.

Dequidt C, Danglot L, Alberts P, Galli T, Choquet D, Thoumine O. 2007. Fast turnover of L1 adhesions in neuronal growth cones involving both surface diffusion and exo/endocytosis of L1 molecules. Mol Biol Cell. 18:3131-43.

Deretic D. 1997. Rab proteins and post-Golgi trafficking of rhodopsin in photoreceptor cells. Electrophoresis. 18:2537-41.

Diefenbach TJ, Guthrie PB, Stier H, Billups B, Kater SB. 1999. Membrane recycling in the neuronal growth cone revealed by FM1-43 labeling. J Neurosci. 19:9436-44.

Ditlevsen DK, Povlsen GK, Berezin V, Bock E. 2008. NCAM-induced intracellular signaling revisited. J Neurosci Res. 86:727-43.

Doherty P, Cohen J, Walsh FS. 1990. Neurite outgrowth in response to transfected N-CAM changes during development and is modulated by polysialic acid. Neuron. 5:209-19.

Doherty P, Fazeli MS, Walsh FS. 1995. The neural cell adhesion molecule and synaptic plasticity. J Neurobiol. 26:437-46.

Doherty P, Fruns M, Seaton P, Dickson G, Barton CH, Sears TA, Walsh FS. 1990. A threshold effect of the major isoforms of NCAM on neurite outgrowth. Nature. 343:464-6.

Doherty P, Furness J, Williams EJ, Walsh FS. 1994. Neurite outgrowth stimulated by the tyrosine kinase inhibitor herbimycin A requires activation of tyrosine kinases and protein kinase C. J Neurochem. 62:2124-31.

Doherty P, Walsh FS. 1994. Signal transduction events underlying neurite outgrowth stimulated by cell adhesion molecules. Curr Opin Neurobiol. 4:49-55.

Doyle E, Nolan PM, Bell R, Regan CM. 1992. Hippocampal NCAM180 transiently increases sialylation during the acquisition and consolidation of a passive avoidance response in the adult rat. J Neurosci Res. 31:513-523.

EauClaire S, Guo W. 2003. Conservation and specialization. The role of the exocyst in neuronal exocytosis. Neuron. 37:369-70.

Farmer A, Elkin A, McGuffin P. 2007.The genetics of bipolar affective disorder. Curr Opin Psychiatry. 20:8–12.

Fasshauer D, Antonin W, Subramaniam V, Jahn R. 2002. SNARE assembly and disassembly exhibit a pronounced hysteresis. Nat Struct Biol. 9:144-51.

Finger FP, Novick P. 1997. Sec3p is involved in secretion and morphogenesis in Saccharomyces cerevisiae. Mol Biol Cell. 8:647-62.

Freedman R. 2003. Schizophrenia. N Engl J Med .349:1738–1749.

Friedrich GA, Hildebrand JD, Soriano P. 1997. The secretory protein Sec8 is required for paraxial mesoderm formation in the mouse. Dev Biol. 192:364-74.

Futerman AH, Banker GA. 1996. The economics of neurite outgrowth - the addition of new membrane to growing axons. Trends Neurosci. 19:144-9.

Gillian AM, Brion JP, Breen KC. 1994. Expression of the neural cell adhesion molecule (NCAM) in Alzheimer's disease. Neurodegeneration. 3:283–291.

Goedert M, Spillantini MG. 2006. Alzheimer's disease. Semin Neurol. 27:32–41.

Gower HJ, Barton CH, Elsom VL, Thompson J, Moore SE, Dickson G, Walsh FS. 1988. Alternative splicing generates a secreted form of N-CAM in muscle and brain. Cell. 55:955-64.

Grindstaff KK, Yeaman C, Anandasabapathy N, Hsu SC, Rodriguez-Boulan E, Scheller RH, Nelson WJ. 1998. Sec6/8 complex is recruited to cell-cell contacts and specifies transport vesicle delivery to the basal-lateral membrane in epithelial cells. Cell. 93:731-40.

Gubkina O, Cremer H, Rougon G. 2001. Mutation in the neural cell adhesion molecule interferes with the differentiation of anterior pituitary secretory cells. Neuroendocrinology. 74:335-46.

Guo W, Roth D, Gatti E, De Camilli P, Novick P. 1997. Identification and characterization of homologues of the Exocyst component Sec10p. FEBS Lett. 404:135-9.

Guo W, Roth D, Walch-Solimena C, Novick P. 1999. The exocyst is an effector for Sec4p, targeting secretory vesicles to sites of exocytosis. EMBO J. 18:1071-80.

Guo W, Sacher M, Barrowman J, Ferro-Novick S, Novick P. 2000. Protein complexes in transport vesicle targeting. Trends Cell Biol. 10:251-5.

Hazuka CD, Foletti DL, Hsu SC, Kee Y, Hopf FW, Scheller RH. 1999. The sec6/8 complex is located at neurite outgrowth and axonal synapse-assembly domains. J Neurosci. 19:1324-34.

Higgins D, Burack M, Lein P, Banker G. 1997. Mechanisms of neuronal polarity. Curr Opin Neurobiol. 7:599-604.

Hinkle CL, Diestel S, Lieberman J, Maness PF. 2006. Metalloprotease-induced ectodomain shedding of neural cell adhesion molecule (NCAM). J Neurobiol. 66:1378–1395.

Hinsby AM, Berezin V, Bock E. 2004. Molecular mechanisms of NCAM function. Front Biosci. 9:2227-44.

Honer WG, Falkai P, Young C, Wang T, Xie J, Bonner J, Hu L, Boulianne GL, Luo Z, Trimble WS. 1997. Cingulate cortex synaptic terminal proteins and neural cell adhesion molecule in schizophrenia. Neuroscience. 78:99-110.

Hsu SC, Hazuka CD, Foletti DL, Scheller RH. 1999. Targeting vesicles to specific sites on the plasma membrane: the role of the sec6/8 complex. Trends Cell Biol. 9:150-3.

Hsu SC, Hazuka CD, Roth R, Foletti DL, Heuser J, Scheller RH. 1998. Subunit composition, protein interactions, and structures of the mammalian brain sec6/8 complex and septin filaments. Neuron. 20:1111-22.

Hsu SC, TerBush D, Abraham M, Guo W. 2004. The exocyst complex in polarized exocytosis. Int Rev Cytol. 233:243-65.

Hsu SC, Ting AE, Hazuka CD, Davanger S, Kenny JW, Kee Y, Scheller RH. 1996. The mammalian brain rsec6/8 complex. Neuron. 17:1209-19.

Hunt JM, Bommert K, Charlton MP, Kistner A, Habermann E, Augustine GJ, Betz H. 1994. A post-docking role for synaptobrevin in synaptic vesicle fusion. Neuron. 2:1269-79.

Inoue M, Chang L, Hwang J, Chiang SH, Saltiel AR. 2003. The exocyst complex is required for targeting of Glut4 to the plasma membrane by insulin. Nature. 422:629-33.

Kadmon G, Kowitz A, Altevogt P, Schachner M. 1990. Functional cooperation between the neural adhesion molecules L1 and N-CAM is carbohydrate dependent. J Cell Biol. 110:209-18.

Karcher SJ, Asai DJ, Staige CJ. 1996. Expression vectors used in project-oriented teaching laboratories. Pages 1–22, in Tested studies for laboratory teaching, Volume 17 (J. C. Glase, Editor). Proceedings of the 17th Workshop/Conference of the Association for Biology Laboratory Education (ABLE). (http://www.ableweb.org/volumes/vol-17/1-karcher.pdf).

Kee Y, Yoo JS, Hazuka CD, Peterson KE, Hsu SC, Scheller RH. 1997. Subunit structure of the mammalian exocyst complex. Proc Natl Acad Sci U S A. 94:14438-43.

Keilhauer G, Faissner A, Schachner M. 1985. Differential inhibition of neurone-neurone, neurone-astrocyte and astrocyte-astrocyte adhesion by L1, L2 and N-CAM antibodies. Nature. 316:728-30.

Kiryushko D, Korshunova I, Berezin V, Bock E. 2006. Neural cell adhesion molecule induces intracellular signaling via multiple mechanisms of Ca2+ homeostasis. Mol Biol Cell. 17:2278-2286.

Kiss JZ, Troncoso E, Djebbara Z, Vutskits L, Muller D. 2001.The role of neural cell adhesion molecules in plasticity and repair. Brain Res Brain Res Rev. 36:175-84.

Kleene R, Schachner M. 2004 Glycans and neural cell interactions. Nat Rev Neurosci. 5:195-208.

Kolkova K, Novitskaya V, Pedersen N, Berezin V, Bock E. 2000. Neural cell adhesion molecule-stimulated neurite outgrowth depends on activation of protein kinase C and the Rasmitogen- activated protein kinase pathway. J Neurosci. 20: 2238– 2246.

Kornblihtt AR, Umezawa K, Vibe-Pedersen K, Baralle FE. 1985. Primary structure of human fibronectin: differential splicing may generate at least 10 polypeptides from a single gene. EMBO J. 4:1755-9.

Kreitzer G, Schmoranzer J, Low SH, Li X, Gan Y, Weimbs T, Simon SM, Rodriguez-Boulan E. 2003. Three-dimensional analysis of post-Golgi carrier exocytosis in epithelial cells. Nat Cell Biol. 5:126-36.

Lahrtz F, Horstkorte R, Cremer H, Schachner M, Montag D. 1997. VASE-encoded peptide modifies NCAM- and L1-mediated neurite outgrowth. J Neurosci Res. 50:62-8.

Leahy RL. 2007. Bipolar disorder: causes, contexts, and treatments. J Clin Psychol. 63:417–424.

Leshchyns'ka I, Sytnyk V, Morrow JS, Schachner M. 2003. Neural cell adhesion molecule (NCAM) association with PKCbeta2 via betaI spectrin is implicated in NCAM-mediated neurite outgrowth. J Cell Biol. 161:625-39.

Lewis DA, Moghaddam B. 2006. Cognitive dysfunction in schizophrenia: convergence of gamma-aminobutyric acid and glutamate alterations. Arch Neurol. 63:1372–1376.

Li L, Chin LS. 2003. The molecular machinery of synaptic vesicle exocytosis. Cell Mol Life Sci. 60:942-60.

Lieberman JA, Perkins D, Belger A, Chakos M, Jarskog F, Boteva K, Gilmore J. 2002. The early stages of schizophrenia: speculations on pathogenesis, pathophysiology, and therapeutic approaches. Biol Psychiatry. 50:884-97.

Lipschutz JH, Guo W, O'Brien LE, Nguyen YH, Novick P, Mostov KE. 2000. Exocyst is involved in cystogenesis and tubulogenesis and acts by modulating synthesis and delivery of basolateral plasma membrane and secretory proteins. Mol Biol Cell. 11:4259-75.

Lipschutz JH, Lingappa VR, Mostov KE. 2003. The exocyst affects protein synthesis by acting on the translocation machinery of the endoplasmic reticulum. J Biol Chem. 78:20954-60.

Lipschutz JH, Mostov KE. 2002. Exocytosis: the many masters of the exocyst. Curr Biol. 12:R212-4.

Lipsky NG, Pagano RE. 1985. A vital stain for the Golgi apparatus. Science. 228:745-7.

Little EB, Edelman GM, Cunningham BA. 1998. Palmitoylation of the cytoplasmic domain of the neural cell adhesion molecule N-CAM serves as an anchor to cellular membranes. Cell Adhes Commun. 6:415-30.

Lowe M. 2000. Membrane transport: tethers and TRAPPs. Curr Biol. Jun. 10: 407-9.

Lupashin V, Sztul E. 2005. Golgi tethering factors. Biochim Biophys Acta. 1744:325-39.

Macia E, Ehrlich M, Massol R, Boucrot E, Brunner C, Kirchhausen T. 2006. Dynasore, a cell-permeable inhibitor of dynamin. Dev Cell. 10:839-50.

Maness PF, Schachner M. 2007.Neural recognition molecules of the immunoglobulin superfamily: signaling transducers of axon guidance and neuronal migration. Nat Neurosci. 10:19-26.

Matern HT, Yeaman C, Nelson WJ, Scheller RH. 2001. The Sec6/8 complex in mammalian cells: characterization of mammalian Sec3, subunit interactions, and expression of subunits in polarized cells. Proc Natl Acad Sci U S A. 98:9648-53.

Matteoli M, Takei K, Perin MS, Südhof TC, De Camilli P. 1992. Exo-endocytotic recycling of synaptic vesicles in developing processes of cultured hippocampal neurons. J Cell Biol. 117:849-61.

Maynard TM, Sikich L, Lieberman JA, LaMantia AS. 2001. Neural development, cell-cell signaling, and the "two-hit" hypothesis of schizophrenia. Schizophr Bull. 27:457-76.

McNew JA, Parlati F, Fukuda R, Johnston RJ, Paz K, Paumet F, Söllner TH, Rothman JE. 2000. Compartmental specificity of cellular membrane fusion encoded in SNARE proteins. Nature. 407:153-9.

Montag-Sallaz M, Montag D, Schachner M. 2003. Altered processing of novel information in N-CAM-deficient mice. Neuroreport. 14:1343-6.

Moore SE, Walsh FS. 1986. Nerve dependent regulation of neural cell adhesion molecule expression in skeletal muscle. Neuroscience. 18:499-505.

Moskalenko S, Henry DO, Rosse C, Mirey G, Camonis JH, White MA. 2002. The exocyst is a Ral effector complex. Nat Cell Biol. 4:66-72.

Muller D, Wang C, Skibo G, Toni N, Cremer H, Calaora V, Rougon G, Kiss JZ. 1996. PSA-NCAM is required for activity-induced synaptic plasticity. Neuron. 17:413-22.

Muller JM, Shorter J, Newman R, Deinhardt K, Sagiv Y, Elazar Z, Warren G, Shima DT. 2002. Sequential SNARE disassembly and GATE-16-GOS-28 complex assembly mediated by distinct NSF activities drives Golgi membrane fusion. J Cell Biol. 157:1161-73.

Murthy M, Garza D, Scheller RH, Schwarz TL. 2003. Mutations in the exocyst component Sec5 disrupt neuronal membrane traffic, but neurotransmitter release persists. Neuron. 37:433-47.

Nankoe SR, Sever S. 2006. Dynasore puts a new spin on dynamin: a surprising dual role during vesicle formation. Trends Cell Biol. 16:607-9.

Nelson RW, Bates PA, Rutishauser U. 1995. Protein determinants for specific polysialylation of the neural cell adhesion molecule. J Biol Chem. 270:17171-9.

Neugebauer KM, Tomaselli KJ, Lilien J, Reichardt LF. 1988. N-cadherin, NCAM, and integrins promote retinal neurite outgrowth on astrocytes in vitro. J Cell Biol. 107:1177-87.

Novick P, Ferro S, Schekman R. 1981. Order of events in the yeast secretory pathway. Cell. 25:461-9.

Novick P, Guo W. 2002. Ras family therapy: Rab, Rho and Ral talk to the exocyst. Trends Cell Biol. 12:247-9.

Ono K, Tomasiewicz H, Magnuson T, Rutishauser U. 1994. N-CAM mutation inhibits tangential neuronal migration and is phenocopied by enzymatic removal of polysialic acid. Neuron. 13:595-609.

Pagano RE, Martin OC, Kang HC, Haugland RP. 1991. A novel fluorescent ceramide analogue for studying membrane traffic in animal cells: accumulation at the Golgi apparatus results in altered spectral properties of the sphingolipid precursor. J Cell Biol. 113:1267-79.

Parlati F, McNew JA, Fukuda R, Miller R, Söllner TH, Rothman JE. 2000. Topological restriction of SNARE-dependent membrane fusion. Nature. 407:194-8.

Peck D, Walsh FS. 1993. Differential effects of over-expressed neural cell adhesion molecule isoforms on myoblast fusion. J Cell Biol. 123:1587-95.

Pelham HR. 2001. SNAREs and the specificity of membrane fusion. Trends Cell Biol. 11:99-101.

Perl AK, Dahl U, Wilgenbus P, Cremer H, Semb H, Christofori G. 1999. Reduced expression of neural cell adhesion molecule induces metastatic dissemination of pancreatic beta tumor cells. Nat Med. 5:286-91.

Persohn E, Pollerberg GE, Schachner M. 1989. Immunoelectron-microscopic localization of the 180 kD component of the neural cell adhesion molecule N-CAM in postsynaptic membranes. J Comp Neurol. 288:92-100.

Pfenninger KH, Ellis L, Johnson MP, Friedman LB, Somlo S. 1983. Nerve growth cones isolated from fetal rat brain: subcellular fractionation and characterization. Cell. 35:573-84.

Pfenninger KH, Friedman LB. 1993. Sites of plasmalemmal expansion in growth cones.Brain Res Dev Brain Res. 71:181-92.

Pfenninger KH, Laurino L, Peretti D, Wang X, Rosso S, Morfini G, Caceres A, Quiroga S. 2003 Regulation of membrane expansion at the nerve growth cone. J Cell Sci. 116:1209-17.

Plappert CF, Schachner M, Pilz PK. 2006. Neural cell adhesion molecule (NCAM-/-) null mice show impaired sensitization of the startle response. Genes Brain Behav. 5:46-52.

Pollerberg EG, Sadoul R, Goridis C, Schachner M. 1985. Selective expression of the 180-kD component of the neural cell adhesion molecule N-CAM during development. J Cell Biol. 101:1921-9.

Pollerberg GE, Burridge K, Krebs KE, Goodman SR, Schachner M. 1987. The 180-kD component of the neural cell adhesion molecule N-CAM is involved in a cell-cell contacts and cytoskeleton-membrane interactions. Cell Tissue Res. 250:227-36.

Polo-Parada L, Bose CM, Landmesser LT. 2001. Alterations in transmission, vesicle dynamics, and transmitter release machinery at NCAM-deficient neuromuscular junctions. Neuron. 32:815-828.

Polo-Parada L, Bose CM, Plattner F, Landmesser LT. 2004. Distinct roles of different neural cell adhesion molecule (NCAM) isoforms in synaptic maturation revealed by analysis of NCAM 180 kDa isoform-deficient mice. J Neurosci. 24:1852-64.

Poltorak M, Frye MA, Wright R, Hemperly JJ, George MS, Pazzaglia PJ, Jerrels SA, Post RM, Freed WJ. 1996. Increased neural cell adhesion molecule in the CSF of patients with mood disorder. J Neurochem. 66:1532–1538.

Poltorak M, Khoja I, Hemperly JJ, Williams JR, el-Mallakh R, Freed WJ. 1995. Disturbances in cell recognition molecules (N-CAM and L1 antigen) in the CSF of patients with schizophrenia. Exp Neurol. 131:266-72.

Popov S, Brown A, Poo MM. 1993 .Forward plasma membrane flow in growing nerve rocesses. Science. 259:244-6.

Prentice HM, Moore SE, Dickson JG, Doherty P, Walsh FS. 1987. Nerve growth factor-induced changes in neural cell adhesion molecule (N-CAM) in PC12 cells. EMBO J. 6:1859-63.

Ranheim TS, Edelman GM, Cunningham BA. 1996. Homophilic adhesion mediated by the neural cell adhesion molecule involves multiple immunoglobulin domains. Proc Natl Acad Sci U S A. 93:4071-5.

Rao Y, Zhao X, Siu CH. 1994. Mechanism of homophilic binding mediated by the neural cell adhesion molecule NCAM. Evidence for isologous interaction. J Biol Chem. 269(44):27540-8.

Riefler GM, Balasingam G, Lucas KG, Wang S, Hsu SC, Firestein BL. 2003. Exocyst complex subunit sec8 binds to postsynaptic density protein-95 (PSD-95): a novel interaction regulated by cypin (cytosolic PSD-95 interactor). Biochem J. 373:49-55.

Rønn LC, Doherty P, Holm A, Berezin V, Bock E. 2000 Neurite outgrowth induced by a synthetic peptide ligand of neural cell adhesion molecule requires fibroblast growth factor receptor activation. J Neurochem. 75:665-71.

Rosen CL, Lisanti MP, Salzer JL. 1992. Expression of unique sets of GPI-linked proteins by different primary neurons in vitro. J Cell Biol. 117:617-27.

Roth D, Guo W, Novick P. 1998. Dominant negative alleles of SEC10 reveal distinct domains involved in secretion and morphogenesis in yeast. Mol Biol Cell. 9:1725-39.

Rutishauser U, Acheson A, Hall AK, Mann DM, Sunshine J. 1988. The neural cell adhesion molecule (NCAM) as a regulator of cell-cell interactions. Science. 240:53-7.

Rutishauser U, Landmesser L. 1996. Polysialic acid in the vertebrate nervous system: a promoter of plasticity in cell-cell interactions. Trends Neurosci. 19:422-7.

Saffell JL, Williams EJ, Mason IJ, Walsh FS, Doherty P. 1997. Expression of a dominant negative FGF receptor inhibits axonal growth and FGF receptor phosphorylation stimulated by CAMs. Neuron. 18:231-42.

Sandi C, Bisaz R. 2007. A model for the involvement of neural cell adhesion molecules in stress-related mood disorders. Neuroendocrinology. 85:158–176.

Sans N, Prybylowski K, Petralia RS, Chang K, Wang YX, Racca C, Vicini S, Wenthold RJ. 2003. NMDA receptor trafficking through an interaction between PDZ proteins and the exocyst complex. Nat Cell Biol. 5:520-30.

Santuccione A, Sytnyk V, Leshchyns'ka I, Schachner M. 2005. Prion protein recruits its neuronal receptor NCAM to lipid rafts to activate p59fyn and to enhance neurite outgrowth. J Cell Biol. 169:341-354.

Sapperstein SK, Walter DM, Grosvenor AR, Heuser JE, Waters MG. 1995. p115 is a general vesicular transport factor related to the yeast endoplasmic reticulum to Golgi transport factor Uso1p. Proc Natl Acad Sci U S A. 92:522-6.

Schachner M, Martini R. 1995. Glycans and the modulation of neural-recognition molecule function. Trends Neurosci. 18:183-91.

Schmid RS, Graff RD, Schaller MD, Chen S, Schachner M, Hemperly JJ, Maness PF. 1999. NCAM stimulates the Ras-MAPK pathway and CREB phosphorylation in neuronal cells. J Neurobiol. 38:542-58.

Schuch U, Lohse MJ, Schachner M. 1989. Neural cell adhesion molecules influence second messenger systems. Neuron. 3:13-20.

Seilheimer B, Schachner M. 1988. Studies of adhesion molecules mediating interactions between cells of peripheral nervous system indicate a major role for L1 in mediating sensory neuron growth on Schwann cells in culture. J Cell Biol. 107:341-51.

Seki T, Rutishauser U. 1998. Removal of polysialic acid-neural cell adhesion molecule induces aberrant mossy fiber innervation and ectopic synaptogenesis in the hippocampus. J Neurosci. 18:3757-66.

Shin DM, Zhao XS, Zeng W, Mozhayeva M, Muallem S. 2000. The mammalian Sec6/8 complex interacts with Ca(2+) signaling complexes and regulates their activity. J Cell Biol. 150:1101-12.

Sjölinder M, Uhlmann J, Ponstingl H. 2002. DelGEF, a homologue of the Ran guanine nucleotide exchange factor RanGEF, binds to the exocyst component Sec5 and modulates secretion. FEBS Lett. 532:211-5.

Söllner T, Whiteheart SW, Brunner M, Erdjument-Bromage H, Geromanos S, Tempst P, Rothman JE. 1993. SNAP receptors implicated in vesicle targeting and fusion. Nature. 362:318-24.

Stork O, Welzl H, Cremer H, Schachner M. 1997. Increased intermale aggression and neuroendocrine response in mice deficient for the neural cell adhesion molecule (NCAM). Eur J Neurosci. 6:1117-25.

Strekalova H, Buhmann C, Kleene R, Eggers C, Saffell J, Hemperly J, Weiller C, Muller-Thomsen T, Schachner M. 2006. Elevated levels of neural recognition molecule L1 in the cerebrospinal fluid of patients with Alzheimer disease and other dementia syndromes. Neurobiol Aging. 27:1–9.

Südhof TC. 1995. The synaptic vesicle cycle: a cascade of protein-protein interactions. Nature. 375:645-53.

Sugihara K, Asano S, Tanaka K, Iwamatsu A, Okawa K, Ohta, Y. 2002 The exocyst complex binds the small GTPase RalA to mediate filopodia formation. Nat Cell Biol. 4:73-78.

Sutton RB, Fasshauer D, Jahn R, Brunger AT. 1998. Crystal structure of a SNARE complex involved in synaptic exocytosis at 2.4 A resolution. Nature. 395:347-53.

Sytnyk V, Leshchyns'ka I, Delling M, Dityateva G, DityatevA, Schachner M. 2002. Neural cell adhesion molecule promotes accumulation of TGN organelles at sites of neuron-to-neuron contacts. J Cell Biol. 159:649-661.

TerBush DR, Maurice T, Roth D, Novick P. 1996. The Exocyst is a multiprotein complex required for exocytosis in Saccharomyces cerevisiae. EMBO J. 15:6483-94.

Todaro L, Puricelli L, Gioseffi H, Guadalupe Pallotta M, Lastiri J, Bal de Kier Joffe E, Varela M, Sacerdote de Lustig E. 2004. Neural cell adhesion molecule in human serum. Increased levels in dementia of the Alzheimer type. Neurobiol Dis. 15:387–393.

Tomasiewicz H, Ono K, Yee D, Thompson C, Goridis C, Rutishauser U, Magnuson T. 1993. Genetic deletion of a neural cell adhesion molecule ariant (N-CAM-180) produces distinct defects in the central nervous system. Neuron. 11:1163-74.

Ullrich O, Reinsch S, Urbé S, Zerial M, Parton RG. 1996. Rab11 regulates recycling through the pericentriolar recycling endosome. J Cell Biol. 135:913-24.

Vawter MP, Hemperly JJ, Hyde TM, Bachus SE, VanderPutten DM, Howard AL, Cannon-Spoor HE, McCoy MT, Webster MJ, Kleinman JE, Freed WJ. 1998. VASE-containing N-CAM isoforms are increased in the hippocampus in bipolar disorder but not schizophrenia. Exp Neurol. 154:1–11.

Vawter MP, Howard AL, Hyde TM, Kleinman JE, Freed WJ. 1999. Alterations of hippocampal secreted N-CAM in bipolar disorder and synaptophysin in schizophrenia. Mol Psychiatry. 4:467–475.

Vawter MP. 2000. Dysregulation of the neural cell adhesion molecule and neuropsychiatric disorders. Eur J Pharmacol. 405:385-95.

Vega IE, Hsu SC. 2001. The exocyst complex associates with microtubules to mediate vesicle targeting and neurite outgrowth. J Neurosci. 21:3839-48.

Vega IE, Hsu SC. 2003. The septin protein Nedd5 associates with both the exocyst complex and microtubules and disruption of its GTPase activity promotes aberrant neurite sprouting in PC12 cells. Neuroreport. 14:31-7.

Wang S, Liu Y, Adamson CL, Valdez G, Guo W, Hsu SC. 2004. The mammalian exocyst, a complex required for exocytosis, inhibits tubulin polymerization. J Biol Chem. 279:35958-66.

Waters MG, Hughson FM. 2000. Membrane tethering and fusion in the secretory and endocytic pathways. Traffic. 1:588-97.

Whyte JR, Munro S. 2001. The Sec34/35 Golgi transport complex is related to the exocyst, defining a family of complexes involved in multiple steps of membrane traffic. Dev Cell. 1:527-37.

Whyte JR, Munro S. 2002. Vesicle tethering complexes in membrane traffic. J Cell Sci. 115:2627-37.

Williams EJ, Furness J, Walsh FS, Doherty P. 1994. Activation of the FGF receptor underlies neurite outgrowth stimulated by L1, N-CAM, and N-cadherin. Neuron.13:583-594.

Wu S, Mehta SQ, Pichaud F, Bellen HJ, Quiocho FA. 2005. Sec15 interacts with Rab11 via a novel domain and affects Rab11 localization in vivo. Nat Struct Mol Biol. 12:879-85.

Yaari R, Corey-Bloom J. 2007. Alzheimer's disease. Semin Neurol. 27:32–41.

Yamakawa H, Seog DH, Yoda K, Yamasaki M, Wakabayashi T. 1996. Uso1 protein is a dimer with two globular heads and a long coiled-coil tail. J Struct Biol. 116:356-65.

Yeaman C, Grindstaff KK, Wright JR, Nelson WJ. 2001. Sec6/8 complexes on trans-Golgi network and plasma membrane regulate late stages of exocytosis in mammalian cells. J Cell Biol. 155:593-604.

Yew DT, Li WP, Webb SE, Lai HW, Zhang L. 1999. Neurotransmitters, peptides, and neural cell adhesion molecules in the cortices of normal elderly humans and Alzheimer patients: a comparison. Exp Gerontol. 34:117–133.

Zakharenko S, Popov S. 1998. Dynamics of axonal microtubules regulate the topology of new membrane insertion into the growing neurites. J Cell Biol. 143:1077-86.

Zhang XM, Ellis S, Sriratana A, Mitchell CA, Rowe T. 2004. Sec15 is an effector for the Rab11 GTPase in mammalian cells. J Biol Chem. 279:43027-34.

9. List of figures

Publications

Chernyshova Y, Leshchyns'ka I, Hsu C H, Schachner M, SytnykV. (submitted). NCAM targets the exocyst complex to growth cone surface membranes to promote exocytosis of TGN-derived organelles.

Acknowledgments

This study has been performed in the Institute for Biosynthesis of Neuronal Structures of the Center for Molecular Neurobiology (ZMNH) at the University of Hamburg. I would like to thank Prof. Melitta Schachner for providing facilities for this research, fruitful discussions and for support and guidance.

I am especially thankful to Dr. Vladimir Sytnyk and Dr. Iryna Leshchyns'ka, who initiated the project, for being great and patient scientific advisors, for their excellent supervision, support, motivation, clever guidance and valuable ideas over the course of my PhD, as well as for their help in writing of our paper and this thesis.

I also would like to thank to all my friends and colleagues, Yevgen Shumeyko, Nadiya Bodrikova, Aksana Andreeva, Oleg Zaitsev, Dmytro Puchkov, Aparna Shetty, Vasudharani Devanathan, Nan Tian, Babett Baraniec, Doreen Westphal, Shen Li and Oleg Senkov for a daily support.

I am grateful to Ute Eicke-Kohlmorgen, Achim Dahlmann, Joseph Thorairajoo, Peggy Putthoff, Fritz Kutschera, Torsten Renz and Eva Kronberg for technical assistance, genotyping and animal care.

I wish to thank our collaborator Dr. Shu-Chan Hsu (Rutgers University,USA) for the pGEX Exo70 construct and anti-Sec8/Exo70 antibody.

Dr. Carol Stocking (Heinrich-Pette-Institut, Hamburg, Germany), thank you very much for helping me to improve the language of this manuscript.

I am also thankful to the biology faculty members of the Dnepropetrovsk National University Dr. Zhernosekov, Prof Dr. Nedzvetsky, Dr. Tykchomyrov, Prof Dr. Ushakova, Prof Dr. Chorna and Dr. Dovzhenko for exciting me to be a scientist.

I wish to thank my parents and all my family in Ukraine that have always encouraged and supported me so far from home.

My special thanks to my husband Vsevolod Bodrikov for the constant help, support, love and patience.